A PHOTOMETRIC INVESTIGATION OF THE FIELDS OF TWO SHORT-PERIOD CEPHEIDS IN CYGNUS

by

Georgi Iliev Mandushev

A thesis submitted in partial fulfillment
of the requirements for the degree of
Master of Science

Department of Astronomy and Physics
Saint Mary's University
Halifax, Nova Scotia
August, 1994

ISBN 0-315-95870-7

Name GEORGI MANDUSHEV

Dissertation Abstracts International is arranged by broad, general subject categories. Please select the one subject which most nearly describes the content of your dissertation. Enter the corresponding four-digit code in the spaces provided.

ASTRONOMY AND ASTROPHYSICS | 0 | 6 | 0 | 6 | U·M·I

SUBJECT TERM **SUBJECT CODE**

Subject Categories

THE HUMANITIES AND SOCIAL SCIENCES

COMMUNICATIONS AND THE ARTS
Architecture 0729
Art History 0377
Cinema 0900
Dance 0378
Fine Arts 0357
Information Science 0723
Journalism 0391
Library Science 0399
Mass Communications 0708
Music 0413
Speech Communication 0459
Theater 0465

EDUCATION
General 0515
Administration 0514
Adult and Continuing 0516
Agricultural 0517
Art 0273
Bilingual and Multicultural 0282
Business 0688
Community College 0275
Curriculum and Instruction 0727
Early Childhood 0518
Elementary 0524
Finance 0277
Guidance and Counseling 0519
Health 0680
Higher 0745
History of 0520
Home Economics 0278
Industrial 0521
Language and Literature 0279
Mathematics 0280
Music 0522
Philosophy of 0998
Physical 0523
Psychology 0525
Reading 0535
Religious 0527
Sciences 0714
Secondary 0533
Social Sciences 0534
Sociology of 0340
Special 0529
Teacher Training 0530
Technology 0710
Tests and Measurements 0288
Vocational 0747

LANGUAGE, LITERATURE AND LINGUISTICS
Language
- General 0679
- Ancient 0289
- Linguistics 0290
- Modern 0291

Literature
- General 0401
- Classical 0294
- Comparative 0295
- Medieval 0297
- Modern 0298
- African 0316
- American 0591
- Asian 0305
- Canadian (English) 0352
- Canadian (French) 0355
- English 0593
- Germanic 0311
- Latin American 0312
- Middle Eastern 0315
- Romance 0313
- Slavic and East European 0314

PHILOSOPHY, RELIGION AND THEOLOGY
Philosophy 0422
Religion
- General 0318
- Biblical Studies 0321
- Clergy 0319
- History of 0320
- Philosophy of 0322

Theology 0469

SOCIAL SCIENCES
American Studies 0323
Anthropology
- Archaeology 0324
- Cultural 0326
- Physical 0327

Business Administration
- General 0310
- Accounting 0272
- Banking 0770
- Management 0454
- Marketing 0338

Canadian Studies 0385
Economics
- General 0501
- Agricultural 0503
- Commerce-Business 0505
- Finance 0508
- History 0509
- Labor 0510
- Theory 0511

Folklore 0358
Geography 0366
Gerontology 0351
History
- General 0578
- Ancient 0579
- Medieval 0581
- Modern 0582
- Black 0328
- African 0331
- Asia, Australia and Oceania 0332
- Canadian 0334
- European 0335
- Latin American 0336
- Middle Eastern 0333
- United States 0337

History of Science 0585
Law 0398
Political Science
- General 0615
- International Law and Relations 0616
- Public Administration 0617

Recreation 0814
Social Work 0452
Sociology
- General 0626
- Criminology and Penology 0627
- Demography 0938
- Ethnic and Racial Studies 0631
- Individual and Family Studies 0628
- Industrial and Labor Relations 0629
- Public and Social Welfare 0630
- Social Structure and Development 0700
- Theory and Methods 0344

Transportation 0709
Urban and Regional Planning 0999
Women's Studies 0453

THE SCIENCES AND ENGINEERING

BIOLOGICAL SCIENCES
Agriculture
- General 0473
- Agronomy 0285
- Animal Culture and Nutrition 0475
- Animal Pathology 0476
- Food Science and Technology 0359
- Forestry and Wildlife 0478
- Plant Culture 0479
- Plant Pathology 0480
- Plant Physiology 0817
- Range Management 0777
- Wood Technology 0746

Biology
- General 0306
- Anatomy 0287
- Biostatistics 0308
- Botany 0309
- Cell 0379
- Ecology 0329
- Entomology 0353
- Genetics 0369
- Limnology 0793
- Microbiology 0410
- Molecular 0307
- Neuroscience 0317
- Oceanography 0416
- Physiology 0433
- Radiation 0821
- Veterinary Science 0778
- Zoology 0472

Biophysics
- General 0786
- Medical 0760

EARTH SCIENCES
Biogeochemistry 0425
Geochemistry 0996
Geodesy 0370
Geology 0372
Geophysics 0373
Hydrology 0388
Mineralogy 0411
Paleobotany 0345
Paleoecology 0426
Paleontology 0418
Paleozoology 0985
Palynology 0427
Physical Geography 0368
Physical Oceanography 0415

HEALTH AND ENVIRONMENTAL SCIENCES
Environmental Sciences 0768
Health Sciences
- General 0566
- Audiology 0300
- Chemotherapy 0992
- Dentistry 0567
- Education 0350
- Hospital Management 0769
- Human Development 0758
- Immunology 0982
- Medicine and Surgery 0564
- Mental Health 0347
- Nursing 0569
- Nutrition 0570
- Obstetrics and Gynecology 0380
- Occupational Health and Therapy 0354
- Ophthalmology 0381
- Pathology 0571
- Pharmacology 0419
- Pharmacy 0572
- Physical Therapy 0382
- Public Health 0573
- Radiology 0574
- Recreation 0575
- Speech Pathology 0460
- Toxicology 0383

Home Economics 0386

PHYSICAL SCIENCES

Pure Sciences

Chemistry
- General 0485
- Agricultural 0749
- Analytical 0486
- Biochemistry 0487
- Inorganic 0488
- Nuclear 0738
- Organic 0490
- Pharmaceutical 0491
- Physical 0494
- Polymer 0495
- Radiation 0754

Mathematics 0405
Physics
- General 0605
- Acoustics 0986
- Astronomy and Astrophysics 0606
- Atmospheric Science 0608
- Atomic 0748
- Electronics and Electricity 0607
- Elementary Particles and High Energy 0798
- Fluid and Plasma 0759
- Molecular 0609
- Nuclear 0610
- Optics 0752
- Radiation 0756
- Solid State 0611

Statistics 0463

Applied Sciences

Applied Mechanics 0346
Computer Science 0984

Engineering
- General 0537
- Aerospace 0538
- Agricultural 0539
- Automotive 0540
- Biomedical 0541
- Chemical 0542
- Civil 0543
- Electronics and Electrical 0544
- Heat and Thermodynamics 0348
- Hydraulic 0545
- Industrial 0546
- Marine 0547
- Materials Science 0794
- Mechanical 0548
- Metallurgy 0743
- Mining 0551
- Nuclear 0552
- Packaging 0549
- Petroleum 0765
- Sanitary and Municipal 0554
- System Science 0790

Geotechnology 0428
Operations Research 0796
Plastics Technology 0795
Textile Technology 0994

PSYCHOLOGY
General 0621
Behavioral 0384
Clinical 0622
Developmental 0620
Experimental 0623
Industrial 0624
Personality 0625
Physiological 0989
Psychobiology 0349
Psychometrics 0632
Social 0451

Table of Contents

Table of Contents (continued)

Saint Mary's University
Department of Astronomy and Physics

Certificate of Examination

David G. Turner

Dr. David G. Turner (Supervisor)
Saint Mary's University

Dr. David A. Clarke
Saint Mary's University

Douglas Forbes

Dr. Douglas Forbes
Sir Wilfred Grenfell College,
Memorial University of Newfoundland

Gary A. Welch

Dr. Gary A. Welch
Saint Mary's University

Dr. Malcolm N. Butler
Graduate Studies Coordinator, Saint Mary's University

List of Figures

List of Figures *(continued)*

List of Tables

Acknowledgements

I would like to thank my thesis supervisor, David Turner, for his continued support, valuable advice and assistance, for allowing me access to his unpublished data and research, and for the new knowledge and skills he taught me.

I would like also to thank Gary Welch for his helpful advice regarding the processing of CCD images and the use of the VISTA routines, as well as for providing me with his unpublished CCD observations of the field of SU Cyg and M92 standards and other data.

My thanks go also to Peter Stetson for allowing me to use his program DAOGROW, Tatsuhiko Hasegawa for his help with getting started with the PGPLOT program, Dave Lane for his assistance with photography and computer-related problems, as well as to faculty members and fellow graduate students who had helped me with advice on many occasions.

Finally, I want to thank my wife, Tomina, whose love, patience and understanding provided support and encouragement during my studies at Saint Mary's.

I gratefully acknowledge the financial support from research grants to Dr. David Turner and from Saint Mary's University scholarships.

Abstract

Photoelectric, photographic and CCD photometry, as well as spectroscopic observations and proper motion data for stars in the fields of the short-period galactic Cepheids V1726 Cygni and SU Cygni are presented and analyzed. The existence of a sparsely populated cluster associated with V1726 Cyg has been confirmed, and a new, loose stellar group has been found in the vicinity of SU Cyg.

The newly obtained distance modulus for C2128+488 (Anon. Platais), the cluster associated with V1726 Cyg, is $V_0 - M_V = 10.98 \pm 0.02$, corresponding to a distance of 1568 ± 13 pc. The spatial coincidence and the close match of the radial velocity, proper motion and age of V1726 Cyg with those of the cluster indicate a high probability of cluster membership for the Cepheid. The space reddening of V1726 Cyg, found from two neighbouring stars, is $E_{B-V} = 0.43 \pm 0.02$ and its luminosity as a cluster member is $\langle M_V \rangle = -3.42 \pm 0.07$. This value is close to that predicted from the PL relation under the assumption that V1726 Cyg is an overtone pulsator, an asumption which is strongly supported by the Fourier parameters of the Cepheid's light curve. It implies, however, an unrealistically small value for the colour term in the PLC relation; a more acceptable value for the colour term is obtained if V1726 Cyg is assumed to pulsate in the fundamental mode.

The newly found group of stars in the vicinity of SU Cyg has a distance modulus of $V_0 - M_V = 10.08 \pm 0.02$ (d = 1040 pc). It contains mostly early A to late F-type stars, with a few early B-type stars whose membership is more uncertain. The nature of this group is not entirely clear; it might be associated with the nearby association Vul OB4, which is at the same distance (Turner, unpublished), or represent a very sparse cluster, probably in its final stages of dissolution.

A reddening of $E_{B-V} = 0.16$ has been determined for SU Cyg from a nearby (20″) star having an accurate MK spectral type. While the Cepheid is spatially coincident with the stellar group, its absolute magnitude implied from possible membership is about $0\overset{m}{.}5$ brighter than that predicted from the PLC relation. This fact, together with the discrepancy between the observed colour of the cluster turnoff and the one expected for a Cepheid with the period of SU Cyg, indicates that the latter is merely projected by chance against the slightly more distant stellar group.

The probable discovery of a new planetary nebula, located about 3′ south of SU Cyg, and a possible new cluster 17′ west of SU Cyg, are also reported.

Introduction

It has been more than 300 years since Edward Piggot discovered the variability of the first Cepheid, η Aquilae. Cepheids remained ordinary variable stars until the turn of the 20th century, when Henrietta Leavitt found that the apparent magnitude of Cepheids in the Small Magellanic Cloud decreased with increasing period and discovered what we now know as the period-luminosity (PL) relation. Later, when the theory of stellar structure developed, it became clear that Cepheids, together with other pulsating stars, can provide valuable information about stellar interiors through pulsation theory. Being very luminous stars, Cepheids are invaluable in determining the extragalactic distance scale. They are easily detected in nearby galaxies and it is expected that with the Hubble Space Telescope it will be possible to observe Cepheids as far as the Virgo cluster of galaxies, thus contributing to the reliable determination of the Hubble constant H_0.

Much of the accuracy of the extragalactic distance scale depends, however, on the quality of the PL calibration. Around the late 1950s it was realized that Cepheids associated with open clusters can provide an independent and accurate calibration of the PL relation, facilitated by the development of the Johnson *UBV* system. Since then a number of projects have been initiated to derive reliable distances to galactic clusters associated with Cepheids (Schmidt 1984; Turner 1986; Caldwell and Coulson 1987; Gieren *et al.* 1994).

This study was suggested to the author by David Turner as a part of an on-going program to study in detail clusters associated with Cepheid variables (Turner 1986; Turner *et al.* 1992; Turner 1992; Turner *et al.* 1994). It presents and analyzes the observational data for two fields surrounding the Cepheids V1726 Cygni and SU Cygni. Both regions do not include any obvious clusters, although the existence of a very sparse cluster near V1726 Cyg has been suggested and subsequently rejected by the discoverer of V1726 Cyg

(Platais 1979; Platais 1986). It was not until the paper by Turner *et al.* (1994) that the reality of the cluster was confirmed. There is no known cluster near SU Cyg; one of the goals of this investigation is to check the suggestion (Turner, private communication) that the few relatively bright stars surrounding the Cepheid might be the more luminous members of a loose, but physically related group of stars associated with SU Cyg.

The study is separated into two parts; the first one is devoted to V1726 Cyg and the nearby cluster C2128+488 (Anon. Platais), and the second part presents the results for the field of SU Cyg.

Part 1. V1726 Cygni and the field of C2128+488 (Anon. Platais)

1.1 Introduction

The variability of V1726 Cyg = BD +48° 3398 was discovered by Platais (1979) during his study of the field of the nearby open cluster M39 in Cygnus. He classified it as a Cepheid variable with low amplitude and a sinusoidal light curve and determined a period of 4.24 days. Platais also pointed to the presence of a sparse cluster of faint stars about 4′ to the east of the Cepheid and showed that the distance to the cluster, as determined from photographic photometry and proper motion studies, was consistent with a possible membership for V1726 Cyg. In a later study of the same cluster Platais (1986) concluded that its existence is not well established, since, in his opinion, the additional photometric and proper motion data gave little evidence that the apparent cluster is something more than a random enhancement of the local star density.

The low amplitude and the sinusoidal light curve of V1726 Cyg (Platais and Shugarov 1981, Berdnikov 1986) make it a good candidate for an overtone pulsator. Given the controversy still surrounding such stars and the fact that there are only a few other known or suspected cluster overtone pulsators (Antonello and Poretti 1986, Antonello *et al.* 1990*a*, Turner 1992; Turner, private communication), the study of the reality of the cluster and its possible association with V1726 Cyg becomes even more interesting.

The reality of the cluster was demonstrated in a recent study by Turner *et al.* (1994) which incorporated, among other data, star counts and radial velocity measurements for several stars in the field. The purpose of the present investigation is to derive an accurate distance modulus for the cluster and to study the question of the membership of V1726 Cyg. Section 2 describes the observational data and reductions, Section 3 presents the analysis of the results, Section 4 is devoted to the properties of the Cepheid V1726 Cyg, and Section 5 presents the conclusions.

1.2 Observational Data and Reductions

1.2.1 Photoelectric photometry

The first photoelectric *UBV* observations for 31 stars in the field of C2128+488 have been published recently by Turner *et al.* (1994). These data are listed in Table 1, where the first two columns identify the stars numbered according to Turner *et al.* (1994) and Platais (1986), respectively, columns 3 to 5 give the photometry, column 6 gives the number of nights on which each star was observed, and the last column lists spectral types from Turner *et al.* (1994) and Platais (1986, 1988) as well as other remarks. Uncertain or very uncertain values are marked by a colon or a double colon, respectively.

These photoelectrically observed stars formed the calibration sequence necessary to tie the photographic measurements to the standard Johnson *UBV* system. Figure 1 shows the finder chart for the field, where the photoelectric standards are the stars numbered 1–31, and the remaining stars (101–220) are those measured photographically. This finder chart was generated by a computer using the rectangular coordinates from the catalogue of Platais (1994). For a more realistic view of the field, one may wish to look at Figure 2, which gives a reproduction of a *B* plate on a scale about twice the original.

1.2.2 Photographic photometry

Ideally, one would like to have photoelectric observations for most of the stars in the field being studied. It is often impossible to achieve this, however, given the need

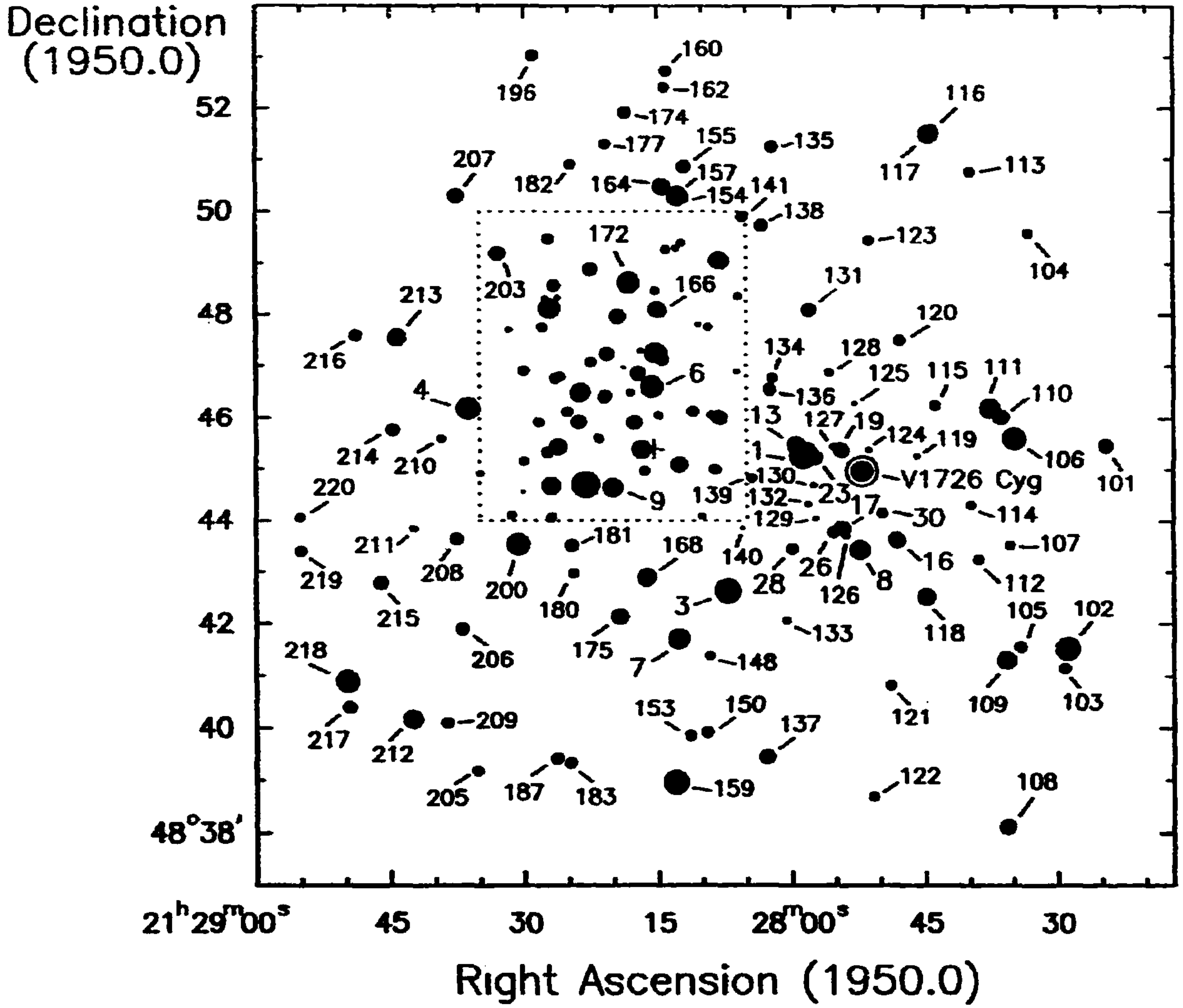

Figure 1a. A finder chart for the field of C2128+488. The photoelectric standards are numbered 1–31; stars 101–220 are those measured photographically. The crowded central region is shown in more detail in Figure 1*b*.

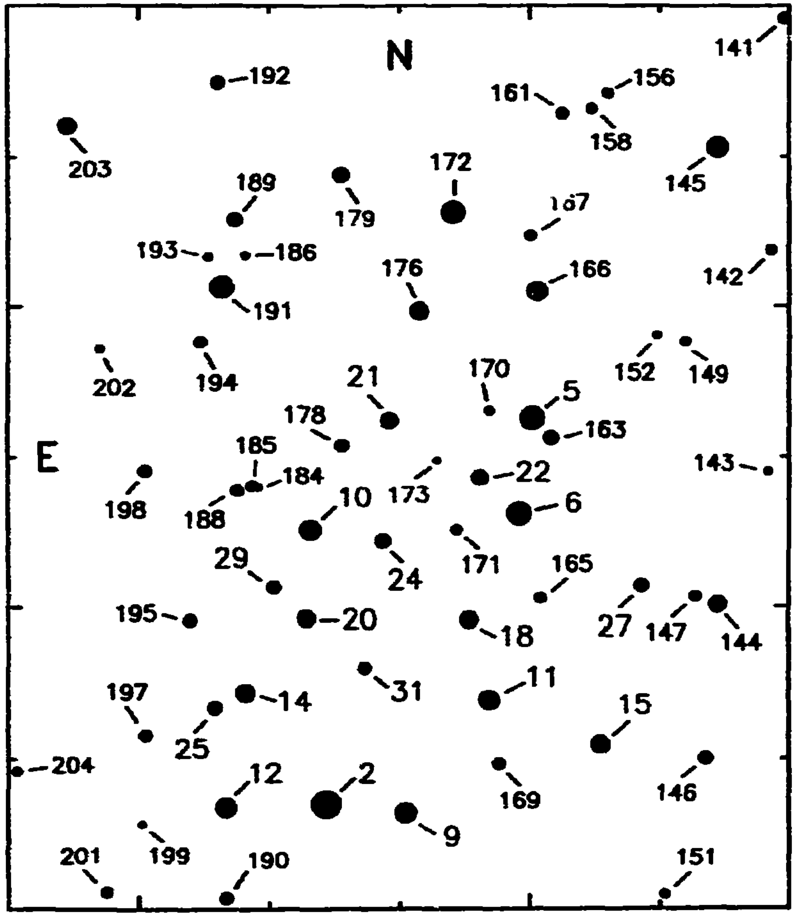

Figure 1*b*. A finder chart for the central region of C2128+488. The photoelectric standards are numbered 1–31; stars 101–220 are those measured photographically.

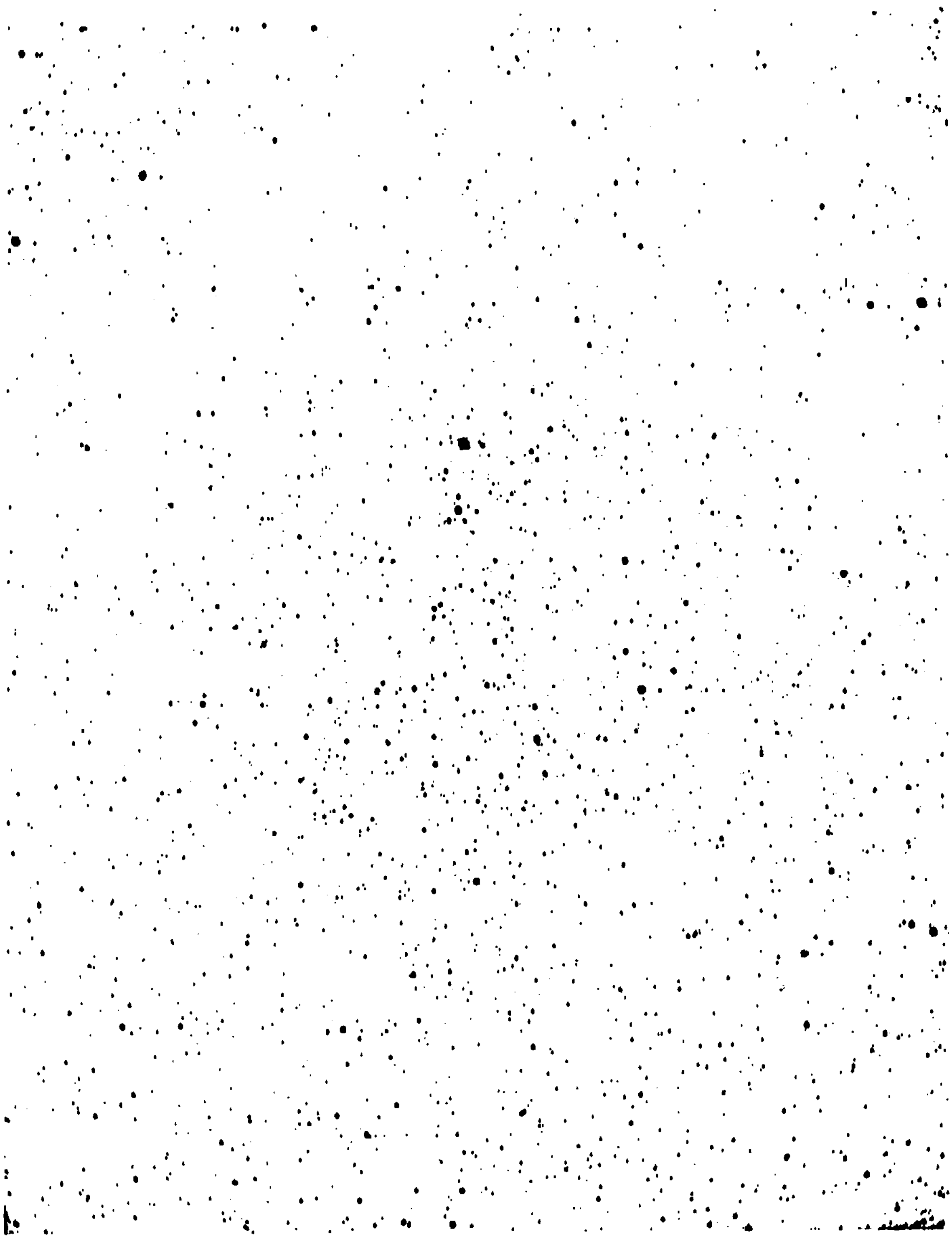

Figure 2. An overview of the region of C2128+488, reproduced from a B plate of the field. V1726 Cyg is the brightest object on this picture; the faintest visible stars have $B \approx 20$. West is up and north is to the left.

Table 1. Photoelectrically observed stars in the field of C2128+488

Star	Platais	V	B–V	U–B	n	Remarks
V1726 Cyg	1821	9.00	+0.90	+0.61	16	F6 Ib
1	1921	11.15	+0.30	+0.19	6	B9 III (pec., shell)
2	2322	11.20	+0.48	–0.10	4	F8 IV[a]
3	2053	11.62	+0.64	+0.15	1	G0:[a]
4	2551	12.00	+0.84	+0.64	1	F0:[a]
5	2197	12.29	+0.28	–0.08	4	B7 Vn
6	2206	12.34	+1.15	+0.95	4	
7	2146	12.58	+1.72	+1.89	1	
8	1826	12.80	+0.63	+0.20	5	
9	2274	12.88	+0.45	+0.42	5	A3 V
10	2333	12.98	+0.37	+0.28	4	A0 V
11	2227	12.99	+0.86	+0.50	4	
12	2399	13.06	+0.24	–0.24	4	B6 Vnn
13	1927	13.32	+0.58	+0.33	4	A7: V
14	2379	13.35	+0.68	+0.21	4	
15	2143	13.45	+0.39	+0.22	4	B9.5 IVn
16	1761	13.46	+0.91	+0.49	6	
17	1852	13.49	+0.72	+0.32	5	
18	2237	13.72	+1.86	+1.84::	3	
19	1859	13.75	+0.40	+0.28	4	
20	2343	13.78	+1.31	+1.00	3	
21	2287	13.83	+1.01	+0.24	3	
22	2233	13.89	+1.78	+1.28	2	double
23	1899	14.15	+0.65	+0.31	6	
24	2295	14.17	+0.48	+0.40	3	
25	2406	14.44	+1.09	+0.95	1	
26	1874	14.47	+0.58	+0.29	6	
27	---	14.50	+1.46	+1.16::	3	
28	---	14.55	+1.94	+2.12:	2	
29	---	14.61	+1.32	+1.35	1	
30	1783	14.71	+0.45	+0.32	2	
31	---	14.91	+1.46	+1.01	2	

[a] According to Platais (1984)

to measure a hundred or more stars, most of them rather faint. Photographic photometry, when done carefully, is capable of providing high-quality photometric data and as several authors have shown (*e.g.* Turner and Welch 1989, Turner *et al.* 1993), it is possible to obtain intrinsic accuracy of the order of $\pm 0^{m}.03$ for the instrumental magnitudes of most measured stars.

The photographic plates used in this study were obtained by Barry Madore on the night of 1981 September 28/29 at the prime focus of the 3.6-m Canada-France-Hawaii Telescope. A total of six plates, two in each of the U, B and V bandpasses were used. The plate information is summarized in Table 2.

Table 2. Plate information for the field of C2128+488

	Plate No.	Exposure Time	Emulsion	Filter	Comments
V	A-1578	7.5^{m}	IIa-D	GG495	Cirrus
	A-1579	5.0^{m}	IIa-D	GG495	Cirrus; Not used
B	A-1580	5.0^{m}	IIa-O	GG385	Cirrus
	A-1581	5.0^{m}	IIa-O	GG385	Cirrus
U	A-1582	10.0^{m}	IIa-O	UG1	Cirrus
	A-1583	10.0^{m}	IIa-O	UG1	Cirrus

All plates were measured with the Saint Mary's University Astro-Mechanics A01 iris photometer. The measuring procedure followed closely that described by Turner and Welch (1989). First each plate was examined for obvious guiding errors, background non-uniformity or other flaws. None were found on all six plates. The wedge setting for the reference beam was set to zero, and neutral-density filters were used in the main beam in order to be able to sample a wider sky annulus around the star, so that the toe of the stellar image lies within the diaphragm. This is a necessary condition to obtain a linear relation between the square of the iris reading, I^2, and the magnitude (Schaefer 1981, Turner and Welch 1989).

An actual measurement consisted of null-meter centring the stellar image and after that taking the iris reading. This technique ensures consistent and reliable centering of the stellar image, leading to higher internal accuracy and reduced scatter around the calibration curve. Each photoelectric standard was measured twice, at the start and at the end of the measuring session, in order to minimize the influence of changing sensitivity. The values of the iris readings for a given standard star were very nearly the same, with differences around 1–2 iris units, which shows the excellent stability of the iris photometer over the measuring period.

All plates were exposed with a Racine-Pickering prism in the optical path in order to obtain secondary images for the brighter stars; these images can be used to extend the photoelectric calibrating sequence to fainter stars. Unfortunately, there was no overlap between the magnitude ranges of the primary and secondary images, and only a few secondary images could be fitted by the extrapolated relation for the primary standards. This left the exact magnitude difference between the primary and secondary images difficult to determine using only these plates. Turner *et al.* (1994) derived $\Delta V = 4.59$, $\Delta B = 4.61$ and $\Delta U = 4.62$ for the field of NGC 7790. These offsets were found to give very consistent results for the secondary images in the V1726 Cyg field and are the values used in this study.

The calibration curves for the six plates are shown in Figures 3, 4 and 5. The data for the primary and secondary images are shown by filled and open circles, respectively. With the measuring technique described above, one would expect a linear relation between I^2 and magnitude. In this case, however, it turned out that the linear relation was between I^4 and magnitude (similar to that found by Turner *et al.* 1986 for the S Vul field):

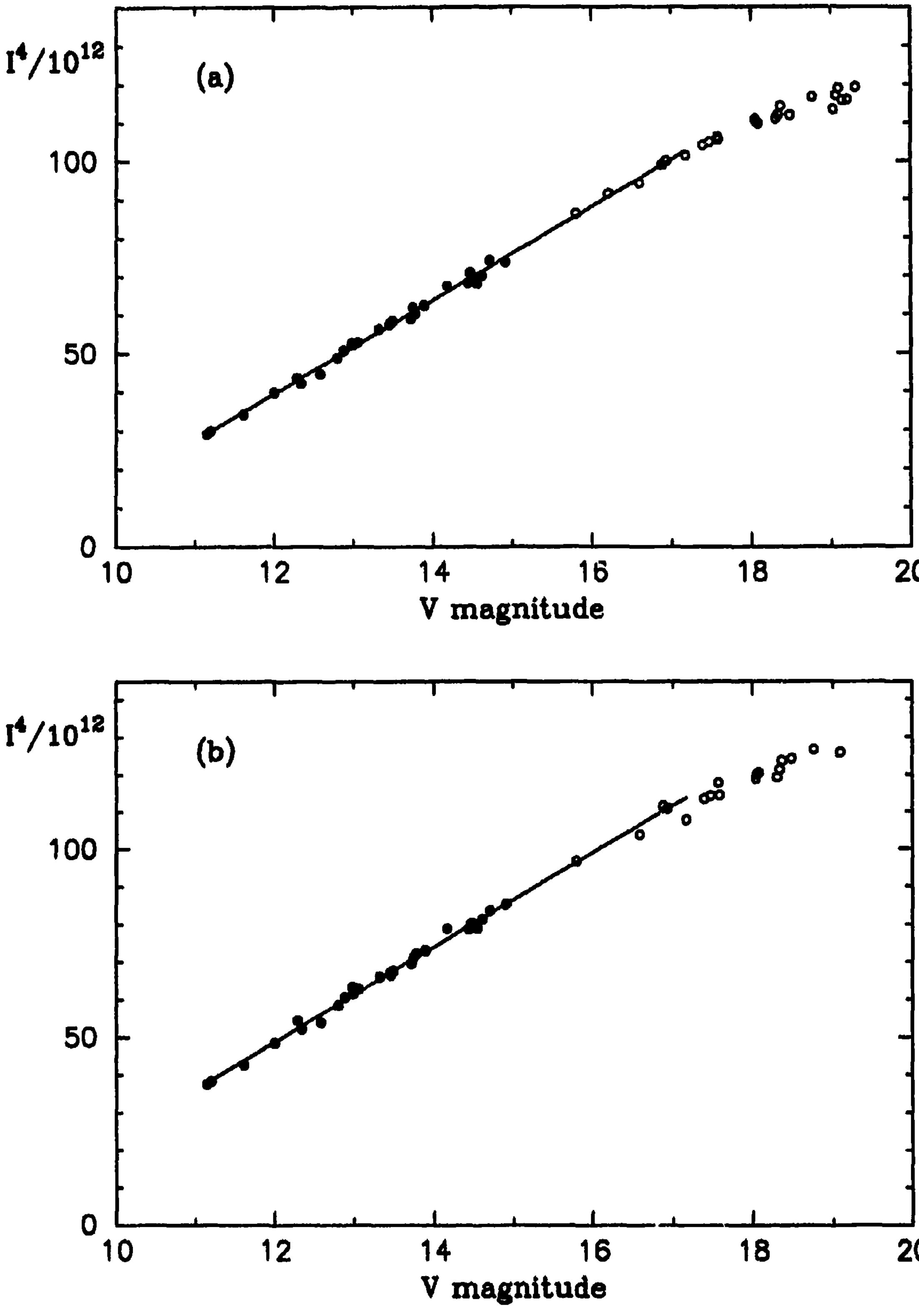

Figure 3. Calibration relations for the *V* plates. *(a)* First *V* plate, *(b)* second *V* plate.

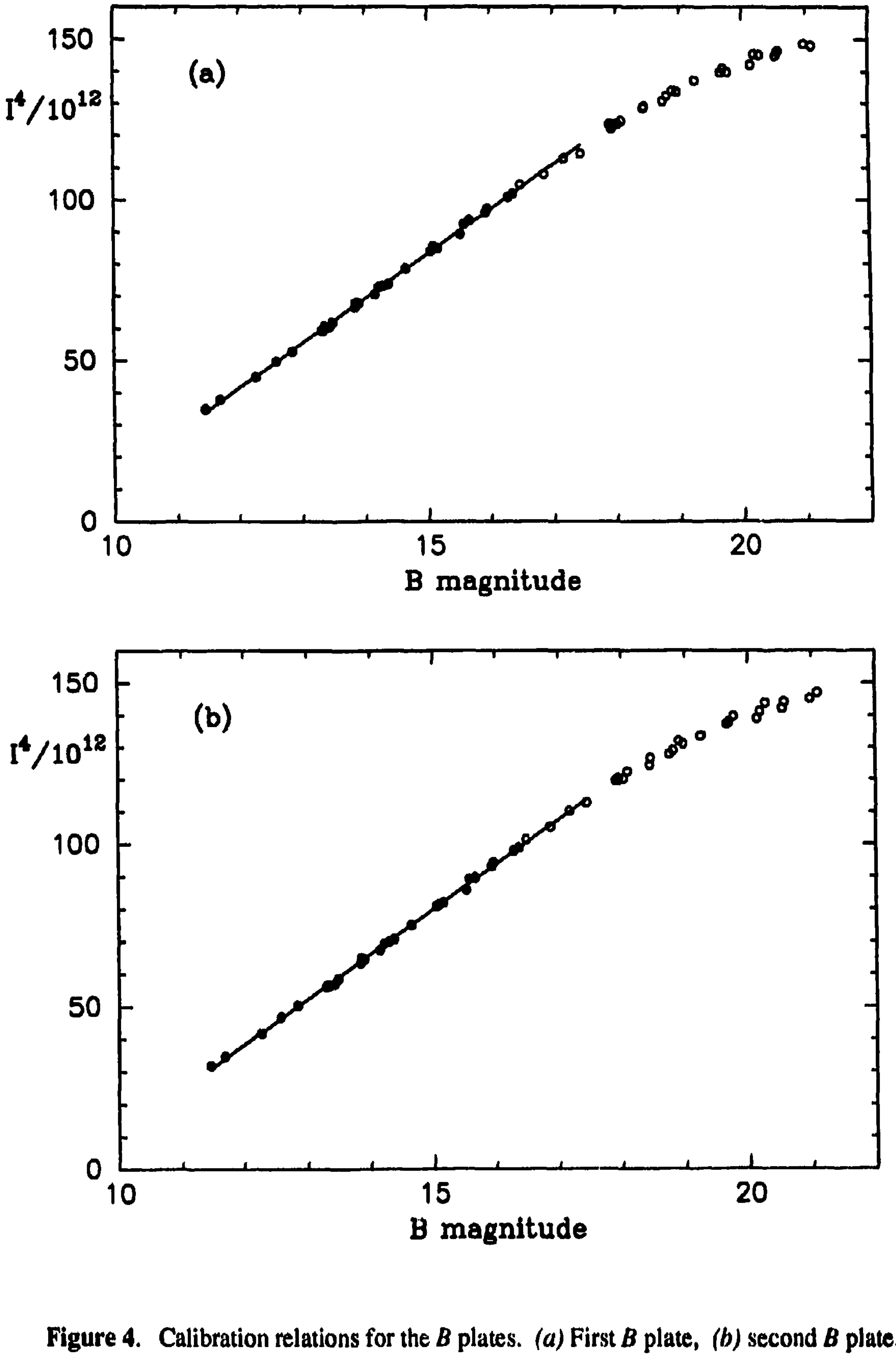

Figure 4. Calibration relations for the *B* plates. *(a)* First *B* plate, *(b)* second *B* plate.

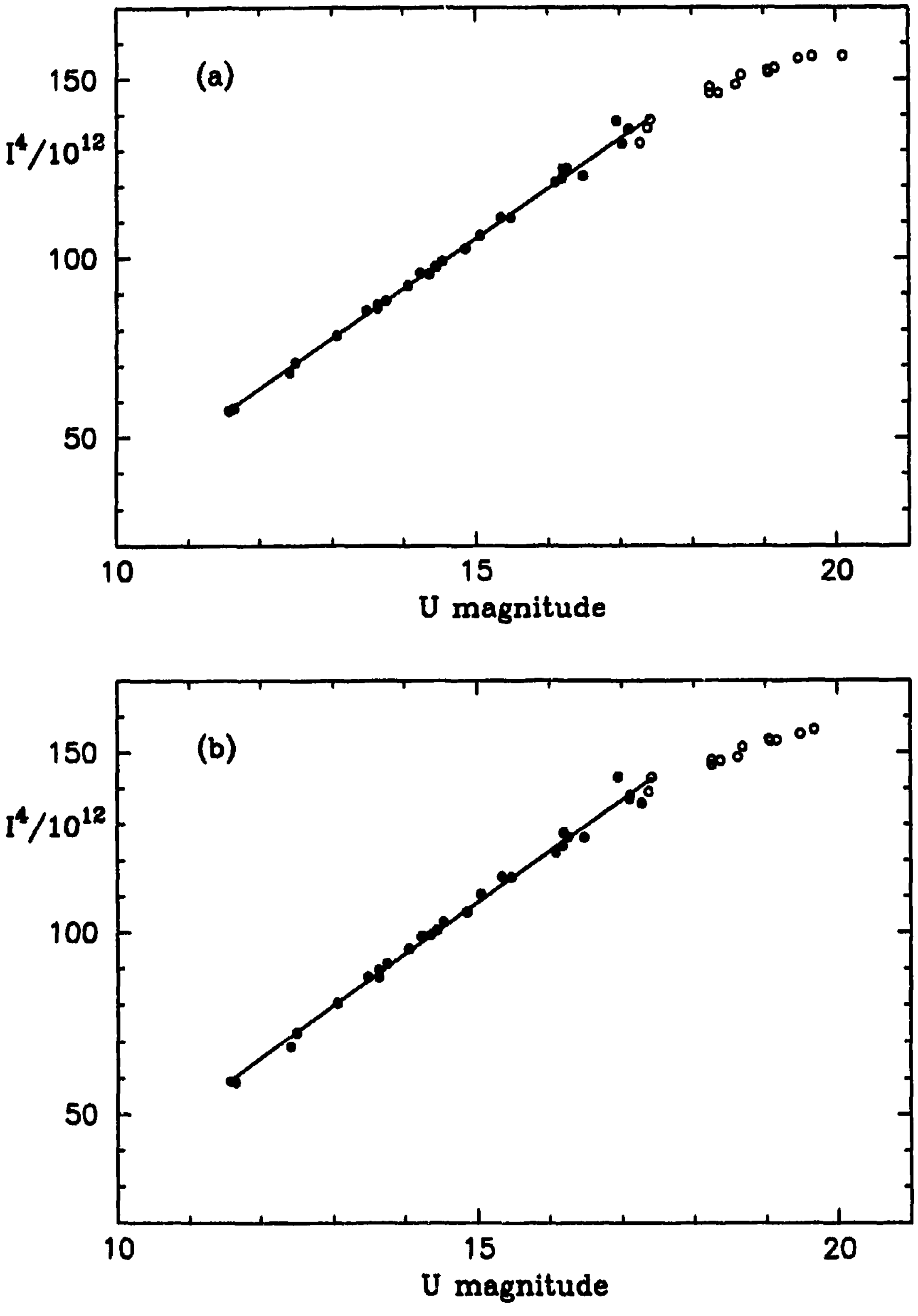

Figure 5. Calibration relations for the *U* plates. (a) First *U* plate, (b) second *U* plate.

$$v = a_1 + b_1 I^4,$$
$$b = a_2 + b_2 I^4,$$
$$u = a_3 + b_3 I^4,$$

where v, b and u are the instrumental visual, blue and ultraviolet magnitudes, I is the iris reading, and the coefficients a_1, b_1, ... were determined by a least squares fit. As can be seen from the figures with the calibration curves, such a linear relation extends over six magnitudes. The straight line in each figure represents the best-fitting line for the given plate. It is plotted approximately to the magnitude limit beyond which the linear relation is no longer valid. Although it is possible in principle to fit shorter line segments to the faint secondary images, it is clear that because of the lower quality of those measurements not much new information will be gained. For various reasons, most often due to duplicity, a few photoelectric standards were not included in the calibrations, and several others were rejected because of large residuals from the fitting line. Figure 6 shows plots of the residuals versus the appropriate magnitude for all six plates. From this plot, and also from Figures 3–5, it is evident that the calibration relations for the B plates are very tight, even for the faint secondary images, whereas the V and U plates exhibit larger scatter. Therefore, in later reductions the b instrumental magnitudes for the program stars, as derived from the relations in Figure 4, were averaged and taken as a basis for judging the quality of the $B-V$ and $U-B$ colours.

Since each plate was measured twice, there were two calibration relations for each plate and correspondingly, four sets of instrumental magnitudes in each bandpass. This allowed us to estimate the quality of the calibrations from the dispersion around the mean magnitude for each star. The results from the V plates exhibited a larger scatter than the B and U plates, and there was a considerable difference between the instrumental magnitudes from the two V plates. Having only two plates, it was difficult to decide which one causes the peculiar results. The appearance of the colour equations, as well as the careful visual

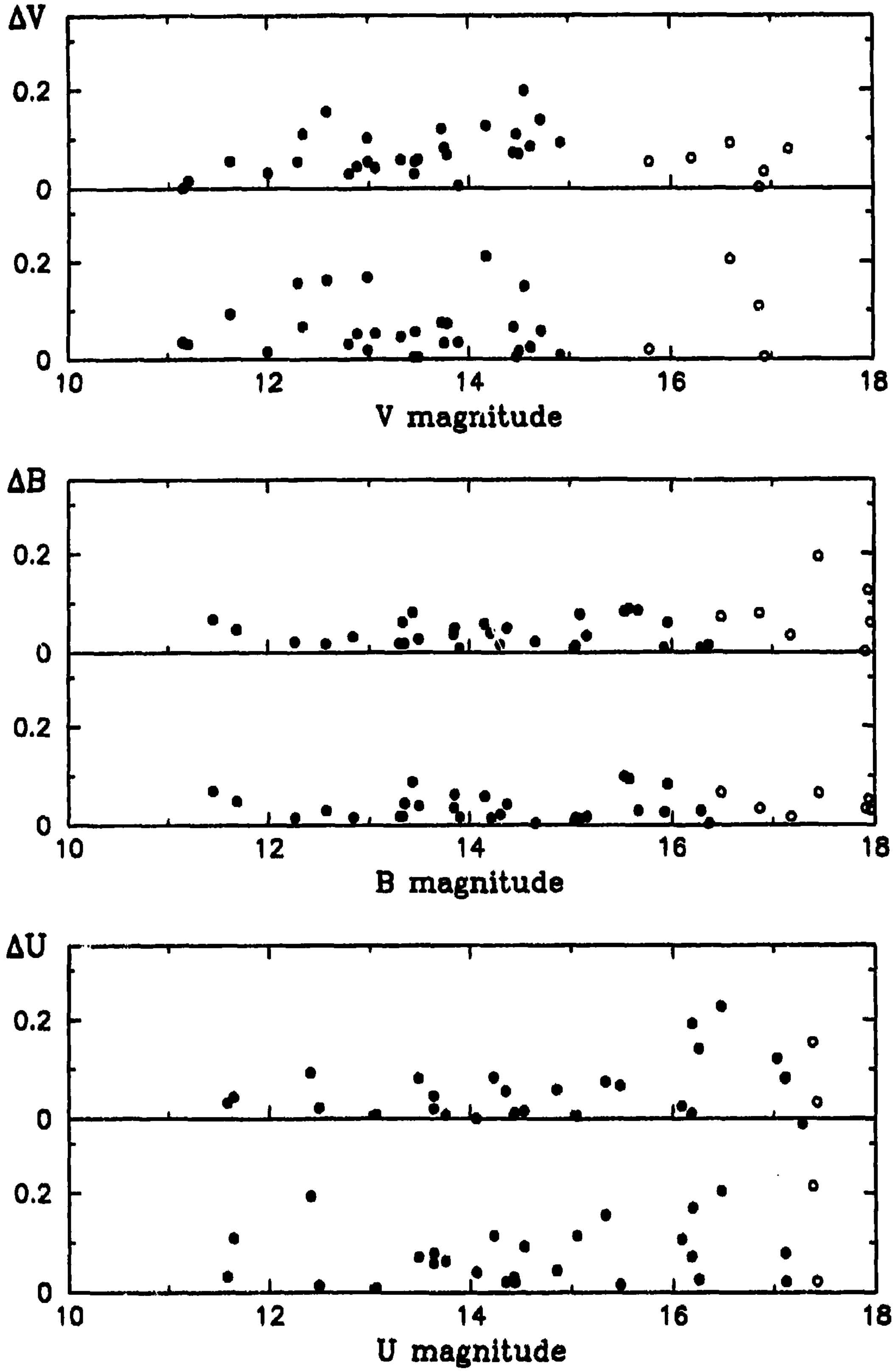

Figure 6. Residuals from the calibration lines for the *V*, *B* and *U* plates. The upper half of each panel shows the residuals for the first plate and the lower half for the second plate in the corresponding bandpass.

inspection of the plates indicated that the second V plate (No. A-1579) should be excluded from the analysis. The reasons for the anomalous data from this plate are not entirely clear, and might include improper fixing (there were noticeable traces of the plate backing), plate–filter mismatch (Turner, private communication), temporary change in the cirrus uniformity, or some other factors. Whatever the true explanation, there is no evidence that the rejection of this plate diminished the overall quality of the photographic photometry.

The transformation to the Johnson UBV system was done using equations which included only the colour terms. This is permissible because the area of the studied field is small, and in their simplest form the equations can be written as:

$$V - v = c_1 + d_1(b - v) \tag{1}$$

$$B - V = c_2 + d_2(b - v) \tag{2}$$

$$U - B = c_3 + d_3(u - b) \tag{3}$$

where v, b and u denote the instrumental magnitudes in the corresponding bandpasses, and V, B and U denote the standard Johnson magnitudes. The coefficients c_1, d_1, ... can be determined by means of least squares fits. As mentioned earlier, the two sets of b instrumental magnitudes derived from the two B plates were in excellent agreement and were averaged to yield a single b magnitude for the given star. This magnitude can be combined with either of the two sets of v or u magnitudes to produce two sets of $b - v$ indices and two sets of $u - b$ indices, as well as two sets of differences $V - v$, all of which can be used in the colour equations. These six relations are plotted in Figures 7–9, where panels (a) show the data for the first plate, and panels (b) for the second plate as explained above. The best linear least squares fits to the transformation equations (1) – (3) are shown by straight lines and tabulated in Table 3. Open circles mark points that were

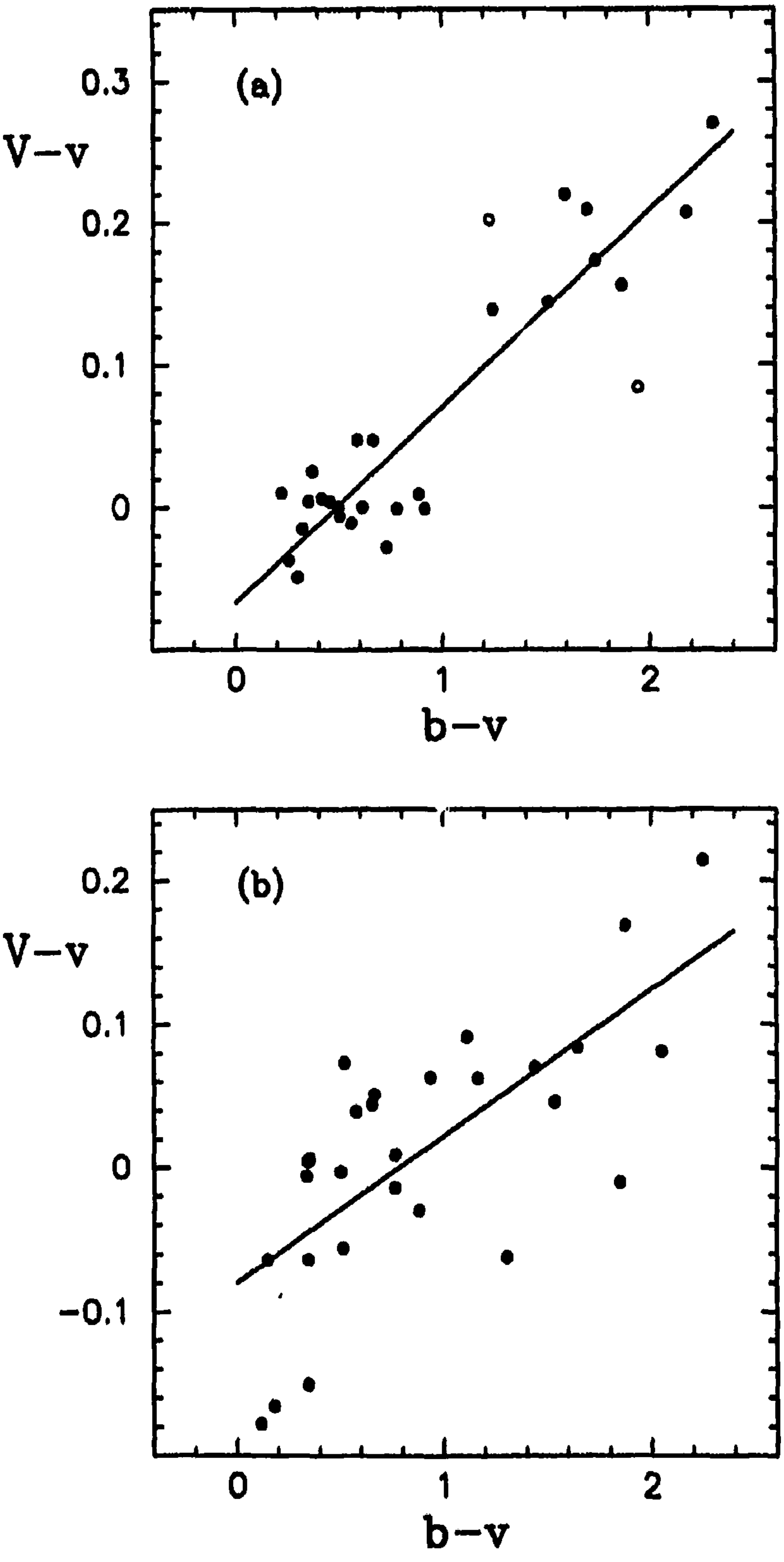

Figure 7. Plot of $V-v$ versus $b-v$ for the *(a)* first and *(b)* second V plates.

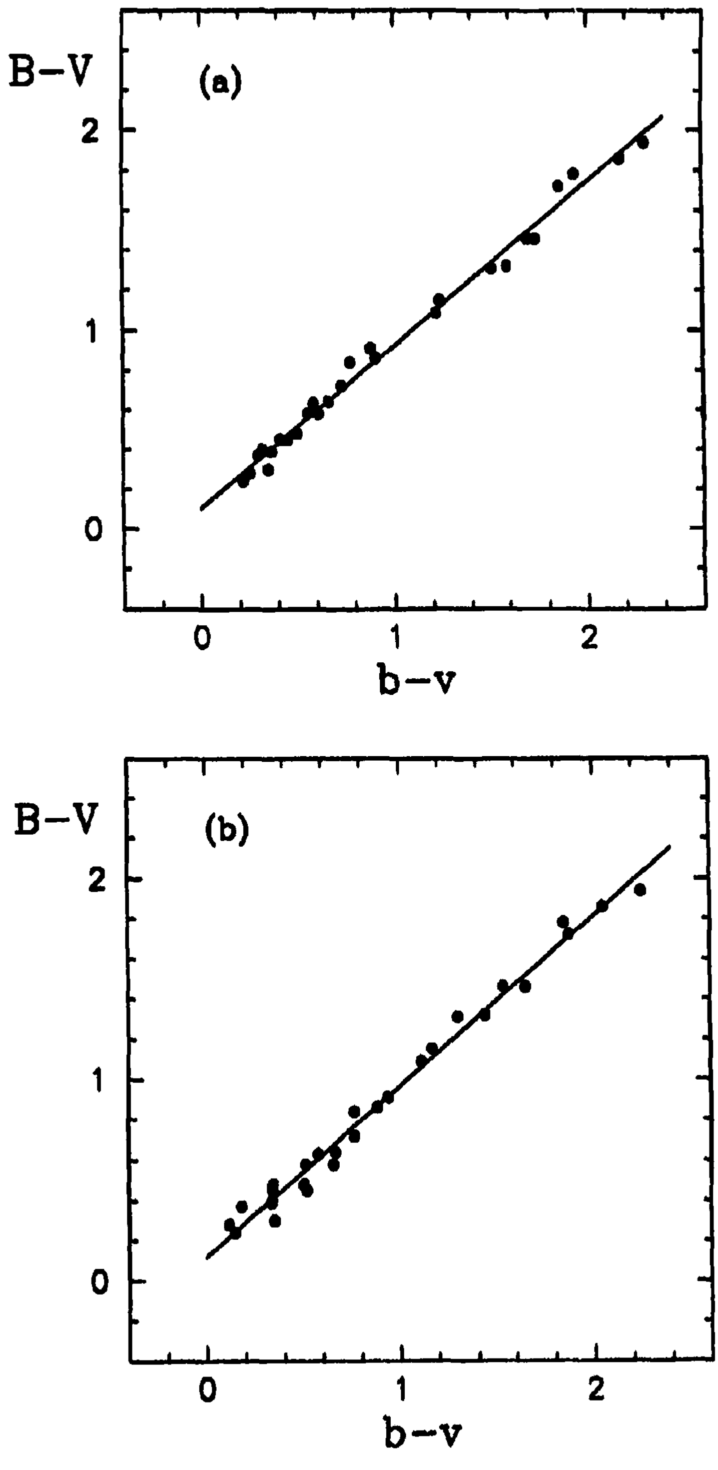

Figure 8. Plot of $B-V$ versus $b-v$ for the *(a)* first and *(b)* second V plates.

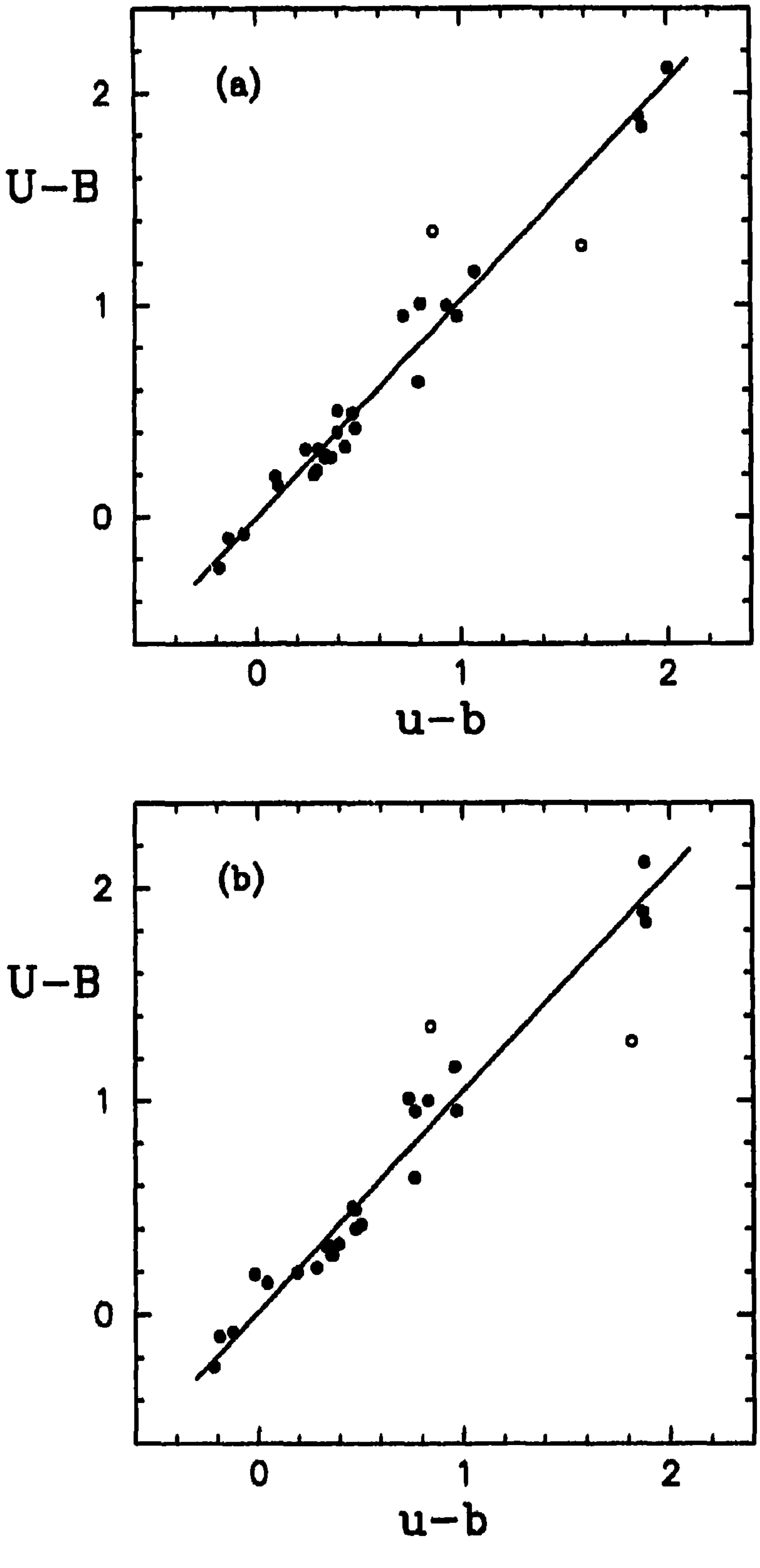

Figure 9. Plot of $U-B$ versus $u-b$ for the *(a)* first and *(b)* second U plates.

rejected because of their large deviation from the fit. As can be seen in Figure 7b, the $(V-v)$ vs. $(b-v)$ plot for the second V plate has a rather anomalous appearance and was one of the reasons for rejecting this plate. The $(B-V)$ vs. $(b-v)$ relations (Figure 8) are quite tight, with the second one having somewhat large dispersion, due to the fact that the instrumental colour index $b-v$ was formed using the v magnitudes from the second V plate. The slopes of the $U-B$ relations are very close to unity, indicating a good match to the Johnson UBV system for the B and U plates. That is not the case for the $B-V$ relations, however, most likely because the V plates do not provide a good match to the Johnson system.

Table 3. Coefficients for the transformation equations (1) – (3)

Equation	Plate	$c_i \pm 1\sigma$	$d_i \pm 1\sigma$	Remarks
(1)	1	−0.067 ± 0.012	+0.138 ± 0.011	
	2	−0.080 ± 0.022	+0.102 ± 0.020	Not used
(2)	1	+0.103 ± 0.018	+0.818 ± 0.015	
	2	+0.121 ± 0.021	+0.846 ± 0.019	Not used
(3)	1	−0.003 ± 0.026	+1.030 ± 0.032	
	2	+0.014 ± 0.032	+1.032 ± 0.040	

With all coefficients for the colour equations known, it is straightforward to calculate the photographic UBV magnitudes for the program stars. The data are listed in Table 4 and the star numbers correspond to those in the finder chart (Figure 1). Many of our program stars have been observed photographically by Platais (1986, 1994). However, Turner *et al.* (1994) have found magnitude-dependent trends in Platais' UBV photometry, in addition to small systematic offsets from the Johnson system. This limits the usefulness of his data somewhat and only the magnitudes and colours derived in the

Table 4. *UBV* photographic photometry for the program stars in C2128+488

Star	Platais	V	B–V	U–B	Star	Platais	V	B–V	U–B	Star	Platais	V	B–V	U–B
101	1410	13.92	0.75	0.40	141	---	14.66	1.33	0.68	181	2356	14.14	0.88	0.37
102	1456	12.00	1.95	2.25	142	2027	15.24	0.58	0.33	182	2357	14.73	0.55	0.28
103	1460	14.56	1.01	0.54	143	---	15.71	0.54	–0.13	183	2361	14.49	0.53	0.35
104	1521	14.88	0.60	–0.01	144	2068	13.61	0.34	0.37	184	---	15.77	0.86	–0.02
105	1534	14.53	0.95	0.32	145	2069	12.82	0.62	0.38	185	---	14.97	0.90	0.19
106	1543	12.15	1.55	1.78	146	2079	14.52	0.63	0.40	186	---	15.71	0.96	0.02
107	---	14.92	0.75	0.42	147	---	14.99	1.25	0.64	187	2385	14.26	0.87	0.27
108	1565	13.60	0.76	0.45	148	2095	14.97	0.73	0.29	188	2389	14.78	0.58	0.29
109	1567	13.03	0.50	0.05	149	---	15.24	1.00	0.19	189	2390	14.31	0.80	0.17
110	1580	13.49	0.58	0.49	150	2101	14.52	0.55	0.37	190	2398	14.72	0.84	0.32
111	1600	12.54	0.35	–0.03	151	---	15.44	0.93	0.08	191	2402	12.43	1.95	2.17
112	1621	14.59	0.72	0.53	152	---	15.70	1.03	0.03	192	2404	14.58	0.62	0.39
113	1639	14.72	0.63	0.36	153	2129	14.62	0.54	0.40	193	---	15.68	0.86	0.18
114	1640	15.00	0.67	0.36	154	2135	15.12	0.78	0.12	194	2418	14.89	0.72	0.39
115	1704	14.64	0.75	0.56	155	2136	14.07	0.85	0.29	195	2423	14.74	0.83	0.17
116	1706	14.63	0.67	0.36	156	2139	15.23	0.80	–0.29	196	---	14.22	0.79	0.30
117	1713	12.77	0.48	–0.12	157	2150	12.63	0.59	0.38	197	2448	14.92	0.63	0.33
118	1723	13.20	0.74	0.32	158	2153	15.27	0.77	0.20	198	2449	14.71	0.63	0.24
119	---	15.57	0.79	0.05	159	2155	11.82	0.37	0.29	199	---	16.01	0.82	0.05
120	1757	14.57	0.64	0.48	160	2169	14.48	0.92	0.10	200	2466	12.13	1.47	1.78
121	1771	14.86	0.91	0.32	161	2170	14.93	0.79	0.26	201	2478	15.03	0.84	0.14
122	---	14.85	1.31	0.46	162	2174	14.75	0.82	0.06	202	---	15.68	0.86	0.00
123	1808	14.83	0.71	0.56	163	2180	14.22	0.48	0.40	203	2500	13.65	0.41	0.28
124	---	15.67	0.87	0.05	164	2181	13.25	0.88	0.31	204	---	15.45	0.77	0.35
125	---	15.86	0.94	0.04	165	2192	15.06	0.63	0.35	205	2538	14.74	0.87	0.07
126	---	15.46	1.11	0.17	166	2194	13.14	0.75	0.21	206	2566	14.26	0.72	–0.18
127	---	15.63	0.90	0.10	167	2199	15.11	0.74	0.24	207	2577	13.71	1.52	1.52
128	1882	15.17	0.77	0.25	168	2217	13.10	0.62	0.40	208	2579	14.24	0.54	0.42
129	---	15.69	0.94	0.08	169	2224	14.77	0.72	0.36	209	2601	14.48	0.66	0.28
130	---	15.60	1.02	0.09	170	---	15.56	0.97	0.10	210	2609	15.17	0.74	0.38
131	1912	13.82	0.65	0.36	171	2246	15.28	0.92	–0.10	211	2656	15.32	0.70	0.29
132	---	15.57	0.91	0.13	172	2247	12.41	1.45	1.65	212	2660	12.87	0.31	–0.16
133	1943	15.15	0.67	0.36	173	---	16.10	0.90	–0.05	213	2689	13.20	0.51	0.54
134	1967	14.92	0.75	0.42	174	2251	14.27	0.45	0.28	214	2699	14.13	0.79	0.28
135	1969	14.34	0.67	0.35	175	2261	13.35	0.52	0.39	215	2729	14.02	0.72	0.33
136	1974	14.29	0.59	0.37	176	2267	13.60	0.80	0.25	216	2778	14.45	0.97	0.28
137	1978	13.62	0.77	0.49	177	2292	14.80	0.80	0.12	217	2789	14.14	0.99	0.43
138	1989	14.21	0.57	0.34	178	2315	14.62	0.57	0.38	218	2792	12.27	0.64	0.04
139	2003	14.92	0.61	0.35	179	2316	13.98	0.94	0.35	219	2867	14.52	1.18	0.25
140	---	16.00	0.79	0.05	180	2354	14.80	1.01	0.34	220	2871	14.84	0.95	0.27

present study are used. For reference purposes we also give in Table 4 the star numbers from the Platais' (1986, 1994) catalogue of the field of M39.

The number of stars measured initially was greater than those listed in Table 4. Some of them, however, did not have reliable measurements in all bandpasses, such as many faint red stars which were on or below the plate limit in B and U, or others which turned out to be close doubles. In order to get the best results, the final analysis was restricted to stars brighter than ~16th magnitude in V and ~17th magnitude in B and U, and within ~8′ of the cluster centre, which are the stars given in Table 4.

The formal uncertainties in the magnitudes and colours were estimated from measurements for the standard stars: ±0.03 in V, ±0.03 in $B-V$ and ±0.06 in $U-B$, with somewhat larger uncertainties for stars fainter than ~15th magnitude. From these errors, as well as from the general appearance of the calibration curves and colour relations, we can conclude that the overall quality of the photographic photometry is very good and is comparable to the high-quality data obtained in a similar study of the field of WZ Sgr (Turner *et al.* 1993).

1.2.3 Radial velocity data

Spectroscopic observations for V1726 Cyg and seven other stars in the field of C2128+488 have been published by Turner *et al.* (1994). Spectral classifications provide independent information on the luminosity of cluster stars, and radial velocity data are very useful for assigning membership probabilities. Table 5, adopted from Turner *et al.* (1994), lists the heliocentric radial velocities for all eight stars. We discuss the radial velocity observations for V1726 Cyg in more detail later in Section 4.

Table 5. Radial velocities for C2128+488 stars

Star	V_R (km s^{-1})
V1726 Cyg	−15.1
1	−15.1
5	−15.4
9	−30.1 [a]
10	−16.1
12	+5.4 [a]
13	+38.9 [a]
15	+14.5 [a]
Cluster mean = −15.4 ± 0.2 km s^{-1}	

[a] Rejected from the mean as a likely non-member

1.3 Analysis

1.3.1 Interstellar Reddening

It is well known that in the optical region interstellar extinction depends on wavelength approximately as λ^{-1} (*e.g.* Krelowski and Papaj 1993) and therefore the term "reddening" is often used as a synonym for absorption. The quality of the derived cluster parameters depends very much on how carefully interstellar extinction has been taken into account. Reddening is often measured by the colour excess

$$E_{B-V} = A_B - A_V = (B-V) - (B-V)_0,$$

where A_V and A_B denote the total absorption in the V and B bandpasses, respectively. The quantities $(B-V)$ and $(B-V)_0$ are respectively the observed (reddened) and intrinsic (dereddened) values for the colour index $B-V$.

A very important characteristic of the extinction in a given region of the sky is the reddening line for that region, expressed by the relation

$$E_{U-B}/E_{B-V} = X + YE_{B-V},$$

where E_{U-B} is defined in the same way as E_{B-V}, X is the slope of the reddening line and Y is the so-called curvature term. In an extensive study FitzGerald (1970) found $X = 0.70$ and $Y = 0.05$ for the entire sky except Cygnus, where X was found to be 0.75. However, Turner (1989) showed that the slope terms differ significantly from one sky region to another and questioned the use of a mean galactic reddening relation to deredden individual stars. He found values for X ranging from 0.62 to 0.80, but very similar curvature terms, with a mean $\langle Y \rangle = 0.02$. Therefore, it is important to use an individual reddening relation appropriate for the region being studied and not rely on "mean" values.

The slope of the reddening line for the field of C2128+488 was determined by Turner *et al.* (1994) from seven spectroscopically observed B and A-type stars (see Table 1). They found $E_{U-B}/E_{B-V} = 0.81 \pm 0.06$, the same as that obtained by Turner (1976) for early-type stars in nearby fields containing the clusters NGC 7062 and NGC 7067. Thus, we adopted a reddening slope of $E_{U-B}/E_{B-V} = 0.81$ for the purpose of dereddening the program stars and assumed a zero curvature term, which is justified by the small range of colour excesses found for this region (see Figure 12).

The colour–colour diagram for the field of C2128+488 is shown in Figure 10, where photoelectrically observed stars (Table 1) are marked by filled circles and stars having only photographic photometry (Table 4) are marked by open circles. The solid curve is the intrinsic relation for main-sequence stars of solar metallicity (Turner, private communication). There seem to be no unreddened early-type stars, and several B stars define the average reddening of $E_{B-V} \approx 0.39$ for cluster members. One can also notice many A and F-type stars reddened roughly by the same amount, as well as a few

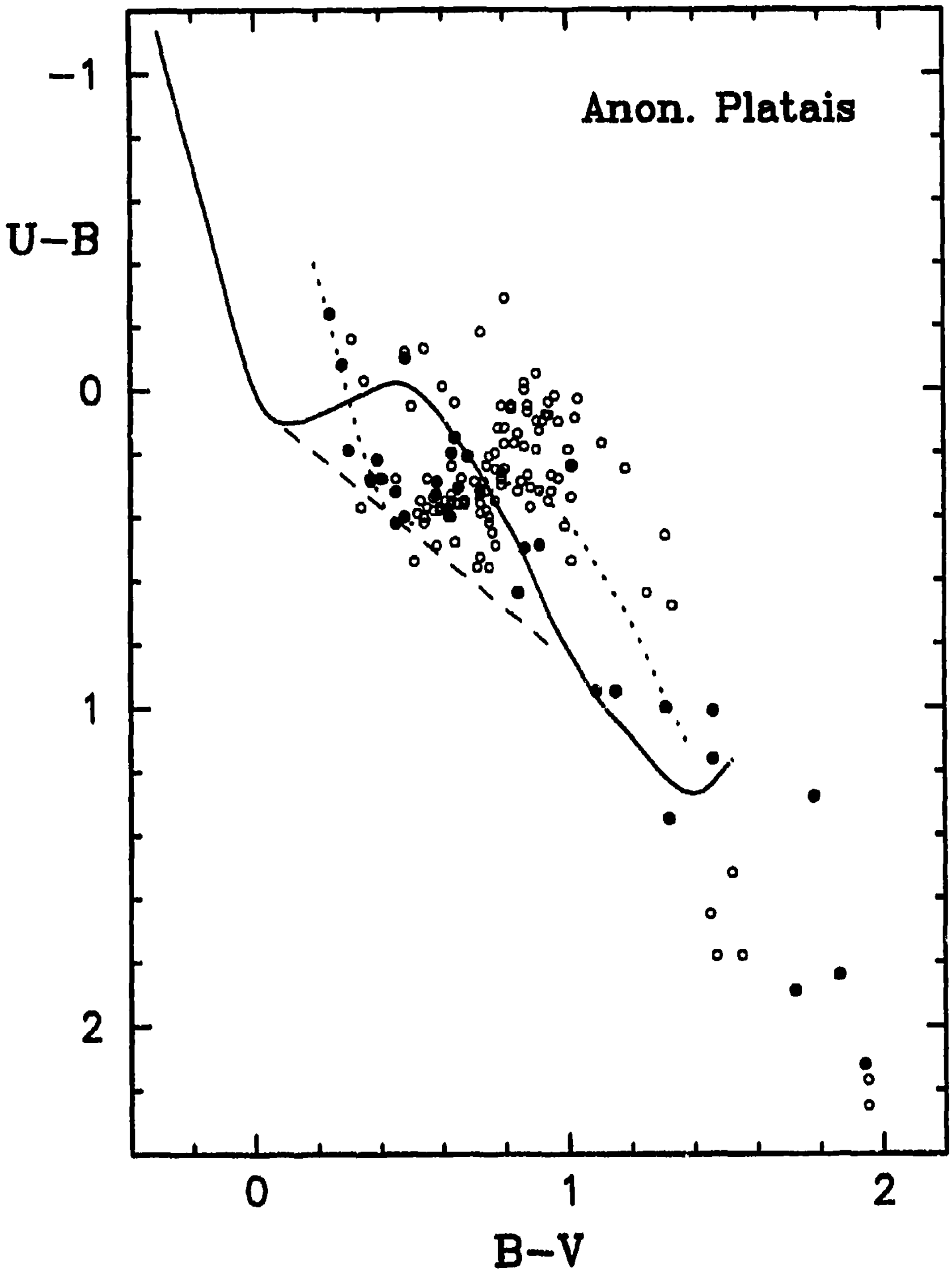

Figure 10. Colour-colour diagram for the field of C2128+488. Filled circles: photoelectrically observed stars; open circles: stars with photographic photometry. The intrinsic relation for main-sequence stars is shown by a solid line; the dotted line shows the same relation reddened by $E_{B-V} = 0.39$. The reddening line appropriate for this field is shown by a dashed line.

unreddened late-type giants in the lower right part of the diagram. A rather curious feature in this plot is the group of about 25 stars above the reddened F6 bump at $(B-V,\ U-B) \approx (0.9,\ 0.1)$. Most of these stars have $V \geq 15$, and as one can see from Figure 3, this is the faint limit of the calibration defined by the primary images. Thus, one possible explanation is a systematic error caused either by the use of secondary images, or by uncertain photoelectric photometry of the faint standards. There is no evidence for this in the calibration relations, however, so these stars are probably heavily reddened B stars, or (rather unlikely) reddened metal-poor F dwarfs.

The dereddening for all program stars (with the exception of those having spectral classifications) was done by a computer program written by the author. It calculates all possible intersections of the reddening line for a given star with the intrinsic relation and gives as output the resulting colour excesses, intrinsic colours and magnitudes. For the purpose of calculating the intersections, the intrinsic relation is assumed to be a sequence of short straight lines connecting the individual pairs $\left((B-V)_0,\ (U-B)_0\right)$.

The multiple dereddening solutions were resolved taking into account the position of the star in the field and, eventually, the resulting colour–magnitude diagram. The few stars which fall below the A2 reddening line (shown by a dashed line in Figure 10) were dereddened to the A2 kink. Their positions on the colour–colour diagram are not necessarily caused by photometric errors — another possibility is rapid rotation which is expected to widen the intrinsic colour relation for dwarfs around spectral type A2 (Turner, private communication).

A reddening map of the field of C2128+488 is presented in Figure 11. It was generated using all stars with known colour excess. The reddening values shown on the map were corrected to an equivalent reddening of a B0 star using the expression

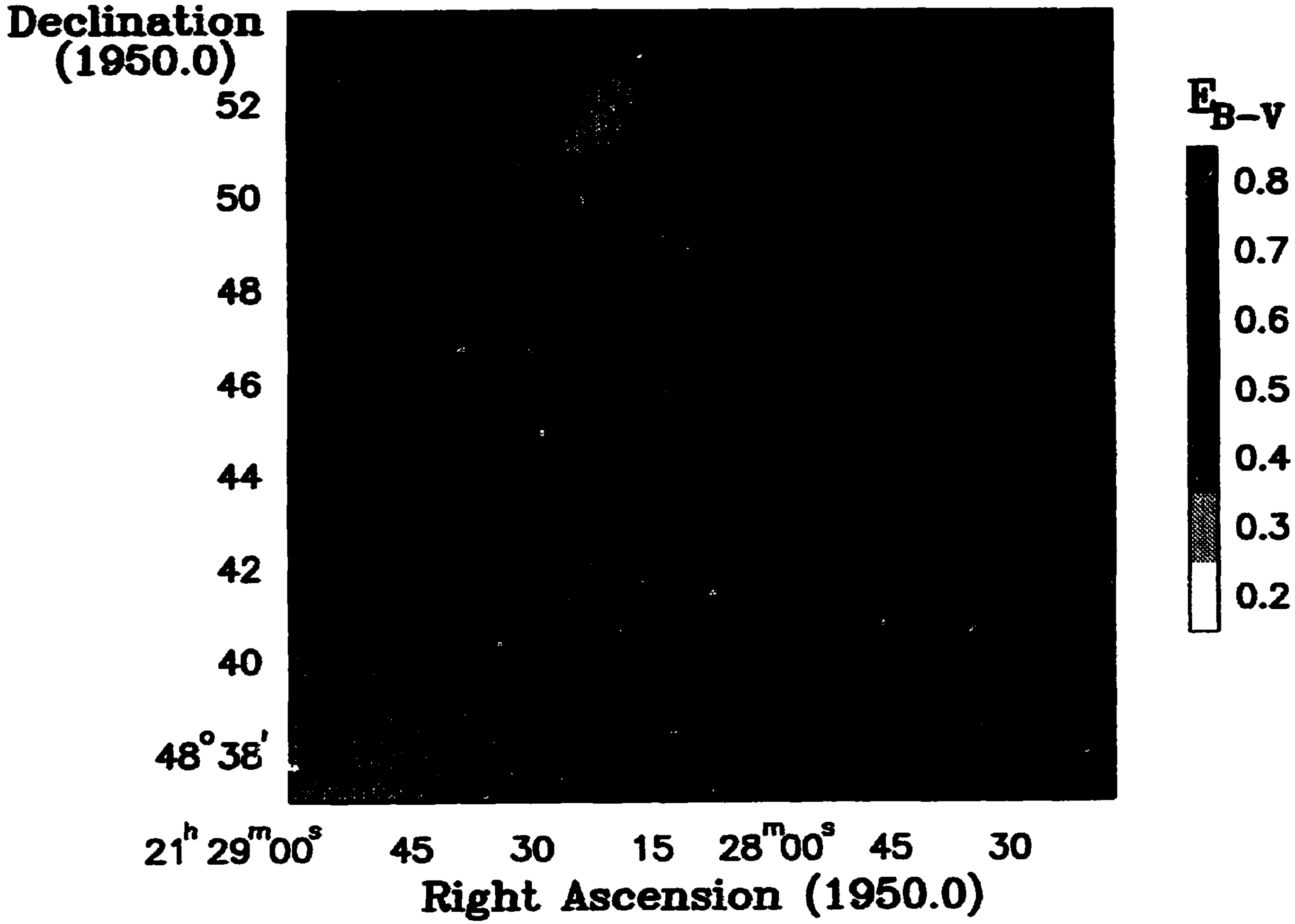

Figure 11. A reddening map for the field of C2128+488 based on the colour excesses for all reddened stars. V1726 Cyg is circled.

$$E_{B-V}(\mathrm{B0}) = \frac{E_{B-V}(\text{observed})}{0.976 - 0.074(B-V)_0},$$

which is based on Buser's (1978) study (Turner, private communication). The reddening pattern in this area is somewhat patchy, with a belt of lower reddening between two higher-reddening regions. The large-scale distribution of absorbing matter implied from Figure 11 is in remarkable agreement with that seen in Figure 2 and in the Palomar Observatory Sky Survey. It is worth mentioning that interpolation of small samples of very irregularly spaced data (such as ours) is not very robust and that the details of this map might change somewhat should new data become available. However, the general features of the map, in particular the area of lower reddening in the middle and the area of high reddening to the west and south of the Cepheid, seem rather well established.

Since cluster members are at a common distance, any differences between their apparent distance moduli must be due to interstellar extinction. The amount of visual extinction is given by

$$A_V = R \times E_{B-V}, \tag{4}$$

where R is the ratio of total to selective absorption. Therefore, in the presence of interstellar extinction

$$V - M_V = (V_0 - M_V) + R \times E_{B-V},$$

where $(V_0 - M_V) = const$. Clearly, on a $(V - M_V)$ versus E_{B-V} plot (called a variable-extinction diagram), unevolved cluster stars should lie on a straight line with a slope equal to R_V and Y-intercept equal to the true distance modulus V_0–M_V.

The variable-extinction diagram for the field of C2128+488 is shown in Figure 12. With the exception of the spectroscopically observed stars (open diamonds), the values for M_V were obtained from the intrinsic color indices $(B-V)_0$ using the zero-age main

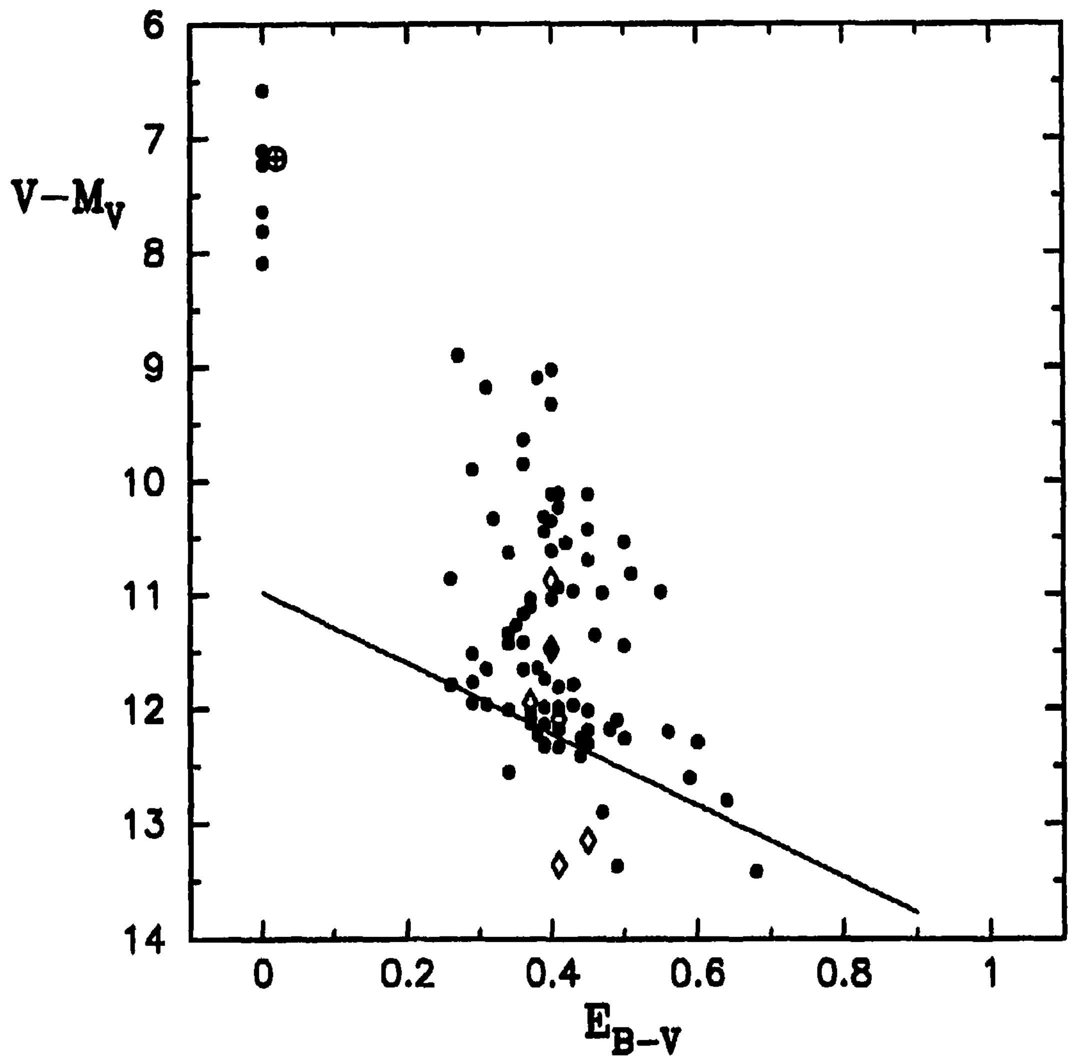

Figure 12. Variable-extinction diagram for C2128+488 stars with luminosities obtained from ZAMS fitting (filled circles) and spectral types (open diamonds). The nearly unreddened cluster M39 is shown by a circled cross. A fit to the lower envelope of likely ZAMS cluster stars is shown by a straight line with slope $R = 3.1$.

sequence (ZAMS) from Turner (1979). There is a well defined lower envelope which we assume represents the cluster main sequence. Two of the spectroscopically observed stars (Nos. 1 and 5) are very close to the envelope, and a third such star (No. 10) seems to be slightly evolved away from the main sequence. The radial velocities for those three stars (Table 4) also indicate that they are probable cluster members.

The lower envelope consists of 19 stars having a range of colour excess about 0.2. Using these stars, and a combination of parametric and non-parametric fitting techniques, Turner *et al.* (1994) derived a value for $R = A_V / E_{B-V} = 3.07 \pm 0.27$. Therefore, we adopted a value of $R = 3.1$ and used Equation (4) to calculate the extinction corrections.

Anon. Platais is seen at the outskirts of M39 (NGC 7092), which at a distance 265 pc is only slightly reddened; McNamara and Sanders (1977) derived $E_{B-V} = 0.02$, similar to Johnson (1953) who found no reddening at all. As can be seen from Figure 12 where M39 is marked by a crossed circle, the farthest unreddened star has a distance modulus of $V - M_V \approx 8.1$ (415 pc). The closest reddened stars are at $V - M_V \approx 8.9$ and they are reddened roughly by the same amount as cluster stars ($E_{B-V} \approx 0.25$ to 0.4). We can conclude, therefore, that the dust clouds responsible for the extinction across C2128+488 are at a distance of about 415 pc or a little further.

1.3.2 Cluster membership, distance and age

Data for the potential cluster members, selected by their positions on the variable-extinction and colour-magnitude diagrams, are listed in Table 6 and the colour-magnitude diagram is presented in Figure 13. These objects include the 19 lower envelope stars from Figure 12, the three spectroscopically observed stars with radial velocities matching that of V1726 Cyg (see Table 4), star No. 111 at the cluster turn-off and V1726 Cyg itself. We consider all these stars to be highly probable cluster members and they are marked by filled circles in Figure 13. The remaining 18 stars in Table 6 (open circles) are within

Table 6. Reduced data for probable C2128+488 members

Star	E_{B-V}	$(B-V)_0$	V_0	Star	E_{B-V}	$(B-V)_0$	V_0
V1726 Cyg[a]	0.46[b]	0.46	7.56	150[a]	0.37	0.19	13.36
1[a]	0.37	−0.06	10.01	153[a]	0.39	0.16	13.40
5[a]	0.41	−0.12	11.03	163[a]	0.37	0.12	13.06
10[a]	0.40	−0.02	11.74	165[a]	0.39	0.26	13.86
19[a]	0.44	−0.03	12.39	167	0.34	0.42	14.06
24[a]	0.37	0.12	13.01	169	0.43	0.31	13.44
26	0.31	0.28	13.50	174[a]	0.26	0.20	13.46
111[a]	0.48	−0.12	11.06	178[a]	0.39	0.20	13.43
114[a]	0.41	0.28	13.73	182[a]	0.29	0.27	13.82
115	0.60	0.17	12.77	183[a]	0.34	0.20	13.43
120	0.50	0.16	13.03	188[a]	0.31	0.28	13.81
123	0.59	0.14	13.00	192	0.41	0.23	13.32
128	0.36	0.43	14.05	193	0.35	0.53	14.59
133[a]	0.41	0.28	13.88	194	0.45	0.29	13.49
134	0.49	0.28	13.39	197[a]	0.37	0.28	13.78
136	0.39	0.22	13.09	198	0.29	0.35	13.80
138	0.36	0.22	13.08	203[a]	0.45	−0.03	12.25
139[a]	0.38	0.25	13.75	204[a]	0.44	0.35	14.08
144[a]	0.29	0.06	12.72	208	0.41	0.14	12.96
146	0.43	0.22	13.19	210	0.45	0.31	13.77
148	0.38	0.37	13.79	211[a]	0.35	0.35	14.18

[a] Highly probable member

[b] Reddening from neighbouring stars

~$0\overset{m}{.}75$ of the cluster main sequence and possibly represent unresolved binaries. The position of star No. 10 suggests that it also might be a multiple system. The short line

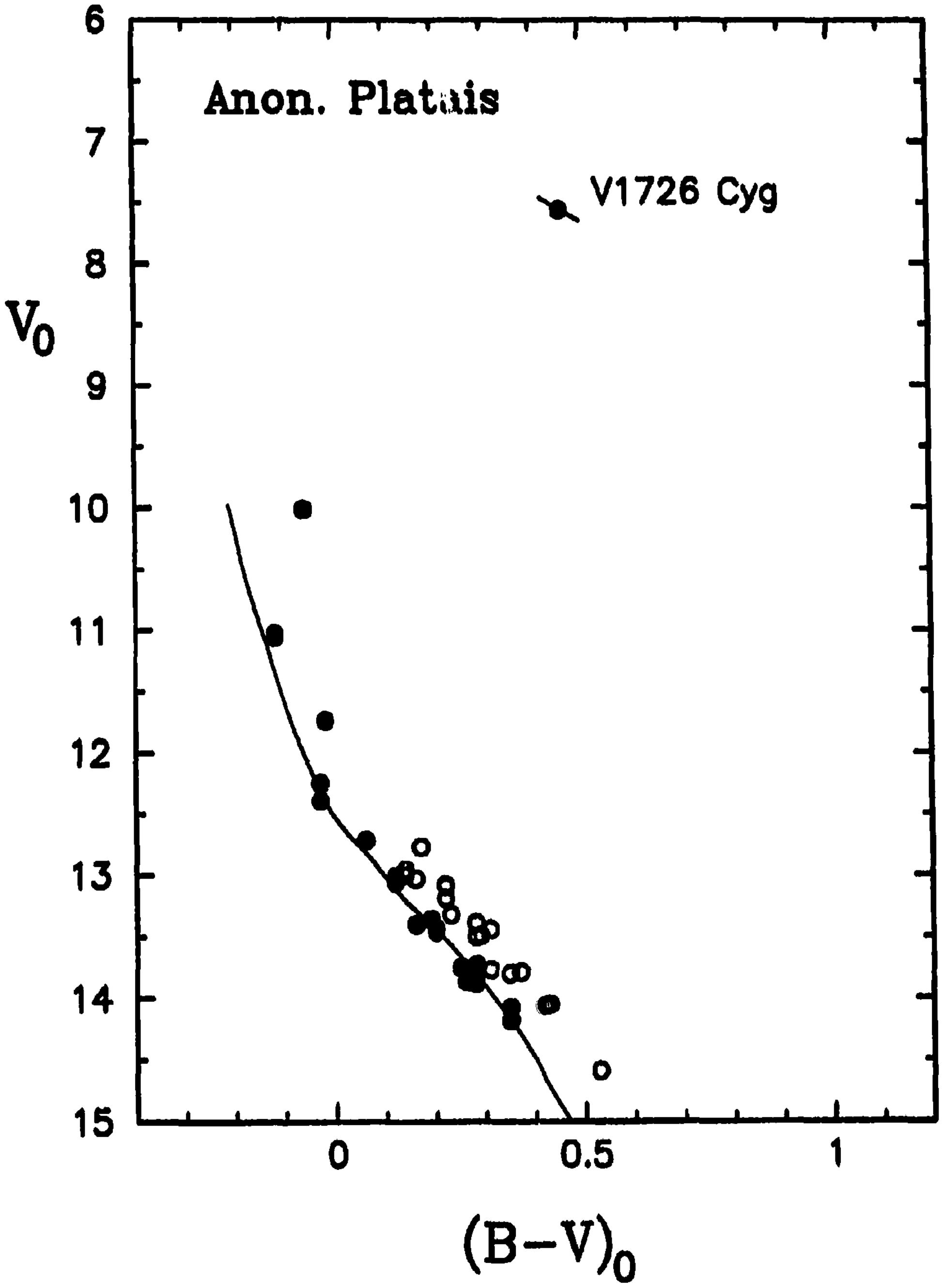

Figure 13. Reddening-free colour-magnitude diagram for highly probable members (filled circles) and other potential members (open circles) of C2128+488. The solid line represents the ZAMS for $V_0 - M_V = 10.98$.

passing through the position of V1726 Cyg indicates the range of change of the Cepheid's magnitude and colour.

Three approaches for determining the distance modulus of C2128+488 were used. They all make use of the sample of 19 lower envelope stars considered to be on the ZAMS. The classical sliding fit technique produced a distance modulus of $V_0 - M_V = 10.96$ with an uncertainty below ±0.05. The second method consisted of fitting a straight line to the sample of 19 main-sequence stars on the variable-extinction diagram. As mentioned earlier, the Y-intercept of this line is equal to the cluster distance modulus. An attractive feature of this approach is that the formal error is obtained directly from the fit, but the method is not applicable to clusters with little or no differential reddening. In our case, the range in colour excess is only $\sim 0^{m}.2$, which translates into larger uncertainty for the Y-intercept: an unweighted least squares fit yielded $V_0 - M_V = 10.97 \pm 0.12$.

The third method was an attempt to quantify the sliding fit technique in the following way: The ZAMS relation that we use is tabulated in intervals of $0^{m}.01$ in intrinsic colour, which means that given the value of $(B-V)_0$ for any star in Table 6, we can find directly the corresponding value of M_V for that star by just looking it up in the ZAMS table. Then, for a given trial distance modulus, it is straightforward to find the difference between the observed and predicted intrinsic visual magnitudes and calculate some statistic based on those differences. A reasonable range of trial distance moduli is easily found from a rough sliding fit. In our case, we applied this technique for trial values of $(V_0 - M_V)$ between 10.8 and 11.2, and chose as a best value for the distance modulus the one that minimized the dispersion about the ZAMS relation. The result is $V_0 - M_V = 10.977 \pm 0.017$, which is in very good agreement with the values from the previous two methods and moreover, in excellent agreement with Turner *et al.* (1994)

who obtained $V_0 - M_V = 10.98 \pm 0.02$. Thus, we adopted for the distance modulus of C2128+488 the value $V_0 - M_V = 10.98 \pm 0.02$ or 1568 ± 13 pc.

Except for the few spectroscopically observed stars, the membership decisions for the program stars were based on photometric criteria alone. In order to obtain more conclusive results, we turned to the proper motion studies of Platais (1994) which include data for most of our cluster stars. His sample contains a mixture of high-quality and lower-quality proper motions, with measuring errors of $\sigma = 0''.0018$ yr^{-1} and $\sigma = 0''.0035$ yr^{-1}, respectively. In Figure 14 we have plotted on the same scale separate vector-point diagrams for the two types of data; only the possible members are shown. The circles have radii of $\sqrt{2}\sigma$, 2σ and $2\sqrt{2}\sigma$; they divide the data into four classes which can be used to estimate the membership probability (Ebbighausen 1942). At the distance to C2128+488, one would expect an approximately Gaussian distribution for the positions on the vector-point diagram since the stellar motions will be small compared to the measuring errors; this appears to be the case for our data taking into account the small sample sizes. There are few stars in both the high-quality and lower-quality samples that fall into Ebbighausen's classes 3 and 4, *i.e.* their cluster membership is doubtful. Clearly, the available proper motion data are not very useful for separating cluster members from field stars, therefore those stars were not rejected. At least, the vector-point diagrams demonstrate that there are no obvious foreground objects among the stars considered to be likely cluster members.

The reality of the cluster and the membership of V1726 Cyg become more convincing when we consider the radial velocity observations for the Cepheid and stars Nos. 1, 5 and 10 (see Table 4). Their mean radial velocity has a standard deviation of only ± 0.5 km s^{-1} which is rather unlikely to happen by chance. This fact, combined with the natural position of all four stars on the colour-magnitude diagram, supports the hypothesis that they are a physically related group of stars.

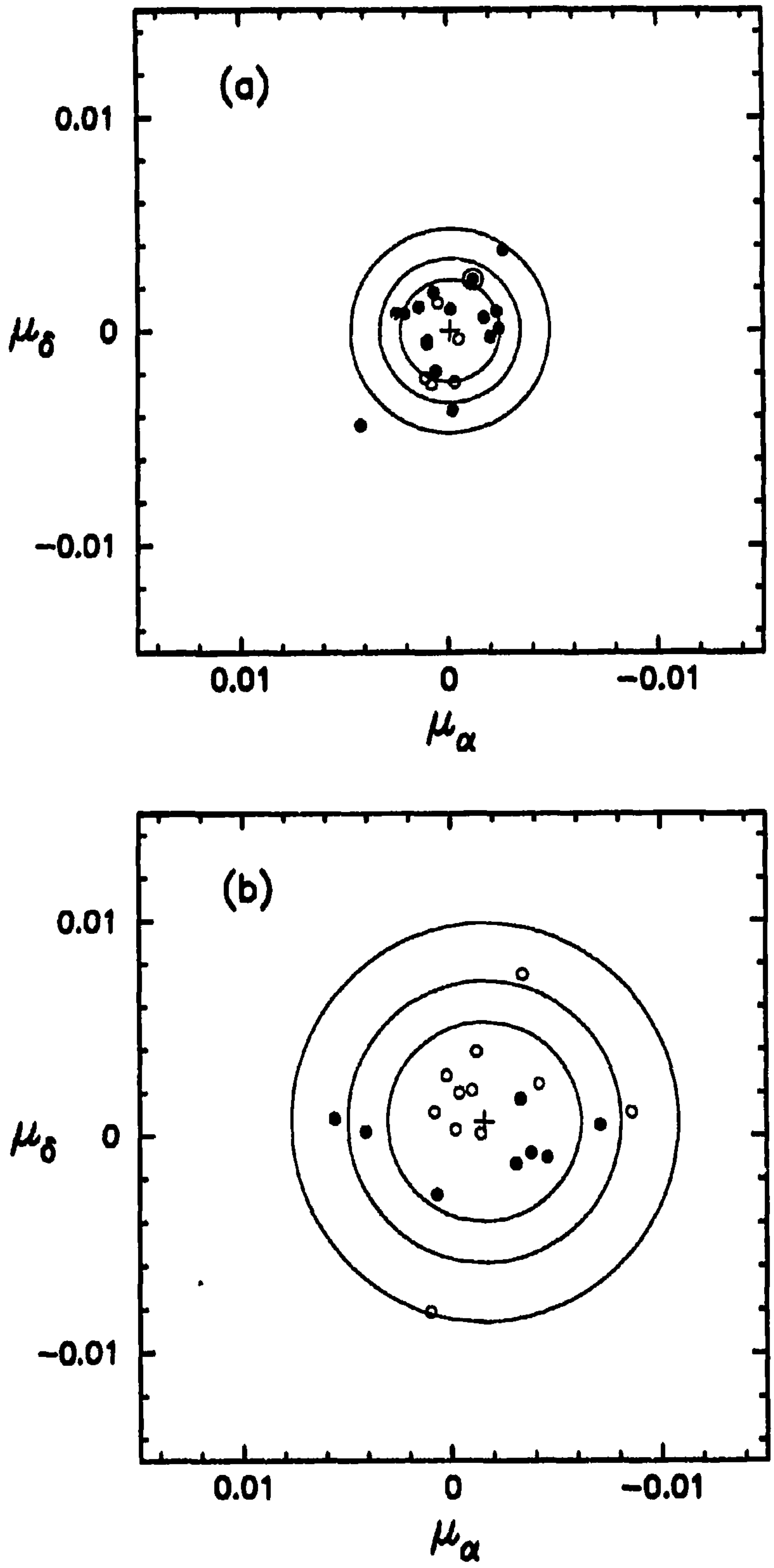

Figure 14. Vector point diagrams for the proper motions of hignly probable members (filled circles) and other potential cluster members (open circles). Separate diagrams are plotted for the high-quality *(a)* and lower-quality *(b)* proper motions, and the circles have radii of $\sqrt{2}\sigma$, 2σ and $2\sqrt{2}\sigma$. The centroid of each distribution is marked by a cross, and V1726 Cyg is circled.

The main-sequence turnoff of C2128+488 is defined by the two bluest stars (Nos. 5 and 111) at $(B-V)_0 = -0.12$ (spectral type B7), which agrees well with the period-turnoff colour relation for other cluster Cepheids (Turner, private communication). We estimated the age of the cluster to be 1.5×10^8 yr assuming solar metallicity and using Maeder and Mermilliod's (1981) models. Turner *et al.* (1994) obtained a similar age (1.9×10^8 yr) using models from Maeder and Meynet (1988). While these estimates may not be very conclusive, they are in good agreement with the age of V1726 Cyg expected from the period-age relation.

1.4 V1726 Cyg

1.4.1 Light and radial velocity variations

The variability of V1726 Cyg was discovered by Platais (1979) who, using only photographic observations collected over a period of three years, classified it as a low-amplitude Cepheid variable and determined a period of 4.24 days. Recognizing the importance of V1726 Cyg as a possible cluster Cepheid, several investigators have carried out further photoelectric observations: Platais and Shugarov (1981), Berdnikov (1986, 1992) and Turner *et al.* (1994). In order to study and establish the properties of V1726 Cyg as well as possible, we collected all its published photoelectric observations. They were adjusted to the system of Turner *et al.* (1994) by shifting each observer's data set (phase, magnitude/colour) with respect to the latter system until the dispersion of the combined sample was minimized. However, this procedure requires a good knowledge of the period of the variable. Since the offsets were small, an approximate period was found using Berdnikov's *V* data, and after every adjustment a new period determination was done until there was no need for further adjustments. This approach assumes that the offsets are colour-independent to which we found no evidence to the contrary. Table 7 summarizes the final offsets (Turner minus other) of the other observers from the system of Turner *et al.* (1994). It should be mentioned that the number of $U-B$ observations is rather small and besides, these data seem to suffer from larger errors than observations in the other bandpasses. Therefore, the values of the $U-B$ offsets given in Table 7 are poorly determined.

Table 7. Magnitude and colour offsets between Turner *et al.* (1994) and the remaining observers

Observer	V	$B-V$	$U-B$
Platais & Shugarov	+0.022	−0.020	---
Berdnikov	−0.019	−0.009	+0.10 ::
Forbes	−0.009	0.000	−0.02 ::

Period determinations were done using the analysis of variance (AoV) technique (Shwarzenberg-Czerny 1989). It is a very fast and computationally simple method, has the advantage that its probability distribution is known for any number of observations and is especially powerful for small sample sizes. Although similar to the phase dispersion minimization (PDM) method (Stellingwerf 1978), the author's experience has shown that the AoV technique produces narrower lines and much less power is transferred to the harmonics, resulting in cleaner periodograms and rejection of spurious signals. Combining all available photoelectric observations in the manner described in the previous paragraph, we obtained the following ephemeris for V1726 Cyg:

$$\begin{aligned} \mathrm{HJD_{max}} = {} & 2444020.5131 + 4.2370383E. \\ & \pm 0.0009 \quad \pm 0.0000003 \end{aligned} \tag{5}$$

In this equation, the first term on the right-hand side is the initial epoch JD_0, the second term is the period of pulsation and E is the number of pulsation cycles since the initial epoch.

The V light curve of V1726 Cyg is presented in Figure 15a, where observations from different observers are shown by different symbols as indicated, and phases were calculated using the ephemeris (5) and the expression

$$f = \mathrm{frac}\left[(\mathrm{JD_{obs}} - \mathrm{JD_0})/P\right] \tag{6}$$

where f is the phase and $\mathrm{JD_{obs}}$ is the heliocentric Julian day of the observation.

The light curve is of small amplitude ($\Delta V \approx 0^{\mathrm{m}}\!.2$) and nearly symmetrical sinusoidal shape — the duration of the rising part of the light curve (the parameter $M-m$) is very close to half of a cycle: $M-m=0.484$. The $B-V$ colour curve is shown in Figure 15b, where the same symbols have been used as in Figure 15a. The $U-B$ colour curve is not plotted since it was nearly impossible to combine observations from different observers and to arrive at a meaningful curve. For example, Berdnikov's mean $U-B$ colours from the two epochs (1983 and 1991) differ by $\sim 0^{\mathrm{m}}\!.15$! It is very unfortunate that the $U-B$ colour curve is so poorly defined because Cepheid $U-B$ colours can be useful for the detection of close companions (Madore 1977, Fernie 1979). For example, the $U-B$ colours of Turner *et al.* (1994) imply a rather small $U-B$ amplitude for V1726 Cyg ($\sim 0^{\mathrm{m}}\!.03$), which might be an indication for the presence of a hot companion.

As mentioned before, a small amplitude and a sinusoidal light curve are often attributes of overtone pulsators. Since this study is primarily concerned with the luminosity of the Cepheid, the question of the pulsational mode of V1726 Cyg is a very important and, as it turns out, a rather difficult one. In the last 15 years many studies

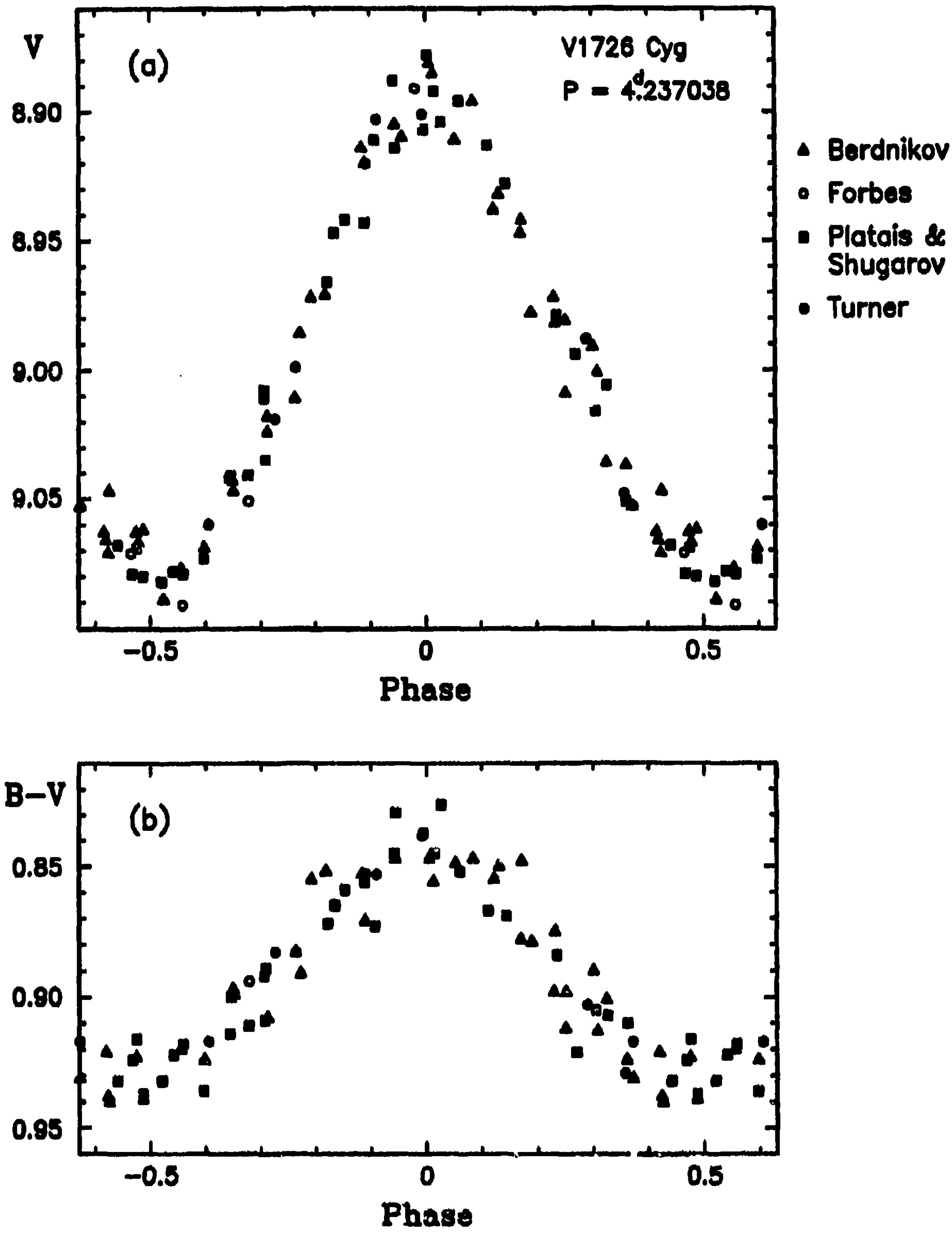

Figure 15. The V light curve *(a)* and the $B-V$ colour curve *(b)* of V1726 Cyg. Different symbols mark the data from different observers as indicated.

(*e.g.* Simon and Lee 1981; Antonello and Poretti 1986; Andreasen 1988; Simon 1988; Antonello *et al.* 1990*a,b*; to name a few) have shown that Fourier decomposition parameters of Cepheid light curves can provide valuable information on the pulsational properties of Cepheids. What concerns us more, however, is that Fourier parameters seem to be a reliable tool for pulsational mode discrimination in short-period Cepheids (Antonello and Poretti 1986; Antonello *et al.* 1990*a,b*, Poretti 1994) when accurate light curves with good phase coverage and a sufficient number of observations are available.

The Fourier decomposition consisted of fitting to the light curve, expressed in terms of the phase f (Equation 6) and magnitude $m(f)$, the series

$$m(f) = m_0 + \sum_{k=1}^{N} \left[a_k \sin(2\pi k f) + b_k \cos(2\pi k f) \right], \qquad (7)$$

where N is the chosen order of decomposition, and the $(2N+1)$ unknown coefficients $(m_0, a_1, b_1, \ldots, a_N, b_N)$ have to be determined from the fit. With the Fourier coefficients known, we can define for each term of order k its Fourier amplitude, H_k, and Fourier phase, ϕ_k, according to the relation:

$$a_k \sin(2\pi k f) + b_k \cos(2\pi k f) \equiv H_k \cos(2\pi k f + \phi_k)$$

or its equivalent

$$H_k^2 \equiv a_k^2 + b_k^2 \; ; \quad \phi_k \equiv \arctan(-a_k / b_k).$$

The actual quantities used in the analysis are the amplitude ratios, R_{k1}, and phase differences, ϕ_{k1}, defined by:

$$R_{k1} \equiv H_k / H_1 ; \quad \phi_{k1} \equiv \phi_k - k\phi_1 \; (+2\pi n).$$

The Fourier parameters for V1726 Cyg (amplitude ratios R_{21} and R_{31}, and phase differences ϕ_{21} and ϕ_{31}) as derived from the V and B light curves, are listed in Table 8 together with their formal errors. Comparison with the same quantities for overtone pulsators (Antonello *et al.* 1990*a*; Poretti 1994) shows that our values are similar to those of other *s*-Cepheids, or more precisely, of the C-*b* subclass of *s*-Cepheids (see also Antonello *et al.* 1990*b*).

Table 8. Fourier decomposition parameters for V1726 Cyg

V data set	B data set
$A_V = 0.187$	$A_B = 0.273$
$\phi_{21} = 3.81 \pm 0.33$	$\phi_{21} = 3.44 \pm 0.45$
$\phi_{31} = 6.72 \pm 0.50$	$\phi_{31} = 6.67 \pm 0.70$
$R_{21} = 0.06 \pm 0.02$	$R_{21} = 0.04 \pm 0.02$
$R_{31} = 0.04 \pm 0.02$	$R_{31} = 0.03 \pm 0.02$

Figure 16 reproduces the diagrams ϕ_{21}–P, ϕ_{31}–P and R_{21}–P from Poretti (1994) (his Figures 1–3) and the position of V1726 Cyg is plotted on each diagram. In the figures, crosses mark C-*a*, or fundamental mode Cepheids, and dots designate C-*b*, or first overtone pulsators. The position of V1726 Cyg is marked by a large triangle. It is clear from the plots that there is a very good chance for V1726 Cyg being an overtone pulsator. The problem is, however, that the light curve of V1726 Cyg has an almost perfectly sinusoidal shape and as a consequence, third order decomposition is not very meaningful, and even the second order amplitude ratios have large uncertainties. In this respect V1726 Cyg is similar to DT Cyg and V1334 Cyg (Poretti 1994). For these Cepheids, it is difficult to establish accurate second and third order terms, and, as a result, their classification as C-*a* or C-*b* variables is rather uncertain. In the case of V1726 Cyg,

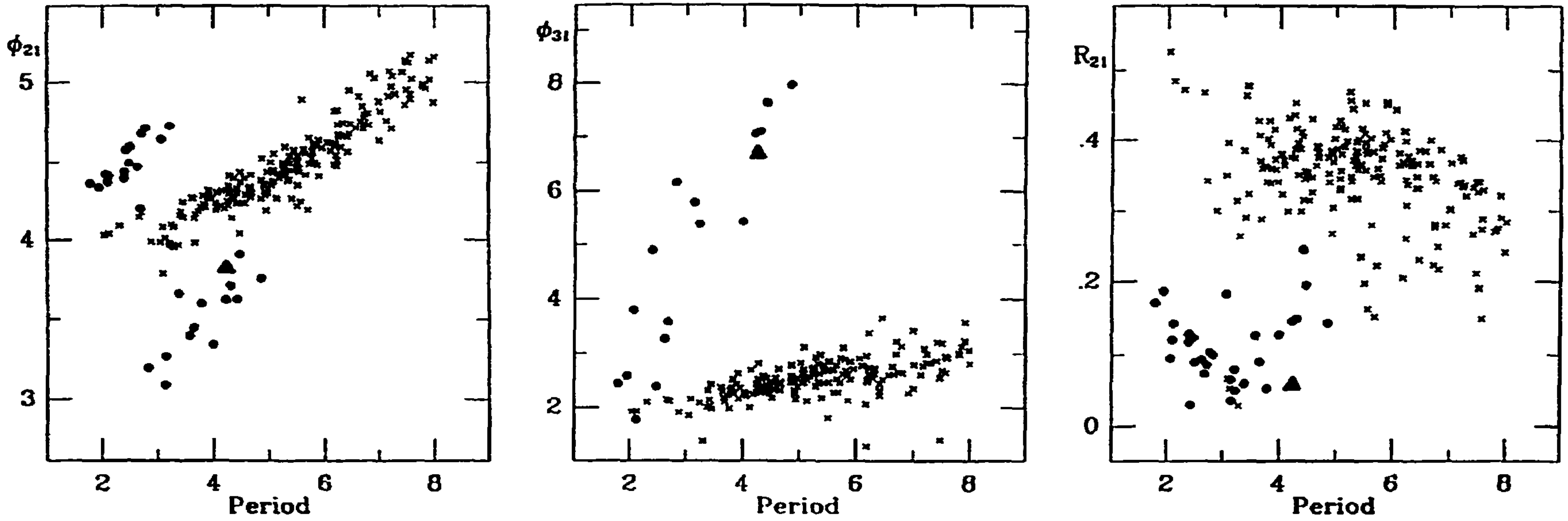

Figure 16. Phase differences ϕ_{21} and ϕ_{31}, and amplitude ratio R_{21} versus period for galactic Cepheids with $P < 7$ days. Crosses indicate C-*a* stars (*i.e.* classical Cepheids), and filled circles mark C-*b* stars (overtone pulsators). V1726 Cyg is marked by a large triangle. *(Reproduced from Poretti 1994).*

the ϕ_{21} value places it on the boundary between C-*a* and C-*b* pulsators (see Figure 16a), the value for ϕ_{31} matches very well the C-*b* domain (Figure 16b, but see the remark about third order fits above) and the position of V1726 Cyg on the R_{21}–period plot (Figure 16c) also suggests a C-*b* classification. To summarize, Fourier decomposition parameters for V1726 Cyg indicate that it is an overtone pulsator (or a C-*b* Cepheid in the terminology of Antonello *et al.* 1990*b*), but this conclusion must be made with a caution because the sinusoidal light curve of V1726 Cyg does not allow precise mode discrimination using the data currently available. New, high accuracy photometric observations are needed to establish firmly the pulsational mode of V1726 Cyg.

The radial velocity curve of V1726 Cyg is presented in Figure 17. It combines observations from Metzger *et al.* (1991) and Turner *et al.* (1994) phased to the same ephemeris as the photometric data, and the plot shows that the two sets of radial velocities are in excellent agreement. Typically for Cepheids, the radial velocity curve is a mirror image of the light curve, but there is a phase offset of about 0.1 between the two. The systemic radial velocity of the Cepheid was found from a low-order Fourier decomposition of the radial velocity curve (it is just the term m_0 in Equation 7, if we substitute magnitudes with radial velocities). We obtained $\gamma = -15.1$ km s^{-1}, in excellent agreement with the study by Metzger *et al.* (1992) who found $\gamma = -15.32$ km s^{-1} for V1726 Cyg. In principle, the radial velocity curve can be used to obtain Fourier parameters for the Cepheid in the same way as photometric data. We did not attempt this, however, because of the small size of the sample and the large scatter in the data.

In the following Table 9 we summarize the parameters of the light, colour and radial velocity variations of V1726 Cyg, derived by means of the Fourier decomposition technique. Note that the notations $(B-V)_{max}$, $(B-V)_{min}$, etc. refer to the colour index at maximum (minimum) light, not to the maximum (minimum) value of the index. Also, angle brackets $\langle\ \rangle$ designate intensity mean values of the corresponding photometric

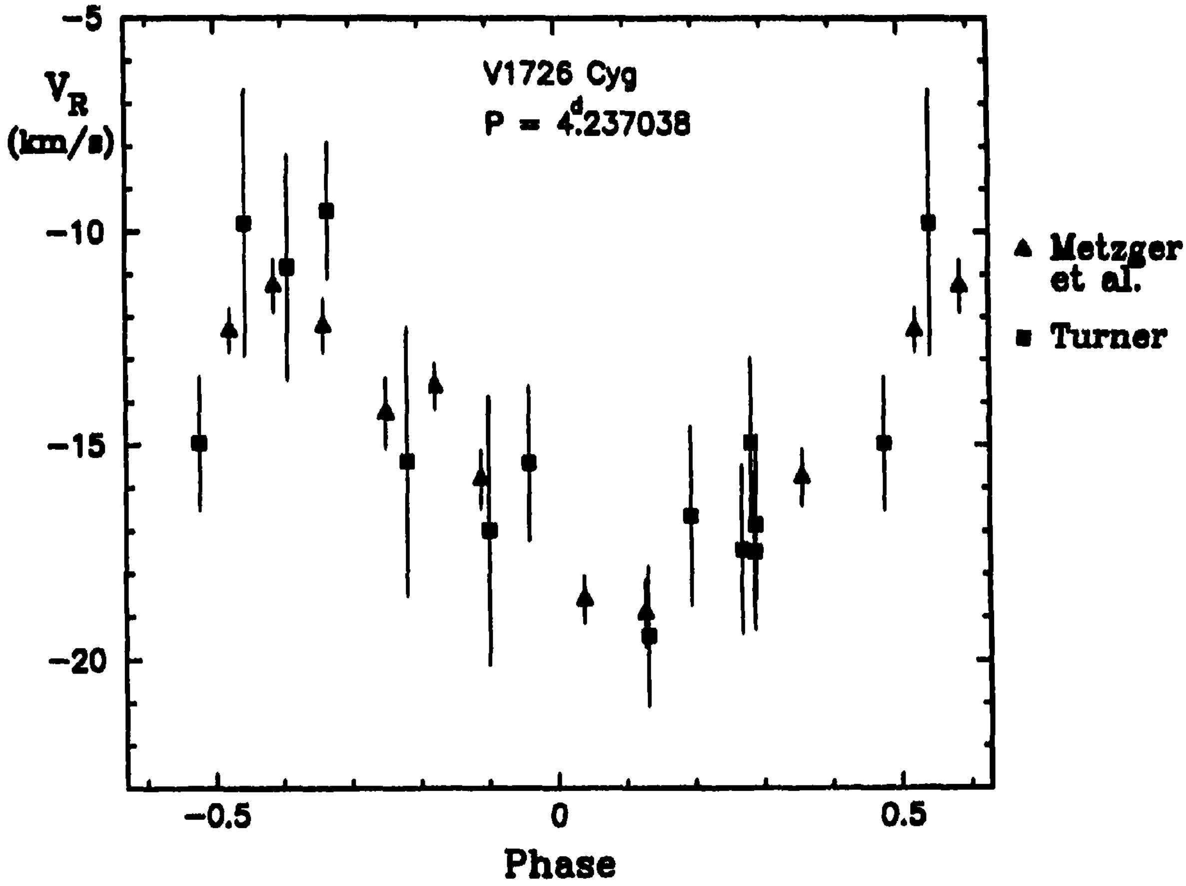

Figure 17. The radial velocity curve of V1726 Cyg. Triangles indicate data from Metzger *et al.* (1991) and the observations of Turner *et al.* (1994) are marked by squares. The uncertainties in the radial velocities are indicated by vertical lines.

quantities. We again note that the values for the $U-B$ colour curve and correspondingly, the U light curve, are of lower accuracy compared to the other quantities.

Table 9. Summary of light and radial velocity variations of V1726 Cyg

V_{max} = 8.892	$(B-V)_{max}$ = 0.84	$(U-B)_{max}$ = 0.57:
V_{min} = 9.079	$(B-V)_{min}$ = 0.93	$(U-B)_{min}$ = 0.62:
$M-m$ = 0.484	$M-m$ = 0.50	
B_{max} = 9.734	U_{max} = 10.30:	
B_{min} = 10.007	U_{min} = 10.62:	
$\langle V\rangle = 8.988 \pm 0.001$	$\langle B\rangle = 9.873 \pm 0.002$	$\langle U\rangle = 10.45 \pm 0.02$:
	$\langle B\rangle - \langle V\rangle = 0.885$	$\langle U\rangle - \langle B\rangle = 0.58$:
$\langle V_R\rangle = -15.1 \pm 0.5$ km s^{-1}, varying between -18.7 and -11.5 km s^{-1}		

1.4.2 Reddening, intrinsic colours and luminosity

As one can see in the reddening map (Figure 11), V1726 Cyg lies in a region of the cluster where the reddening seems to vary considerably — the individual colour excesses for stars around the Cepheid span a range of almost $0\overset{m}{.}3$ in E_{B-V}. Fortunately, V1726 Cyg is closely bracketed by two stars (19 and 30), which have colour excesses of $E_{B-V}(B0) = 0.44$ and $E_{B-V}(B0) = 0.49$, respectively. Assuming that on such a small scale (~1′) interstellar extinction changes smoothly, simple interpolation yields $E_{B-V}(B0) = 0.46 \pm 0.02$ as a value appropriate for the location of V1726 Cyg. Nearly the same result ($E_{B-V}(B0) = 0.47$) is obtained using isoreddening contours similar to those drawn on the reddening map. Adopting $E_{B-V}(B0) = 0.46$ and converting to a colour excess appropriate for a star with the observed colours of the Cepheid, we obtain a reddening of $E_{B-V} = 0.43 \pm 0.02$ for V1726 Cyg. Given a mean $B-V$ colour index of 0.89 (Table 9), the intrinsic colour of V1726 Cyg is $(\langle B \rangle - \langle V \rangle)_0 = 0.46 \pm 0.02$.

An independent estimate for the reddening of V1726 Cyg can be obtained from its spectral type. Turner *et al.* (1994) have considered several sources of intrinsic colours of supergiants and found that the average value appropriate for an F6 Ib supergiant is $(\langle B \rangle - \langle V \rangle)_0 = 0.46 \pm 0.02$, which is identical to the one found from the Cepheid's space reddening.

In the previous section it was found that V1726 Cyg is a highly probable member of C2128+488, as judged from the Cepheid's position, radial velocity and proper motion. Assuming that this is indeed so, we find that the corresponding absolute magnitude of V1726 Cyg is $M_V = -3.42 \pm 0.07$. An important question then is, how does this value compare with the one predicted from the Cepheid period-luminosity (PL) relation? We must consider the fact that there is a strong possibility for V1726 Cyg being an overtone pulsator and compare both possible luminosities. The ratio of fundamental and first overtone periods can be estimated from the period ratios of known double-mode Cepheids (Szabados 1988). If the observed period of $4^{d}.237038$ is the first overtone, the predicted ratio is $P_1/P_0 = 0.6864$, where P_0 is the fundamental period which enters the PL relation. Using Turner's (1992) PL relation, we obtain $M_V = -2.99 \pm 0.07$ if V1726 Cyg pulsates in the fundamental mode, and $M_V = -3.47 \pm 0.07$ if it pulsates in the first overtone. Clearly, the latter value is much closer to the luminosity found for V1726 Cyg from assumed cluster membership. Thus, a best agreement between the available observational data and the luminosity of the Cepheid as a cluster member is achieved when we assume that V1726 Cyg is an overtone pulsator, besides the other evidence for overtone pulsation presented in Section 4.1.

An important piece of information not considered so far in these arguments is the intrinsic colour of V17∠6 Cyg. As Turner *et al.* (1994) have pointed out, with

$(\langle B\rangle - \langle V\rangle)_0 = 0.46$, V1726 Cyg is bluer than other Cepheids of similar period whether it is pulsating in the fundamental mode (P_0 = $4^{\mathrm{d}}_{\cdot}23704$) or in the first overtone ($P_0 = 6^{\mathrm{d}}_{\cdot}17284$). Such a colour might be caused by the presence of a hot companion, which is not unusual for Cepheids. However, Turner *et al.* (1994) conclude that V1726 Cyg is most probably a single star, taking into account the appearance of its spectrum and the identical reddening obtained from its spectral type and from photometry.

They also investigated the influence of the blue colour of V1726 Cyg on the colour term α in the period-luminosity-colour (PLC) relation

$$M_V = A \log P + \alpha(\langle B\rangle - \langle V\rangle)_0 + C$$

and found that when V1726 Cyg is included in the sample as a fundamental mode pulsator, the colour term is $\alpha = 2.1 \pm 0.2$, whereas $\alpha = 0.5 \pm 0.2$ is obtained if V1726 Cyg is considered to be a first overtone pulsator. The latter value is clearly at odds with current results for galactic and Magellanic Clouds Cepheids (see Turner *et al.* 1994). Moreover, in their numerical simulations of how the PLC relation is empirically determined, Brodie and Madore (1980) showed that a small value for α is rather unlikely given the present accuracy of photometry and reddening determinations. Another point in support of fundamental mode pulsation is the period-turnoff colour relation derived from other cluster Cepheids (Turner, private communication), which is matched very well by V1726 Cyg if $P_0 = 4^{\mathrm{d}}_{\cdot}23704$, but requires a bluer cluster turnoff if $P_0 = 6^{\mathrm{d}}_{\cdot}17284$. Thus, although the light curve parameters and the blue colour of V1726 Cyg favour its classification as an overtone pulsator, we have arrived at an even stronger argument that it pulsates in the fundamental mode. It is clear that with the current data we cannot resolve this problem without knowing independently either the Cepheid's pulsation mode or its distance, and that further, high-accuracy observations are needed to settle the question about the pulsation mode of V1726 Cyg.

1.5 Summary and conclusions

We have presented and analyzed photoelectric and photographic photometry, as well as radial velocity observations, for the Cepheid V1726 Cyg and other stars in the field of the galactic cluster C2128+488 (Anon. Platais). The picture of C2128+488 emerging from this study is of a sparse, medium-age (~2×10^8 yr) cluster at a distance of 1570 pc, with only about 20 to 40 probable members found here. The spatial coincidence and the close match of the radial velocity, proper motion and age of V1726 Cyg with those of cluster stars present solid arguments for cluster membership.

The Cepheid itself has a low-amplitude ($\Delta V \approx 0^{m}_{.}2$), nearly symmetrical light curve commonly seen in overtone pulsators. The Fourier decomposition parameters also strongly suggest V1726 Cyg is an overtone pulsator, despite the uncertainties associated with higher-order decomposition of nearly sinusoidal light curves. The luminosity of the Cepheid inferred from its cluster membership is very close to that predicted from the period-luminosity relation if we assume pulsation in the first overtone. This assumption, however, leads to an unrealistically small value for the colour term β in the period-luminosity-colour relation. On the other hand, the colour term obtained assuming fundamental mode pulsation is quite reasonable, but the corresponding luminosity places the Cepheid about $0^{m}_{.}15$ closer than the cluster.

Undoubtedly, more detailed study of the cluster and V1726 Cyg is needed to resolve the problems outlined above. Especially important is to obtain high-precision (~$0^{m}_{.}005$ or better) photometry for the Cepheid for two reasons: *(i)* Hopefully it will allow the derivation of reliable F ..ier parameters and eventually, the establishment of the pulsation mode of the Cepheid; *(ii)* Presently, the $U-B$ colour curve of V1726 Cyg is very poorly determined. The $U-B$ amplitude is useful for the detection of close companions and it seems that the presence of a blue companion of V1726 Cyg can alleviate some of the problems with the color term in the PLC relation.

Part 2. The field of SU Cygni

2.1 Introduction

SU Cyg = BD +28° 3460 is a short-period, bright Cepheid located on the boundary between Cygnus and Vulpecula, about 2°.5 from the galactic equator. It is known to be a member of a multiple system (Madore 1977), and most of the recent studies of SU Cyg have focused on the properties of its two companions with the eventual goal of a better determination of the Cepheid's characteristics (Böhm-Vitense 1985; Böhm-Vitense and Proffitt 1985; Evans 1988; Evans and Bolton 1990).

Around 1978 Nancy Evans noted that there is a loose cluster visible around SU Cyg and proposed a more detailed investigation of that region (Turner, private communication). The only photometric study of the field around SU Cyg was done shortly before that by Feltz and McNamara (1976) as a part of their program to derive colour excesses for classical Cepheids. They obtained *UBV* and *uvbyβ* photometry for four early-type stars within 1° of SU Cyg and derived colours, reddenings and distances for those stars. Clearly, any study of the reality of the suspected sparse grouping and its relation to the Cepheid requires much more data, and in this second part of the thesis we report the results of a detailed photometric investigation of the field of SU Cygni.

There are several clusters and stellar groups not very far from SU Cyg, but it is unclear whether any of them can be reasonably associated with the Cepheid. For example, a sparse nearby cluster and distant OB associations (Vul OB1, Vul OB2 and Vul OB4) are located about 2° southeast of SU Cyg in the field of the two long-period Cepheids S Vul and SV Vul (Turner 1980; Turner *et al.* 1986). The open clusters NGC 6834 and Czernik 41 are also a few degrees away, but their size and brightness exclude possible association with SU Cyg. Therefore, this study deals only with the immediate vicinity of

SU Cyg (~30′ in diameter), where the existence of a possible cluster has been suggested by Nancy Evans.

In this part, section 2 describes the observational data and reductions, section 3 presents the analysis of the results and section 4 presents the conclusions. Since SU Cyg has been studied extensively, many of its properties (light and colour curves, period, radial velocity, etc.) are assumed to be well known. More information on observed and inferred parameters of SU Cyg can be found in the following sources: Schaltenbrand and Tammann (1971), Fernie (1979) and the references therein, and Feltz and McNamara (1980) for photometric data; Böhm-Vitense (1985), Evans (1988), Evans and Bolton (1990), and the references there for radial velocity data and studies of other properties of the Cepheid and its companions.

2.2 Observational Data and Reductions

2.2.1 Photoelectric photometry

The main source of photoelectric photometry for stars in the SU Cyg field are the observations of Turner (unpublished), who obtained *UBV* photometry for ten stars within a few arc minutes of the Cepheid with the #4 16" telescope at Kitt Peak National Observatory. On the finder chart of the field (Figure 18) these are the stars numbered 1 to 10. Four additional stars have been observed by Feltz and McNamara (1976), and one of those stars (marked FM3) is also shown on the finder chart. Thus, the available photoelectric data consist of 14 stars whose *UBV* observations and other relevant information are listed in Table 10. The first two columns identify the stars by their numbers in Figure 18 and BD or SAO designations, the next three columns list the *UBV* photometry, column 6 gives the number of nights on which each star was observed, and the last column lists spectral types and other information.

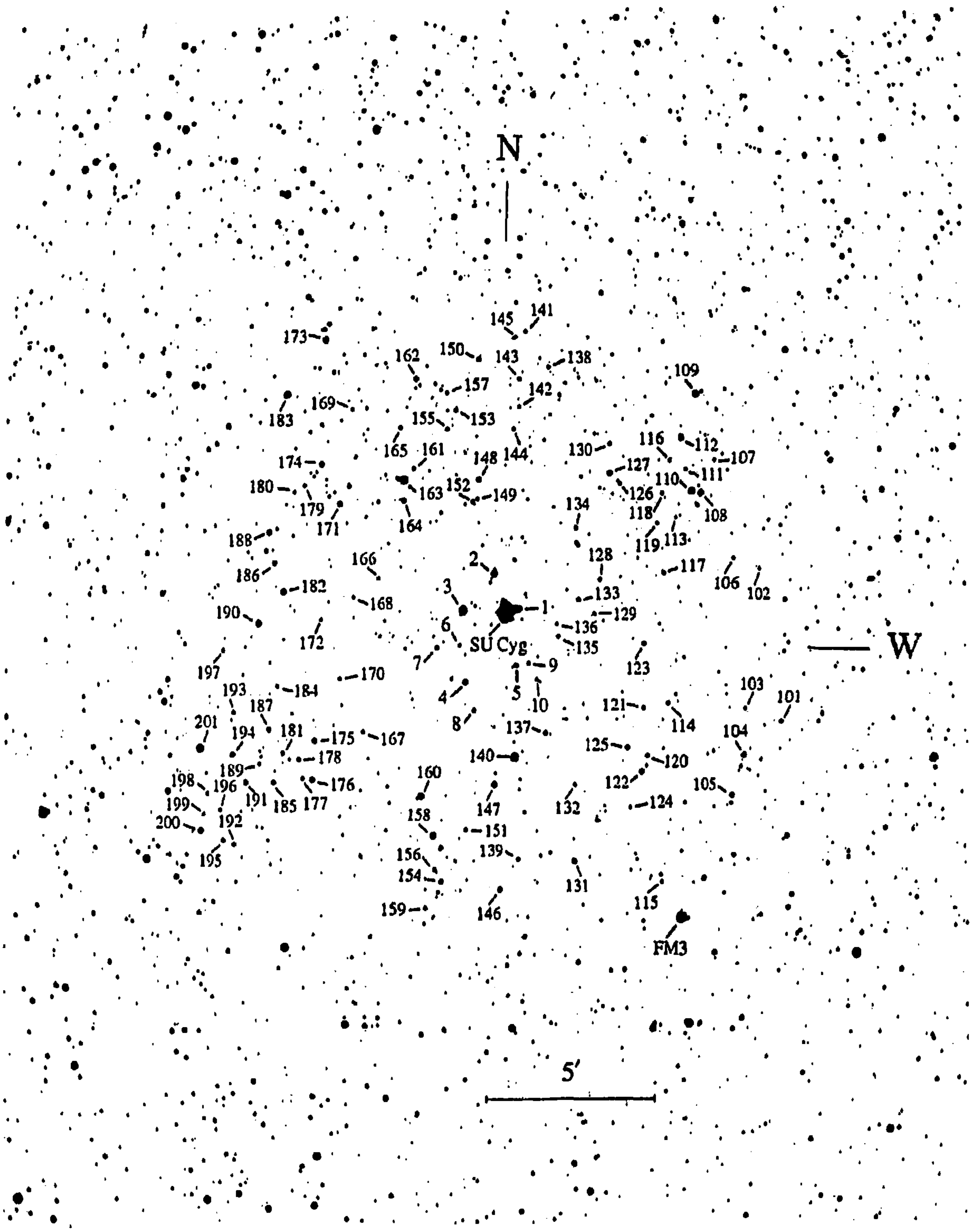

Figure 18. A finder chart for the field of SU Cyg. The photoelectric standards are numbered 1–10 and stars 101–201 are those measured photographically. FM3 is Feltz and McNamara's (1976) star 3.

Table 10. Photoelectric *UBV* photometry for stars in the filed of SU Cyg

Star	BD/SAO	V	B–V	U–B	n	Remarks
SU Cyg	+28 3460	6.884	0.590	0.258	–	F2-G0 I-II [a]; triple
1		10.918	0.221	0.127	5	A2 V [b]
2		10.897	0.552	0.106	5	
3		9.964	1.302	1.349	4	
4		11.787	0.668	0.260	4	
5		12.660	0.270	0.246	4	
6		13.705	1.412	1.290	2	
7		12.910	0.916	0.572	2	
8		13.045	0.532	0.302	2	
9		13.511	1.556	1.563	2	
10		13.460	1.604	1.468	2	
FM 3	+28 3457	9.210	0.089	−0.434	4	B3
FM 4	+28 3469	9.550	0.056	−0.123	4	B5
FM 7	87604	10.290	0.025	−0.184	4	A0
FM 8	+29 3734	9.240	−0.002	−0.452	4	B8

[a] Spectral type from Kholopov *et al.* (1985)

[b] Spectral type from Turner (private communication)

Only the ten stars observed by Turner were used to tie the photographic photometry to the Johnson *UBV* system. Of the four stars observed by Feltz and McNamara, three (FM4, FM7 and FM8) are too far from SU Cyg, and the last one (FM3) turned out to be too bright and not measurable on the iris photometer. Thus, none of them could be used for calibration purposes.

Besides the *UBV* photometry, Feltz and McNamara (1976) obtained *uvbyβ* observations which can be used to find the colour excesses and absolute magnitudes of their four stars. Analyzing Feltz and McNamara's photometry, Turner *et al.* (1987) found colour-dependent errors in their data and noted that Schmidt's (1975) Strömgren photometry seems to be free of such errors. Therefore, we adjusted Feltz and

McNamara's (1976) observations to the system of Schmidt (1975) using the three stars they have in common. Table 11*a* gives the original and corrected β, c_1 and c_0 indices; here c_0 designates the reddening-free value of c_1 and it was found using the expression $c_0 = c_1 - 0.25E_{b-y}$, as quoted by Feltz and McNamara (1976).

Table 11*a*. Strömgren photometry for stars in the field of SU Cyg

Star	β	β (corr.)	c_1	c_1 (corr.)	c_0
FM 3	2.654	2.675	0.502	0.509	0.464
FM 4	2.826	2.823	1.004	1.047	1.024
FM 7	2.848	2.841	0.889	0.924	0.903
FM 8	2.679	2.697	0.556	0.567	0.538

With the values of β and c_0 known, we used Crawford's (1978) calibrations to derive the absolute magnitudes as follows. First, the uncorrected absolute magnitudes were obtained from the M_V vs. β calibration. After that, using the c_0 vs. β_{ZAMS} relation, we calculated β_{ZAMS}, *i.e.* the value of β which a ZAMS star would have for the given c_0. Then the absolute magnitudes, corrected for evolutionary or other luminosity effects, can be found from the difference $\Delta\beta = \beta_{ZAMS} - \beta$ by means of the relation $\Delta M_V = 10\Delta\beta$, as given by Crawford (1978). The results from the calculations are listed in the following Table 11*b*, where M_V^c denotes the final, corrected absolute visual magnitude:

Table 11*b*. Absolute magnitudes from Strömgren photometry

Star	β	$M_V(\beta)$	β_{ZAMS}	ΔM_V	M_V^c
FM 3	2.675	−1.25	2.734	0.59	−1.84
FM 4	2.823	+0.85	2.915	0.92	−0.07
FM 7	2.841	+0.98	2.871	0.30	+0.68
FM 8	2.697	−0.71	2.751	0.54	−1.25

2.2.2 CCD photometry

Two fields north and south of SU Cyg were imaged by Welch (unpublished) on the night of 1985 June 25/26 with the Lowell Observatory 31″ telescope. Each field was observed in the *B* and *V* bandpasses. Unfortunately, the limitations of the technology of that time did not allow imaging in the *U* bandpass. A finder chart for the two fields is shown in Figure 19, which is a mosaic combining the north and south images; SU Cyg is the brightest object at the centre. The combined image has dimensions 521×584 pixels, which at a scale of $0\farcs838$ per pixel corresponds approximately to $7\farcm3 \times 8\farcm2$. Two additional images (one each in *B* and *V*) of a standard field near M92 were also taken. The exposure information for the CCD images is summarized in Table 12.

Table 12. Exposure information for the CCD observations

	Image No.	Exposure Time	Filter	Siderial Time	Comments
V	A179	15^m	GG495	$17^h\,51^m$	Standard Field
	A181	4^m	GG495	$19^h\,22^m$	Northern Field
	A183	4^m	GG495	$19^h\,41^m$	Southern Field
B	A180	30^m	GG385	$18^h\,16^m$	Standard Field
	A182	8^m	GG385	$19^h\,30^m$	Northern Field
	A184	8^m	GG385	$19^h\,49^m$	Southern Field

The preliminary image reductions (dark subtraction, flat fielding, removal of cosmic ray hits, etc.) were done by Gary Welch. Further image reductions and the photometry were performed by the author using the VISTA package and the DAOPHOT stellar photometry routines (Stetson 1987). The purpose of using the CCD images was twofold: firstly, to obtain photometry for the faint stars in the immediate vicinity of

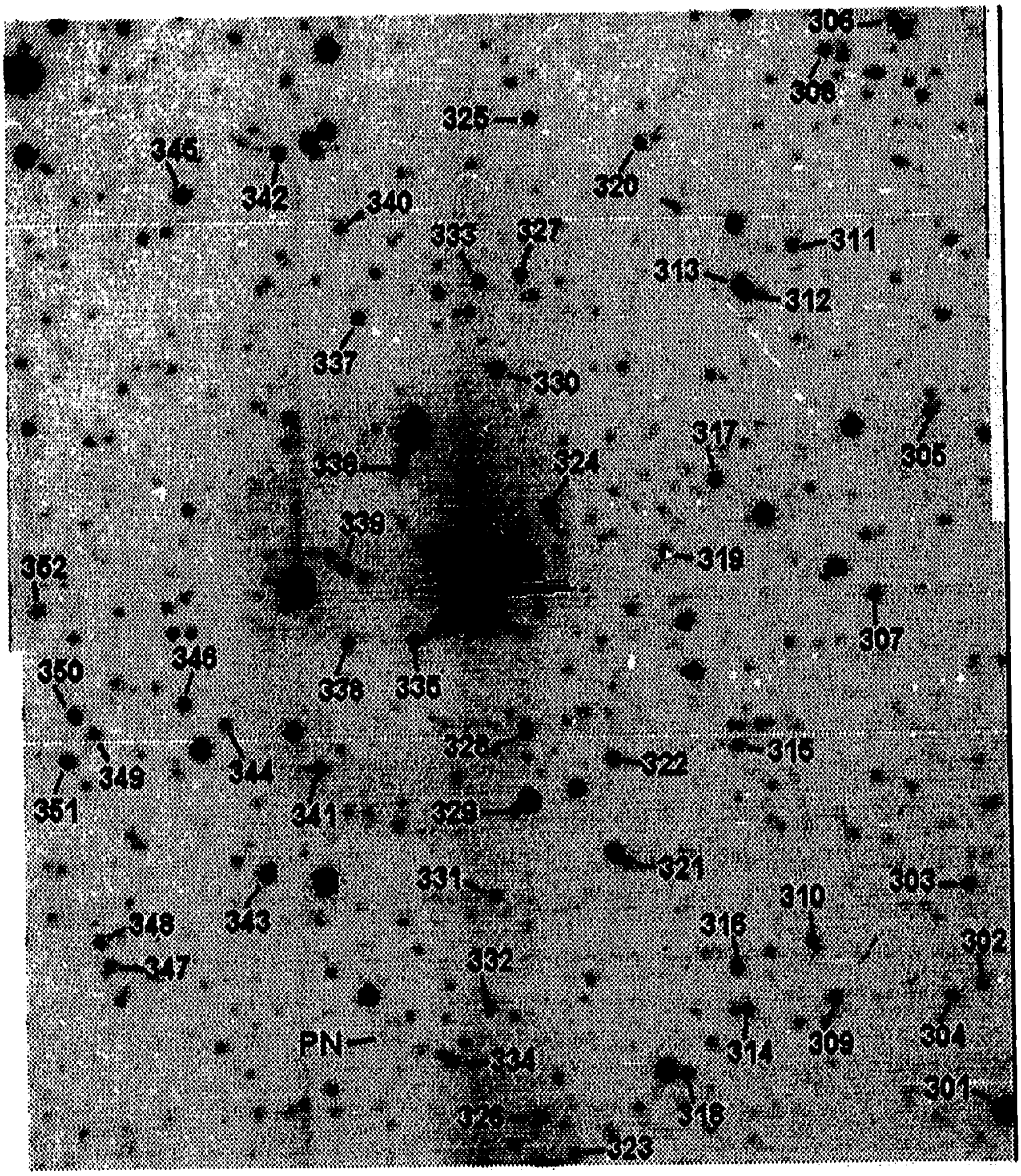

Figure 19. A finder chart for the CCD images of the two fields north and south of SU Cyg. The Cepheid is the brightest object at the centre; the newly discovered planetary nebula is marked PN.

SU Cyg; and secondly, to check how well the CCD photometry matches the photoelectric photometry for the common stars in the field.

For the CCD photometry, all stars with sufficient number of counts were chosen. In practice these were the stars found by the DAOPHOT routine FIND when a 4σ detection threshold was set. Many of the faintest stars were rejected on the later stages of the reduction, since they had considerably larger photometric errors than the average for the other stars. The reasons for the large errors might include adjacent bad rows, uneven background, undetected close companions, or just low signal-to-noise ratio.

The field of SU Cyg is moderately crowded, so simple aperture photometry was not applicable except for a few isolated stars. The instrumental magnitudes of the program stars were derived using a procedure based on the recommendations in Stetson (1987). Several bright, isolated stars were chosen and used to obtain the point-spread function (PSF) for each image. With the PSF available, we divided the program stars into as many groups as necessary (usually two or three), and for each group subtracted all stars not members of that group. The result was an image containing well separated single stars and ideal for aperture photometry. Figure 20 shows an image "cleaned" using the method described above. The images of the standard field were processed in the same way.

After performing aperture photometry for all program stars on the "clean" images, we used the DAOGROW routine (Stetson 1990) to fit the growth curves and obtain the instrumental magnitudes. The transformation to the Johnson *UBV* system was done by means of colour equations similar to equations (1) to (3) in Part 1. The only difference was the inclusion of extinction corrections, which were calculated using extinction coefficients from Welch (private communication). The equations can be written as:

$$V - v_0 = c_1 + d_1(b - v)_0 \qquad (8)$$

$$B - V = c_2 + d_2(b - v)_0 \qquad (9)$$

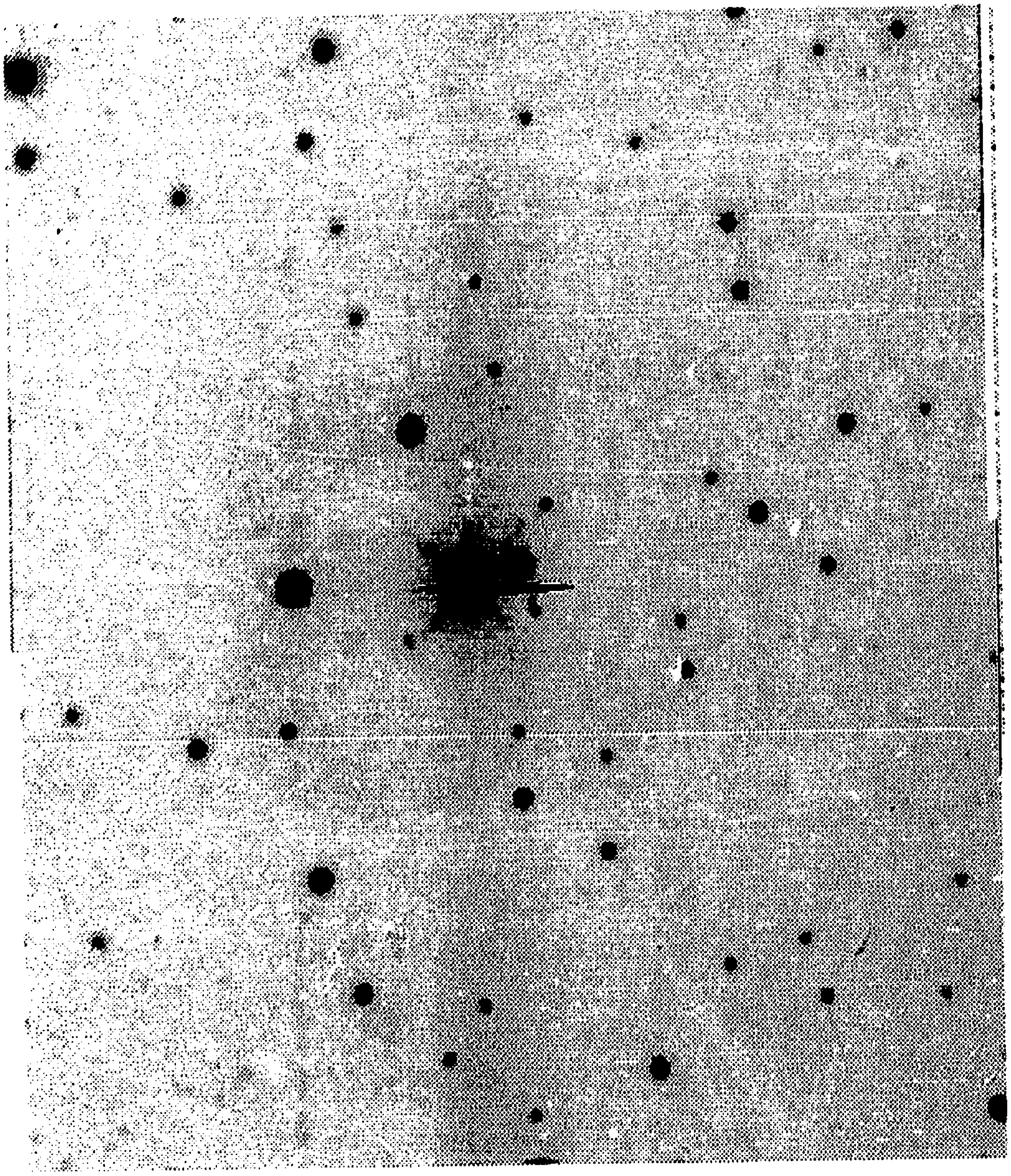

Figure 20. An example of a "cleaned" CCD image, where all close neighbours of the program stars have been removed using the procedure described in the text.

where v_0 and $(b-v)_0$ are the instrumental visual magnitude and $b-v$ colour index, respectively, corrected for extinction, and V and $B-V$ denote the corresponding Johnson magnitude and colour index.

The coefficients c_1, d_1, ... were determined by means of least squares fits, using two sets of standard magnitudes and colours: Turner's *UBV* data (Table 10) and V, $B-V$ data from Lindsey Davis, KPNO (Welch, private communication). The second data set contains magnitudes and colours for 23 stars south of the globular cluster M92, but we used only the 17 brightest standards. The two standard sets do not have common stars, so it was impossible to compare them directly. We estimated the consistency between the two sets by transforming the CCD instrumental magnitudes of Turner's standards to the Johnson *UBV* system using Davis' standards, and comparing the results with the original Turner's photoelectric magnitudes. The agreement was very good, and the residuals were comparable with the uncertainties in Turner's data. The residuals showed a trend with $B-V$, but only for $B-V > 1.4$, which is outside of the colour range of interest in the present study. Therefore, we used both sets of standard stars without any adjustments to obtain the coefficients in equations (8) and (9).

Figure 21 shows plots of the data used in the least squares fits; the straight lines represent the best-fit solutions of the transformation equations. Davis' observations are marked by filled circles, Turner's data are shown by open circles, and the few points which were rejected due the their large deviations from the fit are shown by plus signs.

The coefficients of the colour equations are given in Table 13. It is clear that the slope of the first line [the coefficient d_1 in equation (8)] is practically zero, therefore for the first colour equation we adopted simply $V = v + 1.766$. The CCD *BV* magnitudes and colours, obtained by means of equations (8) and (9), are given in Table 14; the stars are identified according to the CCD finder chart in Figure 19.

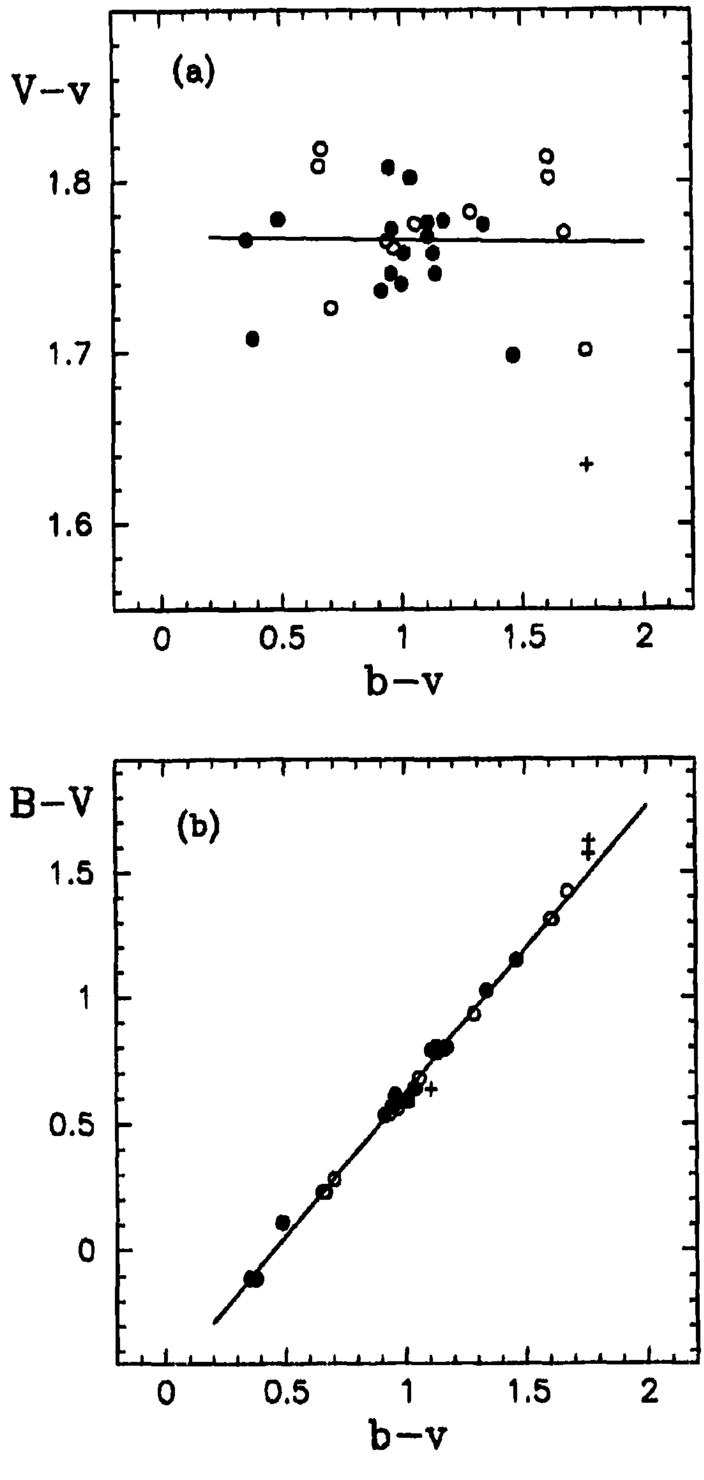

Figure 21. Transformation relations for the CCD magnitudes and colours. *(a)* plot of $V-v$ versus $b-v$, *(b)* plot of $B-V$ versus $b-v$. The observations by Davis are shown by filled circles, Turner's data are marked by open circles and the rejected points are shown by plus sugns.

Table 13. Coefficients for the transformation equations (8) and (9)

Equation	$c_i \pm 1\sigma$	$d_i \pm 1\sigma$	Remarks
(8)	+1.768 ± 0.019	−0.002 ± 0.017	Adopted $c_1 = +1.766$, $d_1 = 0$
(9)	−0.516 ± 0.016	+1.139 ± 0.015	

Table 14. CCD *BV* photometry for faint stars in the vicinity of SU Cyg

Star	V	B−V	Star	V	B−V	Star	V	B−V
301	14.632	+0.737	319	15.235	+0.715	337	14.553	+0.640
302	15.180	+1.187	320	14.713	+1.403	338	15.074	+0.975
303	14.852	+1.303	321	15.117	+2.116	339	14.458	+0.638
304	15.047	+0.900	322	14.564	+0.666	340	15.080	+0.864
305	14.835	+0.805	323	14.928	+1.446	341	14.665	+1.468
306	14.604	+1.813	324	14.372	+0.633	342	14.572	+1.628
307	14.936	+0.774	325	14.657	+2.102	343	13.872	+1.795
308	14.803	+2.074	326	14.628	+1.211	344	15.212	+1.045
309	14.263	+0.729	327	14.884	+1.469	345	14.162	+0.935
310	14.927	+2.130	328	14.982	+1.602	346	14.580	+0.546
311	14.766	+1.587	329	15.224	+0.763	347	15.140	+0.727
312	13.208	+0.296	330	14.374	+1.237	348	15.002	+0.759
313	14.268	+0.615	331	15.194	+0.685	349	15.169	+1.483
314	14.695	+0.709	332	14.865	+1.200	350	14.462	+2.252
315	15.085	+0.923	333	14.732	+0.538	351	15.001	+1.076
316	14.511	+0.552	334	14.647	+0.659	352	15.142	+1.383
317	14.417	+0.569	335	14.475	+0.693			
318	14.868	+0.662	336	14.475	+0.716			

In the course of study of the CCD images the author has discovered what seems to be a new planetary nebula, located about 20″ southwest of star 8. It is labeled PN on the CCD finder chart (Figure 19); Figure 22 shows magnified and enhanced *V* and *B* images of the planetary nebula. Its equatorial coordinates for the epoch 2000.0, measured with

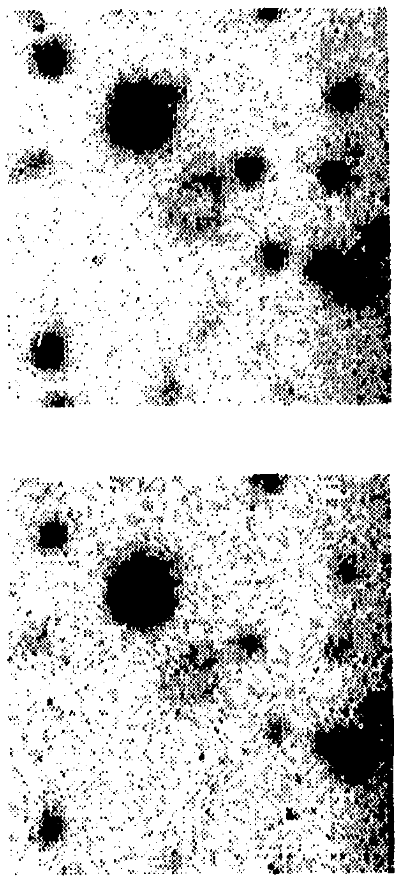

Figure 22. Visual (top) and blue (bottom) images of the newly discovered planetary nebula (at the centre) near SU Cyg. The bright star to the upper left of the nebula is star 8.

respect to SU Cyg are: $\alpha = 19^h 44^m 52^s$, $\delta = +29° 12' 38''$. The planetary nebula has an elliptical shape, with a major axis of ~14″ and a minor axis of ~12″; the brighter northwest edge might be caused by a faint star. Integrated magnitudes of $V = 16.0$ and $B = 16.5$ were measured using VISTA, but the planetary nebula is barely above the sky background so these magnitudes should be regarded as estimates only. The object is not visible on the paper copies of the POSS nor on the David Dunlap Observatory glass copies (Turner, private communication). While the elliptical shape, obvious image structure and different appearance in the V and B bandpasses almost exclude the possibility that this object is an artifact, an additional deep image is needed in order to confirm its existence.

2.2.3 Photographic photometry

The photographic plates used in this study were obtained by John Takala on the nights of 1987 August 19/20 and 20/21, and by David Turner on the night of 1991 August 6/7, with the 48″ telescope of the University of Western Ontario. A total of 12 plates were taken: three in V, four in B and five in U. The exposure information for the plates is summarized in Table 15 on the next page.

All plates were measured using the Saint Mary's University iris photometer and the same techniques as those described in Part 1 of the thesis; the only difference was the absence of secondary images. The initial examination of the plates revealed that one of them was off-centred and covered only a small part of the field, and another one had the guider prism in the field of view and so both plates were rejected. Thus, two V, three B and five U plates were measured altogether.

As opposed to the calibration relations for the field of V1726 Cyg, all of which were linear for I^4 vs. magnitude, the appropriate relations for the SU Cyg field were either

Table 15. Plate information for the field of SU Cyg

	Plate No.	Exposure Time	Emulsion	Filter	Observer	Comments
V	1738	15^m	103a-D	GG495	Takala	Off-centred; not used
	1744	30^m			Takala	
	1781	60^m			Turner	
B	1736	10^m	103a-O	GG385	Takala	
	1740	20^m			Takala	Guider in field; not used
	1743	25^m			Takala	
	1782	47^m			Turner	
U	1737	30^m	103a-O	UG2	Takala	
	1742	60^m			Takala	
	1753	60^m			Takala	
	1754	60^m			Takala	
	1783	98^m			Turner	

I vs. magnitude, or I^2 vs. magnitude, where I is the iris reading. Examples of calibrations for two plates in each bandpass are shown in Figures 23, 24 and 25. Open circles depict points that were not included in the final calibrations. Most often star #1 was rejected, perhaps because its iris data were influenced by the scattered light from the Cepheid. As a whole, the photographic data are somewhat noisier compared with the calibrations for the V1726 Cyg field, most likely because different types of emulsion have been used — the scatter in the iris readings is dominated by emulsion granularity (Turner and Welch 1989), which is larger for 103a-O/103a-D emulsions.

With several plates available in each bandpass, it was possible to estimate the quality of the calibrations from the scatter around the mean instrumental magnitudes. For every star measured in a given bandpass, we calculated the differences between the magnitudes from the individual plates and the average instrumental magnitude for that

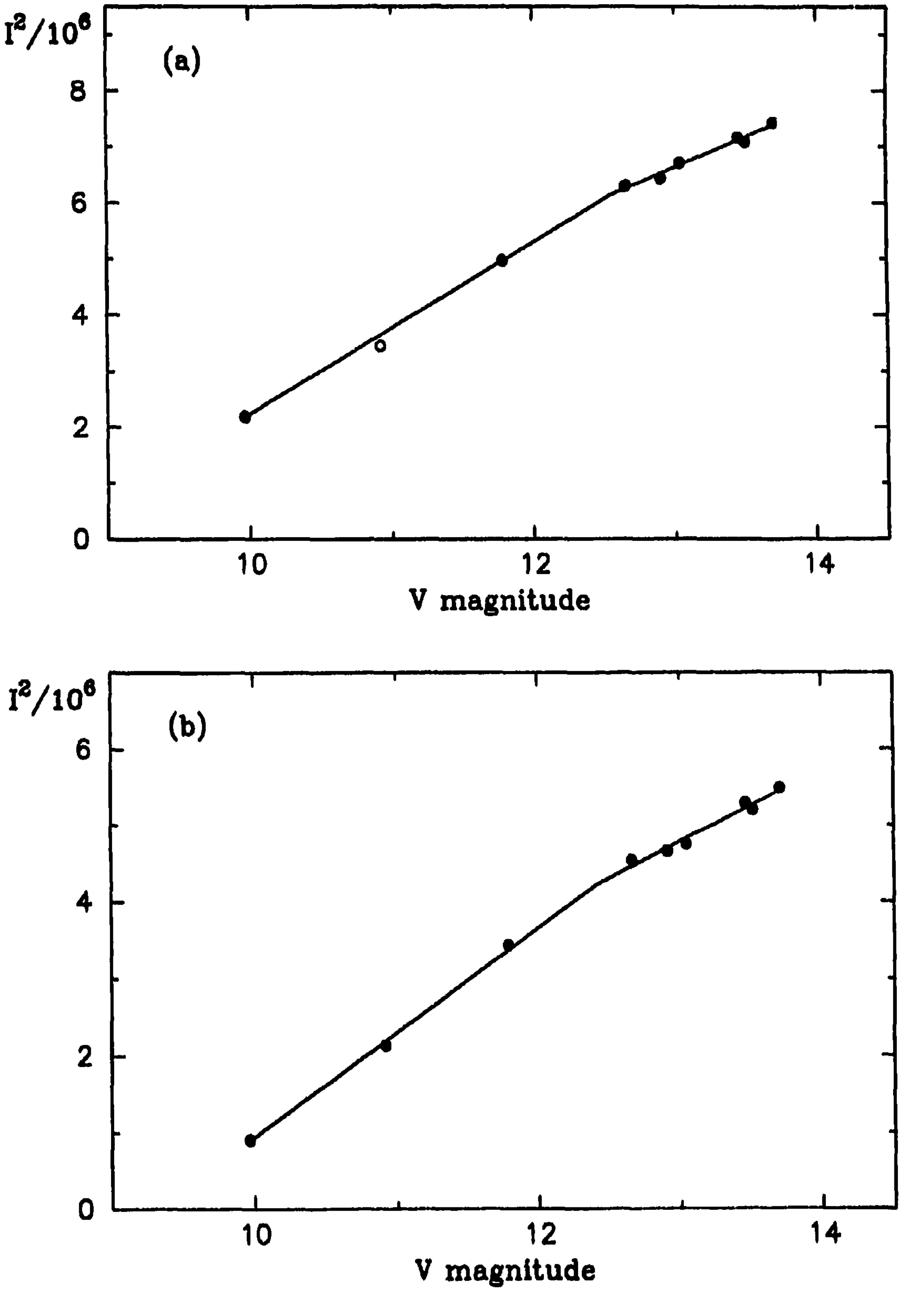

Figure 23. Two examples of calibration relations for the *V* plates. *(a)* second *V* plate, *(b)* third *V* plate.

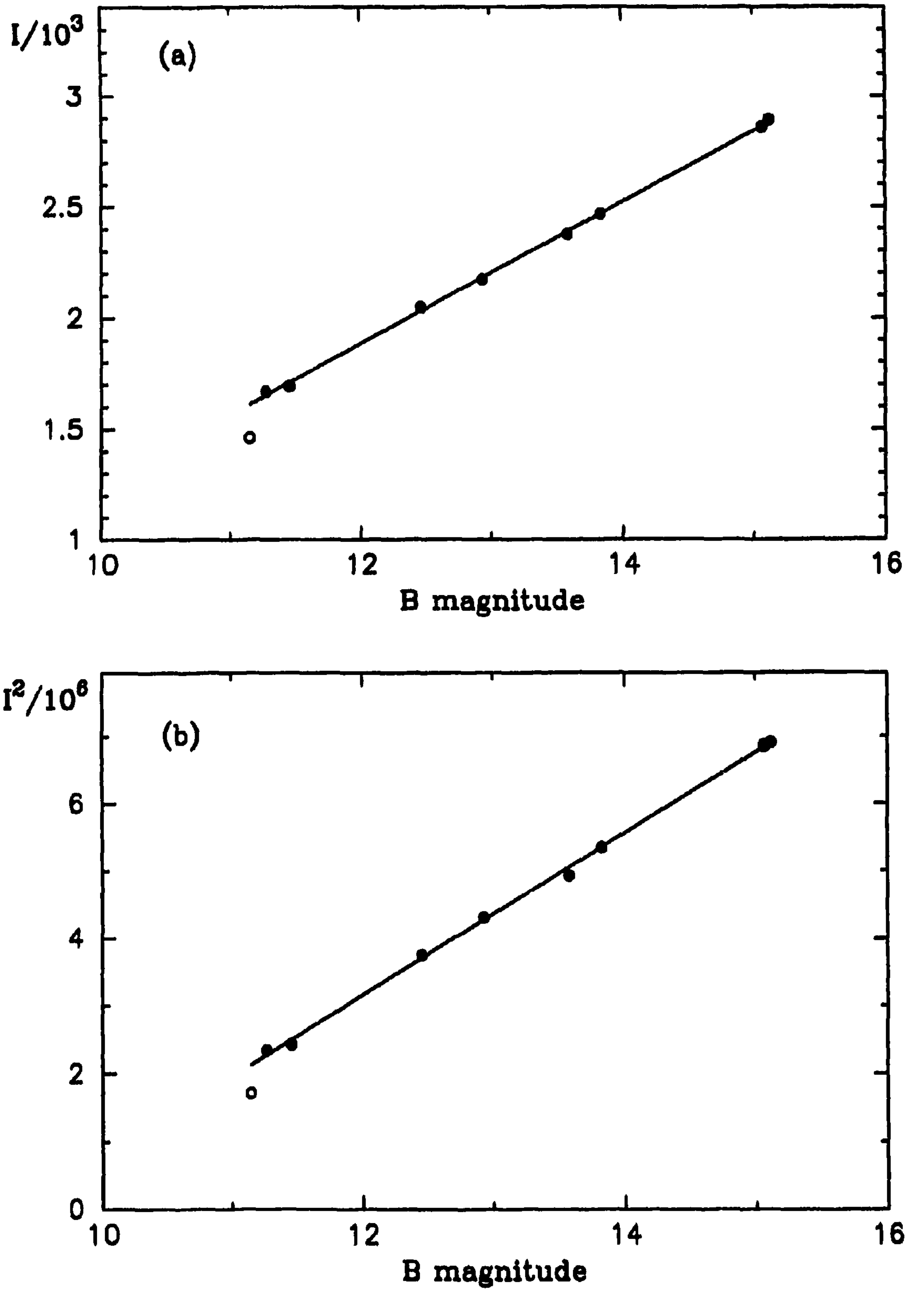

Figure 24. Two examples of calibration relations for the *B* plates. *(a)* first *B* plate, *(b)* third *B* plate.

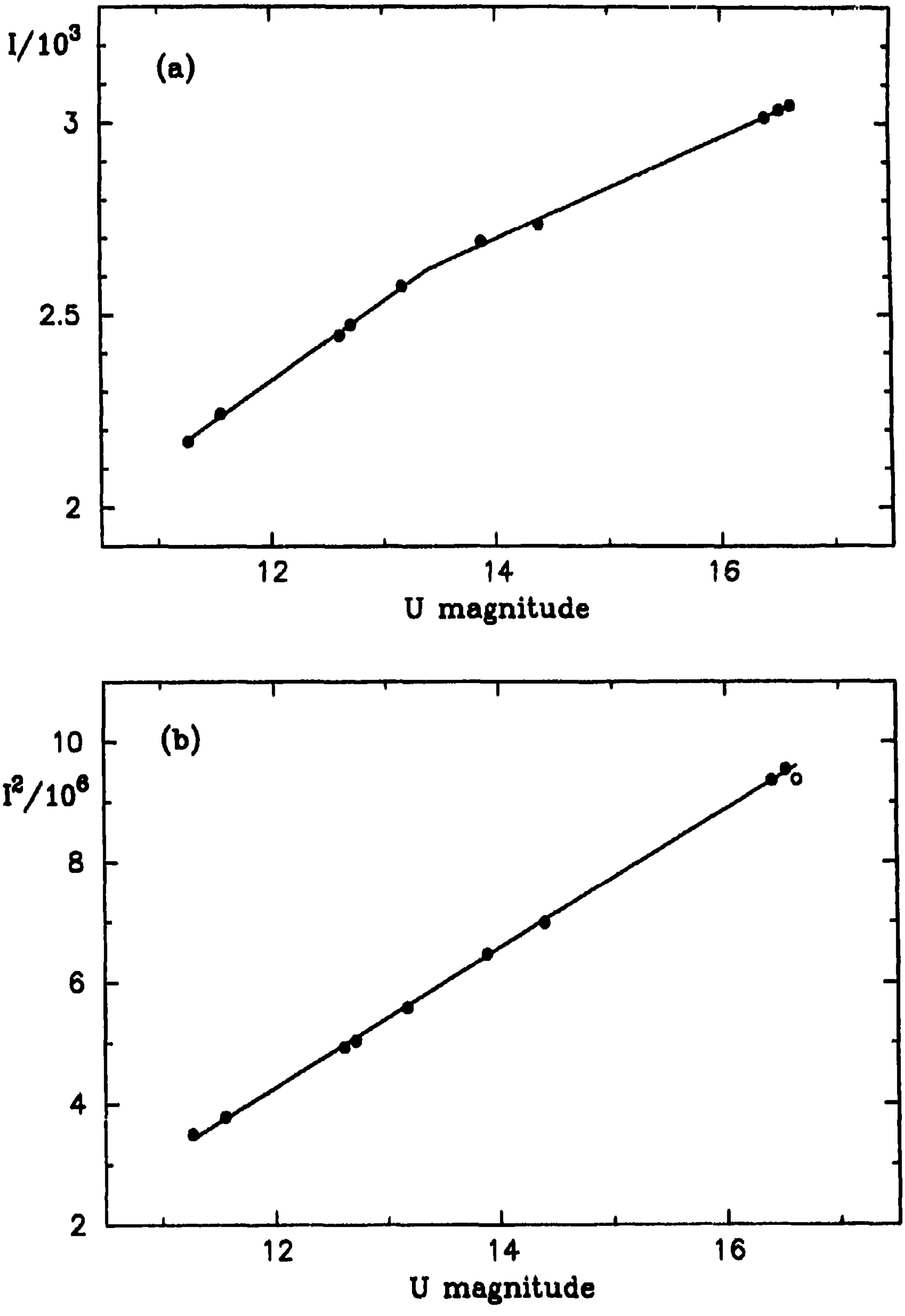

Figure 25. Two examples of calibration relations for the *U* plates. *(a)* third *U* plate, *(b)* fifth *U* plate.

bandpass. The results are summarized in Table 16, where $\overline{\Delta v}$, $\overline{\Delta b}$ and $\overline{\Delta u}$ designate the mean of those differences.

Table 16. Plate-to-plate magnitude differences

Plate #	$\overline{\Delta v}$	$\overline{\Delta b}$	$\overline{\Delta u}$
1	---	0.084	0.042
2	0.033	---	0.076
3	0.034	0.051	0.060
4		0.052	0.077
5			0.045

It is clear that the data from the first *B* plate suffer from larger uncertainties than the remaining two plates, and that plate was excluded from further analysis. Its rejection brought down the average dispersion for the *B* plates from $0\overset{m}{.}040$ to $0\overset{m}{.}031$, which is comparable to the mean dispersions for *V* and *U* plates: $0\overset{m}{.}020$ and $0\overset{m}{.}034$, respectively.

The transformation to the Johnson *UBV* system was performed in exactly the same way as in part 1, *i.e.* using equations which included only the colour terms:

$$V - v = c_3 + d_3(b - v) \qquad (10)$$

$$B - V = c_4 + d_4(b - v) \qquad (11)$$

$$U - B = c_5 + d_5(u - b) \qquad (12)$$

where v, b and u denote the instrumental magnitudes in the corresponding bandpasses, and V, B and U denote the standard Johnson magnitudes. In Figure 26, we have plotted the data used in the transformation equations, as well as the best least squares fits which are shown by straight lines. The coefficients c_3, d_3, ... of the colour equations are tabulated in Table 17.

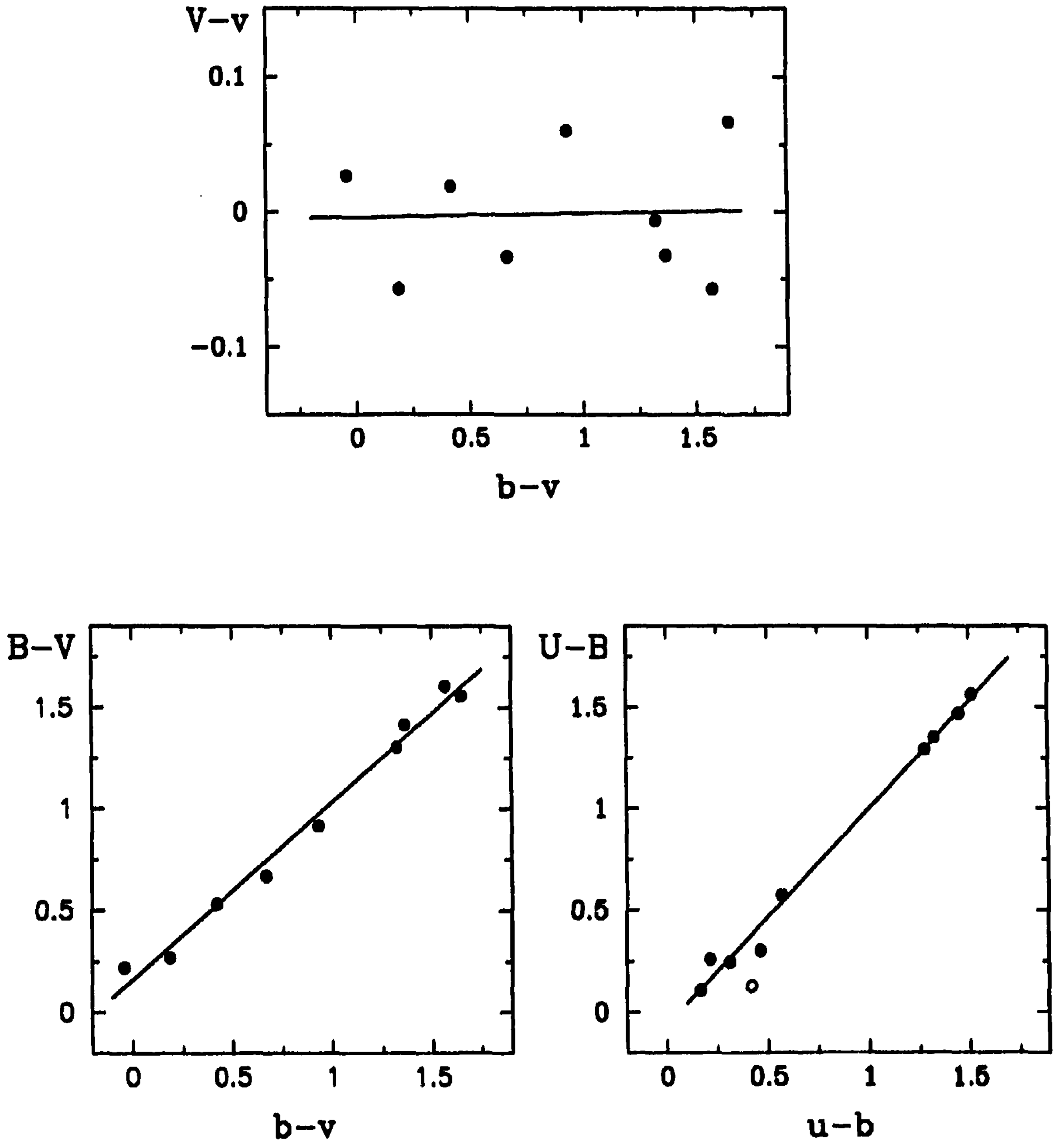

Figure 26. Transformation relations for the photographic plates. Top: plot of $V-v$ versus $b-v$; bottom left: plot of $B-V$ versus $b-v$; bottom right: plot of $U-B$ versus $u-b$.

Table 17. Coefficients for the transformation equations (10) – (12)

Equation	$c_i \pm 1\sigma$	$d_i \pm 1\sigma$	Remarks
(10)	−0.004 ± 0.031	+0.003 ± 0.029	Adopted $c_3 = 0$, $d_3 = 0$
(11)	+0.160 ± 0.041	+0.872 ± 0.039	
(11)	−0.064 ± 0.038	+1.062 ± 0.039	

The photographic *UBV* magnitudes, calculated by means of the transformation equations (10) to (12), are listed in Table 18, where the star numbers correspond to those in Figure 18. For several stars there are no V and $B-V$ data because of close companions which did not allow iris measurements on the V plates. For a few of those stars, marked by an asterisk in Table 18, we managed to obtain the missing V and $B-V$ data from CCD photometry. Star 125, which looked normal on the photographic plates, turned out to be a close double on the CCD images; its companion is star 301 in Table 14. The *UBV* data quoted in Table 18 are the combined values for star 125. Subtracting the contribution from the companion, we obtain true values of $V_{125} = 12.13$ and $(B-V)_{125} = 1.15$.

Another object deserving special notice is star 163. We found that the positions of this star on the photographic plates and on the POSS photographs differ by $\sim 15''$, implying very large proper motion. A search through several proper motion catalogues revealed that star 163 is included in the NLTT catalogue (Luyten 1979, 1980) as LP 337-0060, and in the earlier LTT catalogue (Luyten 1961) as LTT 15763. It has a proper motion of $0\farcs321$ per annum, which implies that this is a nearby, probably unreddened star.

2.2.4 Radial velocity data

The only star in the SU Cyg field with radial velocity observations (except the Cepheid itself) is star 1, which has been observed by Turner (private communication). All his observations are listed in Table 19 below. Clearly, the spread in the radial velocity

Table 18. Photographic *UBV* photometry for the field of SU Cyg

Star	V	B–V	U–B	Star	V	B–V	U–B	Star	V	B–V	U–B
101	12.76	1.06	1.08	135*	13.87	1.48	1.19	169	13.84	0.60	0.28
102	13.56	0.43	0.22	136	14.14	0.75	0.52	170	13.46	1.89	1.49
103	13.66	0.38	0.42	137	12.60	0.36	0.18	171	12.00	1.65	1.96
104	11.84	1.54	2.08	138	13.04	1.19	1.11	172	14.01	0.69	0.37
105	12.09	0.61	0.07	139	13.34	1.56	1.51	173	11.45	0.96	0.40
106	13.75	0.53	0.19	140	10.07	1.82	2.10	174	11.98	1.87	2.38
107	13.46	0.45	0.34	141	13.69	1.27	1.23	175	11.92	0.58	-0.09
108	11.36	1.11	0.63	142	14.04	1.31	1.21	176	11.90	1.24	1.00
109	11.36	1.21	0.96	143	13.43	0.45	0.25	177	13.41	0.48	0.29
110	11.27	1.76	2.34	144	13.50	0.37	0.39	178	13.05	0.51	0.37
111	13.74	1.61	1.35	145	---	--	1.58	179	13.68	0.58	0.20
112	---	--	0.95	146	11.87	0.72	0.04	180	14.16	1.59	0.98
113	14.04	1.56	0.78	147	11.47	0.28	0.29	181	13.07	0.34	0.23
114	12.99	0.27	0.27	148	12.04	1.93	2.22	182	11.93	0.60	-0.06
115	13.33	0.56	0.29	149	13.56	0.51	0.26	183	11.11	0.71	0.27
116	13.37	1.29	1.21	150	12.64	1.89	2.07	184	13.58	2.63	0.80
117	---	--	1.77	151	13.03	0.42	0.40	185	12.59	1.84	2.20
118	13.20	1.34	1.10	152*	13.52	0.35	0.50	186	12.73	0.70	0.29
119	13.97	1.87	1.19	153	---	--	0.43	187	12.50	0.65	0.03
120	12.93	1.60	2.00	154	---	--	0.21	188	12.10	1.26	0.98
121	13.25	0.20	0.23	155	13.09	0.34	0.32	189	13.52	0.49	0.56
122	12.00	0.21	0.22	156	---	--	1.26	190	11.24	0.41	0.11
123	12.80	0.69	0.08	157	13.60	0.96	0.67	191	12.09	1.54	1.70
124	13.85	0.52	0.25	158	11.22	0.64	0.10	192	13.05	0.23	0.21
125†	12.03	1.11	0.89	159	12.99	0.79	0.33	193	13.09	1.29	1.54
126*	13.82	0.55	0.62	160	11.12	1.57	1.88	194	12.23	1.77	1.90
127	12.02	0.43	0.14	161	13.57	0.53	0.74	195	12.81	1.35	1.42
128	13.07	0.41	0.31	162	12.12	2.00	2.28	196	13.54	0.32	0.41
129*	13.93	0.60	0.47	163	10.50	0.83	0.56	197	13.76	0.58	0.37
130	13.25	1.31	1.19	164	12.68	0.52	0.25	198	13.51	1.60	1.54
131	12.06	1.33	1.19	165	13.67	1.71	1.43	199	14.11	0.66	0.49
132	13.71	1.77	1.48	166	14.08	1.38	1.17	200	11.98	1.64	2.00
133	12.69	0.82	0.31	167	13.36	0.77	0.23	201	10.49:	0.17:	0.14:
134	13.25	1.10	1.09	168	14.13	1.95	1.07				

† Has a close companion. Corrected photometry: $V = 12.13$, $B - V = 1.15$

* V and $B - V$ data from CCD photometry

data far exceeds the quoted observational errors and this is most certainly a binary star. Its mean radial velocity of $\langle V_R \rangle = -23.6 \pm 7.1\ \mathrm{km\,s^{-1}}$ is practically equal to the systemic radial velocity of $\langle V_R \rangle = -21.5 \pm 0.1\ \mathrm{km\,s^{-1}}$ for SU Cyg (Evans 1988). Without knowledge of some properties of the second star in the system, it is difficult to say whether this is a mere coincidence or the two systems are physically related. According to Turner (private communication), there is no trace of the companion in the spectrum of star 1, which implies a magnitude difference $\Delta V \gtrsim 2$. That would make the intrinsic distance modulus of star 1 considerably smaller than the one expected for the Cepheid from the PLC relation.

Table 19. Radial velocity data for star 1

JD	V_R $(\mathrm{km\,s^{-1}})$
2445906.909	−5.2 ± [illegible].5
5908.762	−19.3 ± 4.1
5909.781	−43.0 ± 3.8
5910.882	−47.1 ± 2.9
5911.777	+12.5 ± 5.[illegible]
6327.770	−43.5 ± 5.0
6328.689	−9.5 ± 3.8
6330.740	−14.3 ± 5.3
6331.689	−42.8 ± 3.3

We tried to derive an orbital period for star 1 using the data in Table 19, and obtained two possible values of 1.2 and 5.4 days. The small number of observations precludes more certain period determination and the question of the orbital period remains open.

2.3 Analysis

2.3.1 Interstellar Reddening

With the exception of star 1, there are no other stars with accurate MK spectral classifications around SU Cyg, so independent determination of the reddening slope for this field is not possible. Therefore, we adopted the same reddening relation, $E_{U-B}/E_{B-V} = 0.75$, as for the nearby (~2°) field of the Cepheid S Vul (Turner 1980), and used it to deredden the program stars.

The colour-colour diagram for the field of SU Cyg is presented in Figure 27. Filled circles mark the stars observed photoelectrically, and stars having only photographic photometry are shown by open circles. The solid line is the intrinsic colour relation for solar-metallicity stars (Turner, private communication). The region of spectral types A2 – F6 is well populated, but no concentration similar to the one present on the colour-colour diagram for the field of V1726 Cyg is observed here. The unusual position of the few stars lying far below the A2 reddening line is caused by the presence of close companions. The other few stars below the line but close to it were dereddened to the A2 bump of the intrinsic relation. As can be seen at the lower right part of the plot, almost half of our sample consists of late-type stars which are quite common in the galactic plane but are of marginal interest to the present study.

Figure 28 shows a reddening map for the field of SU Cyg, generated using the colour excesses (adjusted to the equivalent for a B0-type star) for all reddened stars having $B-V<1$. The map shows that there is a significant spatial variation of the extinction in this field, with values of E_{B-V} between $0\overset{m}{.}15$ and $0\overset{m}{.}5$. The Cepheid lies on the boundary between a low-extinction area to the west of the centre and a high-extinction region running from north-east to south-west. The latter seems to correspond to an apparent dust obscuration visible on the POSS photographs.

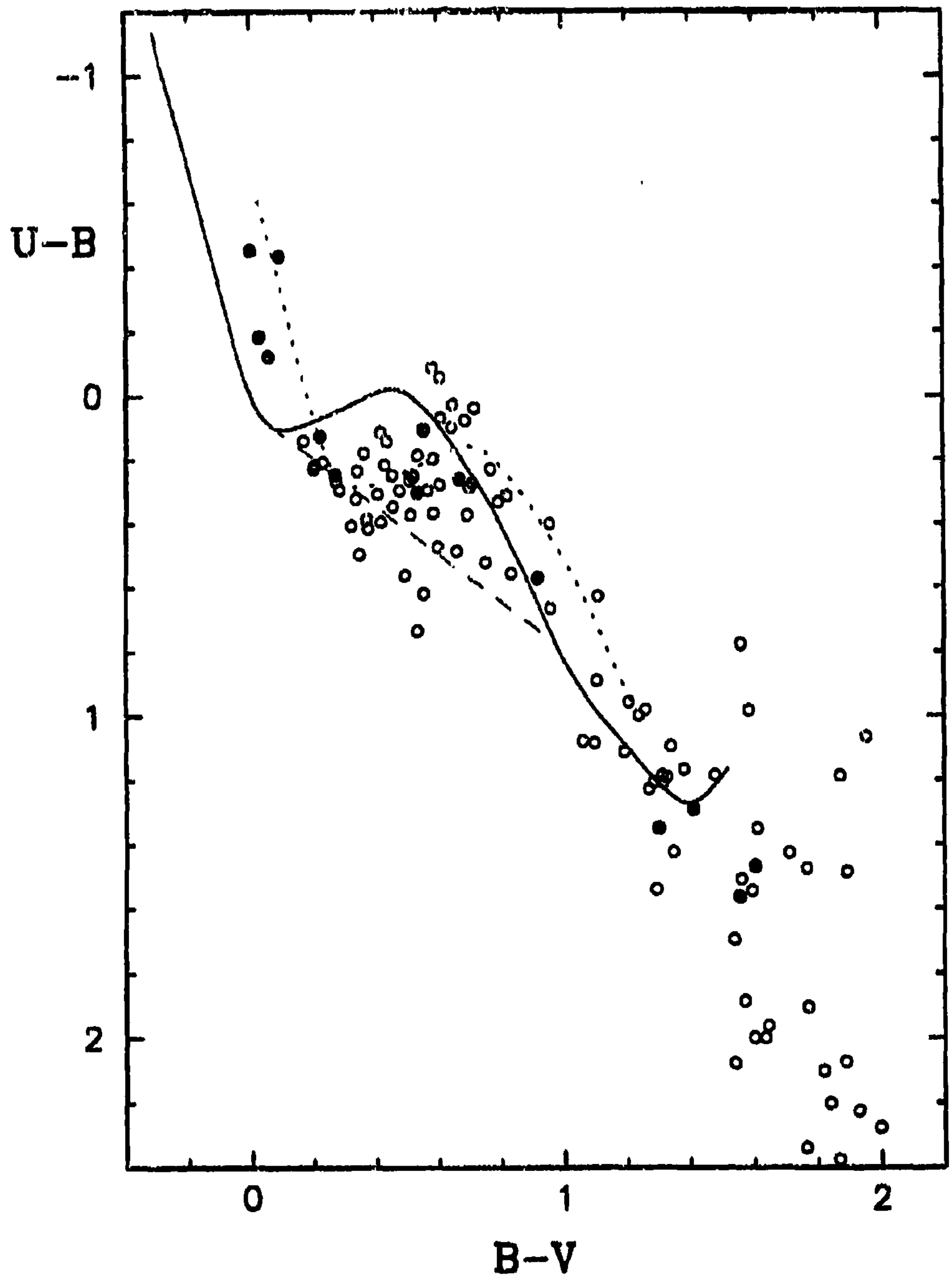

Figure 27. Colour-colour diagram for the field of SU Cyg. Filled circles: photoelectrically observed stars; open circles: stars with photographic photometry. The intrinsic relation for main-sequence stars is shown by a solid line; the dotted line shows the same relation reddened by $E_{B-V} = 0.22$. The reddening line appropriate for this field is shown by a dashed line.

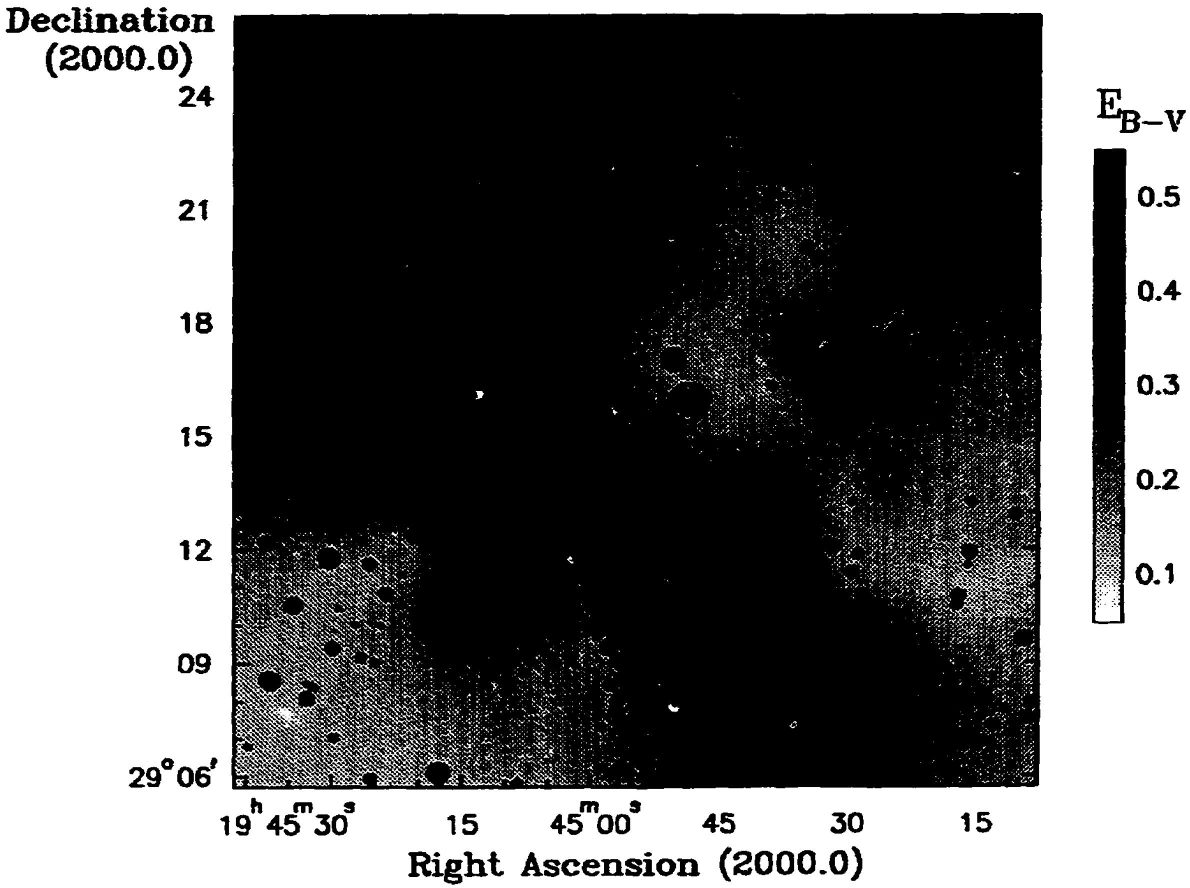

Figure 28. A reddening map for the field of SU Cyg based on the colour excesses for all reddened stars. SU Cyg is circled.

The reddening map was very useful in deriving extinction corrections for the stars having only BV CCD photometry (Table 14). Their colour excesses were estimated from a plot of isoreddening contours drawn every $0^{m}.01$, and the resulting mean values indicate that most of those stars are reddened F and G dwarfs. Table 20 presents reddenings and other relevant data for the combined sample of stars with photoelectric (numbers 1–FM8), photographic (102–201) and CCD (301–351) photometry. The values of M_V were obtained using the zero-age main sequence from Turner (1979).

Table 20. Reduced data for stars in the field of SU Cyg

Star	E_{B-V}	$(B-V)_0$	$V-M_V$	Star	E_{B-V}	$(B-V)_0$	$V-M_V$	Star	E_{B-V}	$(B-V)_0$	$V-M_V$
1	0.17	0.06	9.08	155	0.29	0.06	11.25	314	0.35	0.36	11.43
2	0.16	0.40	7.38	157	0.06	0.90	7.16	315	0.21	0.71	9.68
4	0.34	0.34	8.65	158	0.17	0.48	7.13	316	0.32	0.23	11.92
5	0.22	0.06	10.82	159	0.06	0.73	7.48	317	0.16	0.41	10.82
7	0.06	0.86	6.71	163	0.00	0.83	4.47	318	0.42	0.24	12.23
8	0.32	0.22	10.50	164	0.27	0.26	9.95	319	0.16	0.55	10.70
FM3	0.27	−0.18	10.87	167	0.17	0.61	8.48	322	0.21	0.46	10.60
FM4	0.12	−0.07	8.85	169	0.33	0.29	10.97	324	0.16	0.47	10.34
FM7	0.11	−0.08	9.45	172	0.45	0.26	11.28	326	0.34	0.87	8.37
FM8	0.16	−0.16	10.38	177	0.29	0.19	10.98	329	0.22	0.54	10.75
102	0.21	0.23	10.97	178	0.38	0.15	10.78	331	0.29	0.40	11.67
105	0.14	0.48	8.00	179	0.25	0.34	10.54	332	0.33	0.87	8.60
106	0.22	0.32	10.72	181	0.19	0.16	10.76	333	0.19	0.35	11.54
107	0.33	0.13	11.28	183	0.37	0.36	7.85	334	0.18	0.48	10.56
114	0.22	0.06	11.15	186	0.38	0.34	9.59	335	0.21	0.48	10.39
115	0.33	0.25	10.64	187	0.18	0.48	8.41	336	0.18	0.54	10.01
121	0.15	0.06	11.41	190	0.50	−0.08	10.39	337	0.20	0.44	10.73
122	0.16	0.06	10.16	192	0.17	0.06	11.21	338	0.17	0.81	9.20
123	0.22	0.48	8.71	197	0.40	0.20	11.28	339	0.16	0.48	10.37
124	0.27	0.26	11.12	201	0.16	0.01	8.88	340	0.23	0.63	10.09
127	0.15	0.29	9.15	301	0.20	0.54	10.16	344	0.30	0.74	9.65
128	0.28	0.13	10.89	302	0.20	0.99	8.26	345	0.26	0.68	8.96
133	0.14	0.69	7.38	304	0.21	0.69	9.74	346	0.31	0.24	11.94
137	0.42	−0.05	11.45	305	0.26	0.55	10.37	347	0.35	0.38	11.75
143	0.24	0.22	10.88	307	0.21	0.56	10.35	348	0.36	0.40	11.48
147	0.23	0.06	9.63	309	0.27	0.46	10.30	351	0.35	0.73	9.49
149	0.26	0.26	10.83	312	0.21	0.09	11.22				
151	0.37	0.06	11.19	313	0.20	0.42	10.59				

The variable-extinction diagram for the field of SU Cyg is presented in Figure 29, where all stars in Table 20 have been plotted. Photoelectrically observed stars are shown by triangles, filled circles mark stars with photographic photometry, and data from CCD photometry are depicted by open circles. The four open diamonds represent the stars observed by Feltz and McNamara (1976); their apparent distance moduli are based on Hβ luminosities (see Table 11*b*). The only unreddened object in the diagram is star 163, which we consider to be unreddened based on its large proper motion and position on the colour-colour diagram. Star 163 has a distance modulus of $V_0 - M_V = 4.47$ (78 pc), beyond which there are no obvious unreddened stars. The closest reddened stars are at $V_0 - M_V = 6.5$ (200 pc), so the dust clouds responsible for their extinction are somewhere between 80 and 200 pc. There is a distinct break at $V_0 - M_V = 7.4$ (300 pc), where the field foreground reddening suddenly increases from $E_{B-V} \approx 0.06$ to an average value of $E_{B-V} \approx 0.15$. We can conclude that there is a relatively nearby (~100 pc) dust cloud producing reddening of $E_{B-V} \approx 0.06$, and a second cloud at a distance of ~300 pc which raises the foreground extinction to $E_{B-V} \approx 0.15$. The foreground reddening remains at this value up to $V_0 - M_V \approx 11$ (1600 pc).

In the variable-extinction diagram one can see a poorly populated but distinct lower envelope which indicates the presence of a sparse group of stars at $V_0 - M_V \approx 10.0$. We identified 16 envelope stars as probable members of that stellar group and used them to obtain an estimate of $R = A_V / E_{B-V}$, the ratio of total to selective absorption. An unweighted least squares fit (shown by a straight line) yielded $R = 3.13 \pm 0.24$, very close to the value $R = 3.0$ found for nearby regions in previous studies (see Turner 1980). The latter value was adopted as appropriate for this field, mainly because our value of R was derived from predominantly photographic photometry.

An interesting sequence of six to eight faint background stars is clearly visible below the group lower envelope. All of them are within a 10′ area around SU Cyg and in

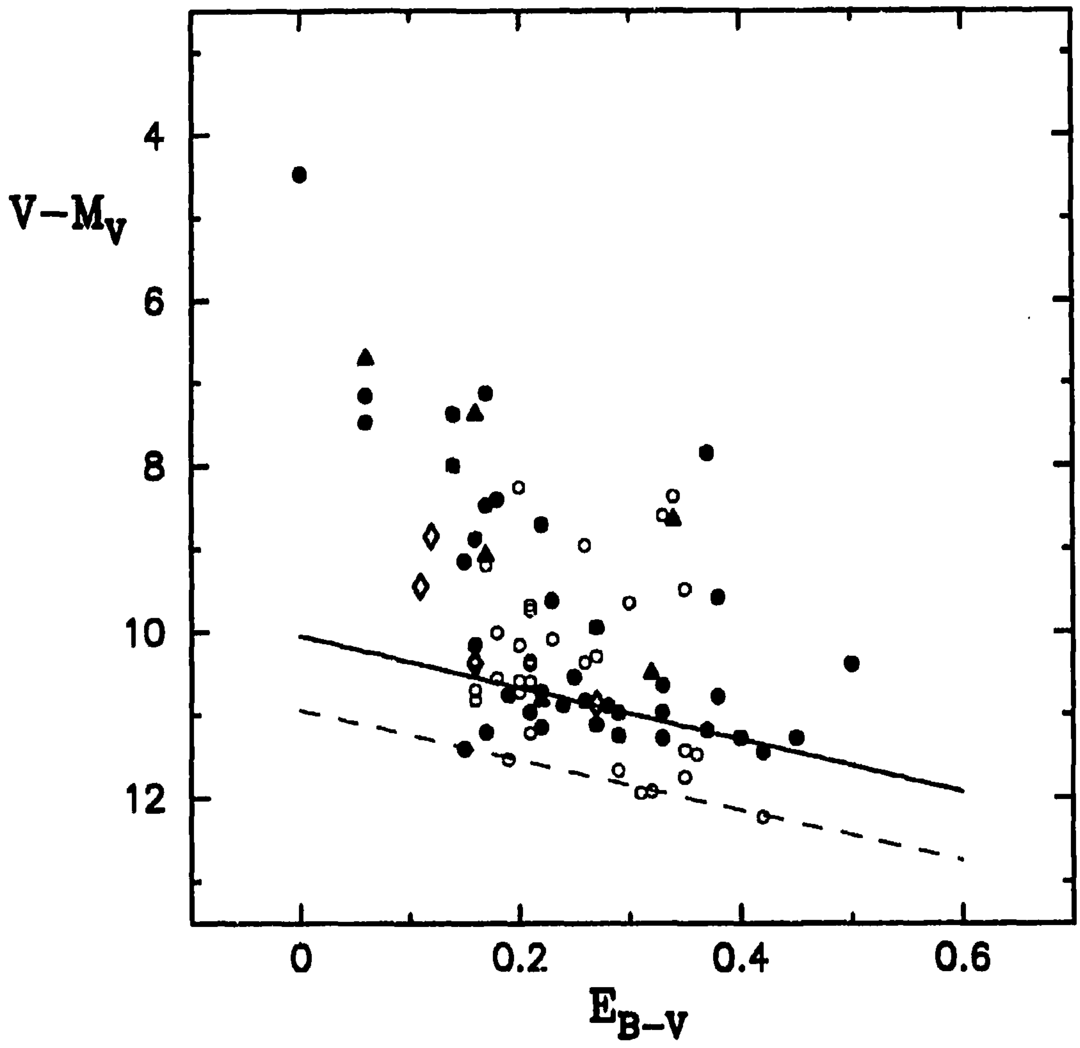

Figure 29. Variable-extinction diagram for stars in the SU Cyg field with luminosities obtained from ZAMS fitting (circles and triangles) and Hβ photometry (open diamonds). Triangles and filled circles represent stars with photoelectric and photographic photometry, respectively. Data from CCD photometry are shown by open circles. The relations appropriate for the two groups at 1040 and 1540 pc are shown by straight lines with a slope of $R = 3.13$.

the author's opinion, these stars represent another, more distant group of late B and A-type stars. The reddening relation for that second group is shown by a dashed line in Figure 29. The corresponding distance modulus is $V_0 - M_V = 10.94$ (1540 pc).

2.3.2 *Membership and distance to the group*

With the value of R fixed, we calculated the extinction corrections for all potential members of the group selected by their positions on the variable-extinction and colour-magnitude diagrams. The data are listed in Table 21 and the colour-magnitude diagram for the group is shown in Figure 30. Besides the 16 lower envelope stars, we have included in Table 21 two of Feltz and McNamara's (1976) stars, as well as a few other stars within $\sim 0^{m}.5$ of the main sequence, which we consider to be probable members.

Table 21. Data for probable group members

Star	$(B-V)_0$	V_0	Star	$(B-V)_0$	V_0	Star	$(B-V)_0$	V_0
5[a]	0.06	12.00	151[a]	0.06	11.92	313[a]	0.42	13.67
FM3[a]	−0.18	8.39	169[a]	0.29	12.84	319	0.55	14.76
FM8[a]	−0.16	8.75	172	0.26	12.67	322[a]	0.46	13.93
106[a]	0.32	13.08	177[a]	0.19	12.53	324	0.47	13.89
122	0.06	11.52	179	0.34	12.92	329[a]	0.54	14.56
128[a]	0.13	12.22	181[a]	0.16	12.49	334[a]	0.48	14.11
137[a]	−0.05	11.35	190	−0.08	9.73	335	0.48	13.85
143[a]	0.22	12.70	197[a]	0.20	12.57	337[a]	0.44	13.95
149[a]	0.26	12.78	307	0.56	14.31	339	0.48	13.98

[a] Highly probable group member

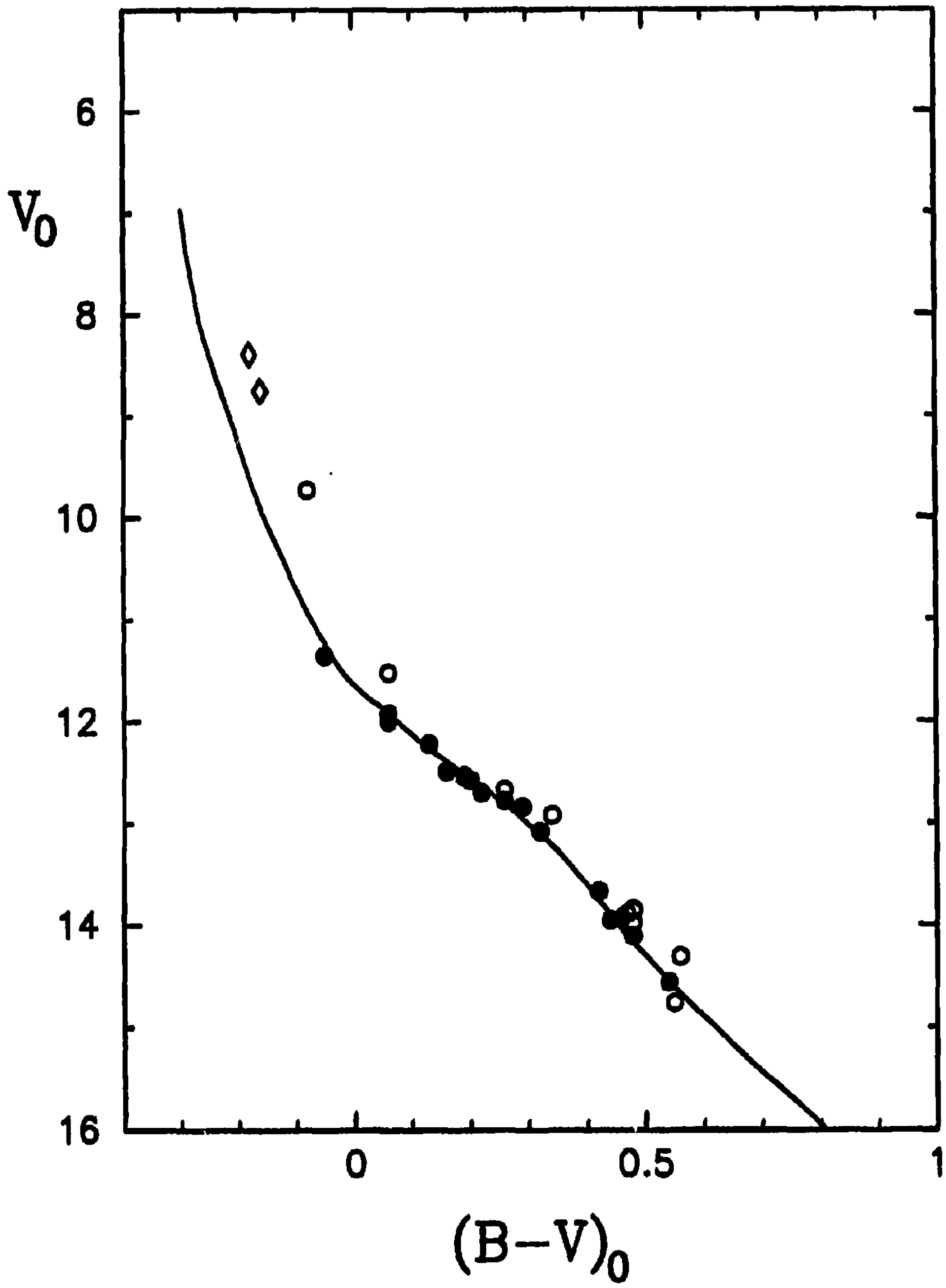

Figure 30. Reddening-free colour-magnitude diagram for highly probable members (filled circles) and other potential members (open circles) of the group at 1040 pc. The positions of Feltz and McNamara's (1976) stars 3 and 8 are shown by open diamonds. The solid line represents the ZAMS for $V_0 - M_V = 10.08$.

The distance to the group was found by means of the modified sliding-fit technique (the third method discussed in section 3.2, Part 1). We applied this method to the 16 members of the group considered to be on the ZAMS and obtained a distance modulus of $V_0 - M_V = 10.08 \pm 0.02$, corresponding to a distance of 1038 ± 10 pc.

The scarcely populated upper main sequence of the group makes the colour of the turnoff point somewhat uncertain. The position of Feltz and McNamara's stars 3 and 8 depends very little on whether their colour excesses are derived from the original *UBV* photometry or through conversion of Strömgren indices. Under the assumption that these two stars are members of the group, the turnoff point is at $(B-V)_0 = -0.18$ (spectral type B4). If they are not associated with the group, its turnoff point will be defined by the single star at $(B-V)_0 = -0.08$ (spectral type B8). Consulting the PPM catalogue (Röser and Bastian 1991), we found that BD +28° 3467, the bright star at the left edge of Figure 1 (about 5′ east of star 200), is a B8 star which has not been observed so far and might be another potential group member. From its rather crude magnitude and spectral type we estimated that it will lie about $1^{\mathrm{m}}\!.5$ above star 190, at $(B-V)_0 \approx -0.08$.

The nature of the stellar group at 1040 pc is not entirely clear. Unlike "normal" open clusters, its members are distributed randomly, without any apparent concentration. The distance modulus of this new group, $V_0 - M_V = 10.08$, is in remarkable agreement with that found by Turner (unpublished) for the nearby Vul OB4 association: $V_0 - M_V = 10.07 \pm 0.04$. It seems possible, therefore, that the group in Figure 30 consists of remote, mostly faint members of Vul OB4. They are not as heavily reddened as the Vul OB4 stars observed by Turner, but the large colour excesses of the latter can be explained by the vast complexes of dust south of SU Cyg, which are well visible on the POSS photographs; the region of SU Cyg, in contrast, is relatively dust-free. The age of the Vul OB4 is estimated by Turner to be $1\text{–}2 \times 10^7$ years, which is comparable to the age of $\sim 4 \times 10^7$ years for the group as determined from the turnoff colour. If the group of stars at $V_0 - M_V = 10.08$ is indeed a part of Vul OB4, it will mean that the association extends far further north than considered before.

Another possibility for the group of stars in Figure 30 is that it might be a part of a larger formation similar to the stellar "sheet" observed by Eggen (1980) in Vela, and that Vul OB4 is also a part of the same formation. In any case, it seems quite plausible to suggest that the newly found group of stars at 1040 pc is related somehow to Vul OB4, although we do not exclude the possibility that the group is a "real" cluster in its final stages of dissolution.

Clearly, there is a need for additional data, especially radial velocities and MK spectral types, in order to resolve the membership question for the upper-main-sequence stars. The use of CCD photometry allowed us to detect lower-main-sequence stars about $0^{m}.2$ redder and $\sim 1^{m}.5$ fainter than in the V1726 Cyg study, so the lower main sequence is well defined. As a more distant goal, it is desirable to obtain photometry for the region south of SU Cyg, between the northern boundary of the Vul OB4 association and the field of the Cepheid. Such a study would be useful for determining the true extent of Vul OB4 and the nature of the anonymous stellar group around SU Cyg.

2.3.3 SU Cygni

In the previous two sections we have presented arguments that SU Cyg is surrounded by a sparse, poorly populated, but relatively young stellar group. Although the group is not recognizable against the dense Milky Way background, its presence is evident on the variable-extinction and colour-magnitude diagrams of the field. The next question that must be answered is whether SU Cyg is physically associated with that group, or we just see the Cepheid projected against it.

The observed photometric properties of SU Cyg were determined using the *UBV* data compilations kindly provided by Leonid Berdnikov. The observations from different sources were in excellent agreement and no corrections were necessary to bring them to a common system. Figure 31 shows the V light curve and the $B-V$ colour curve of the Cepheid as derived from the combined data. The phases were calculated using the newly determined period of $P = 3\overset{d}{.}8455466$. The parameters of the light and colour variations of SU Cyg, obtained by means of Fourier decomposition, are summarized in Table 22.

Table 22. Summary of the light and colour variations of SU Cyg

V_{max} = 6.444	$(B-V)_{max}$ = 0.404	$\langle V \rangle = 6.865$
V_{min} = 7.194	$(B-V)_{min}$ = 0.706	$\langle B \rangle = 7.431$
$M-m$ = 0.285	$\langle B \rangle - \langle V \rangle$ = 0.566	$\langle U \rangle = 7.76$:
$\phi_{21} = 4.20 \pm 0.03$	$R_{21} = 0.375 \pm 0.009$	
$\phi_{31} = 2.22 \pm 0.05$	$R_{31} = 0.171 \pm 0.008$	

$$\mathrm{HJD}_{max} = \underset{\pm 0.0002}{2447789.5873} + \underset{\pm 0.0000003}{3.8455466}E$$

The colour excess of SU Cyg can be found from the reddening of its closest neighbour, star 1. The latter has an MK spectral classification of A2 V (Turner, private communication), and its colour excess is $E_{B-V}(\mathrm{B0}) = 0.17$. Since star 1 is only about 20″ to the west of the Cepheid, we can assume that SU Cyg has the same colour excess of $E_{B-V}(\mathrm{B0}) = 0.17$, corresponding to a reddening of $E_{B-V} = 0.16$ for a star with the observed colours of the Cepheid. Referring to the colour indices in Table 22, we find that the intrinsic colour of the Cepheid at maximum, minimum and mean light is $(B-V)_{0\,max} = 0.24$, $(B-V)_{0\,min} = 0.55$, and $(\langle B \rangle - \langle V \rangle)_0 = 0.41$, respectively.

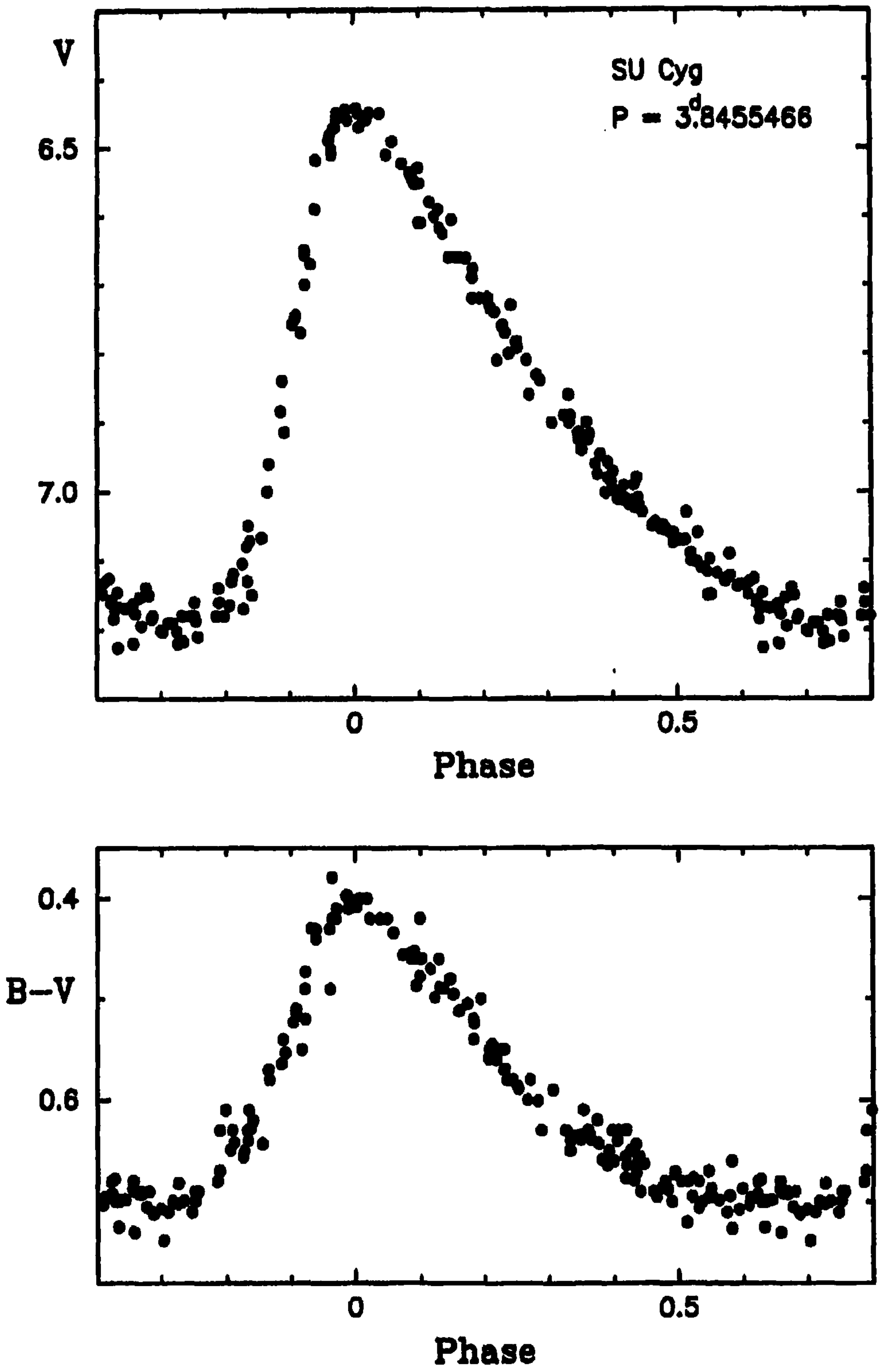

Figure 31. The V light curve (top) and and the $B-V$ colour curve (bottom) of SU Cyg. The phases correspond to the newly determined period shown in the top panel.

These values must be corrected for the influence of the two companions, SU Cyg B (B7.5 V) and SU Cyg C. The exact magnitude difference between SU Cyg and the companions is unknown. The spectral type of SU Cyg C is also unknown, although Evans and Bolton (1990) estimate that it is not earlier than A0 V. The same authors use a colour difference of $\Delta(B-V)=+0.04$ between the Cepheid and SU Cyg B, which implies a magnitude difference of $\Delta V=3.08$. We should note, however, that the derivation of a magnitude difference from the colour difference for small values of $\Delta(B-V)$ is very sensitive to small changes in $\Delta(B-V)$ and therefore not very reliable — a change of 0.01 in $\Delta(B-V)$ for $\Delta(B-V)\approx 0.05$ leads to a change of ~0.20 in ΔV.

If we adopt Evans and Bolton's (1990) correction of $\Delta(B-V)=0.04$, the true intrinsic colour of SU Cyg is $(\langle B\rangle-\langle V\rangle)_0=0.45$ for a mean spectral type of F6 I-II, in good agreement with the value of $(B-V)_0=0.46$ expected from various calibrations of the colours of FG supergiants (*e.g.* Fernie 1963, Johnson 1966, Kron 1978). Moreover, the implied value of the magnitude difference, $\Delta V=3.08$, also agrees with the estimates of other researchers ($\Delta V=2.97$, Böhm-Vitense and Proffitt 1985; $\Delta V=3.1$, Fernie 1979). Therefore we adopted values of $(\langle B\rangle-\langle V\rangle)_0=0.45$ and $\Delta V=3.08$ as appropriate for the Cepheid and SU Cyg B. Depending on the properties of SU Cyg C, the intrinsic colour may be a few hundredths of a magnitude redder, since even a faint early-type companion will affect Cepheid's colours (see Turner 1985); the magnitude difference, on the other hand, is unlikely to change when the light from the second companion is accounted for.

For a magnitude difference of $\Delta V=3.08$, the intrinsic apparent magnitude of the Cepheid is $\langle V\rangle_0=6.45$. If SU Cyg is a member of the group, its implied absolute visual magnitude is $M_V=-3.63$, whereas the absolute magnitude expected from the period-luminosity-colour (PLC) relation is $M_V=-3.06$. The latter value was found by adding a colour correction of -0.189 to the absolute magnitude obtained from Turner's (1992) period-luminosity relation; a colour term of $\beta=2.1$ (Turner *et al.* 1994), and an offset from the centre of the instability strip of $\Delta(B-V)_0 = -0.09$ (Turner, private communication) were used to find the colour correction.

Thus, SU Cyg seems to be too bright to be a member of the group of stars at $V_0 - M_V = 10.08$. There is almost half a magnitude difference between the distance modulus implied by a group membership and the one inferred from the PLC relation. It is hardly possible to reconcile the two distances by assuming other magnitude (or colour) differences, since any decrease in ΔV in order to make the group absolute magnitude smaller will be cancelled out by the diminishing colour term. Similar reasoning can also be applied to supposed reddening errors.

The colour of the main-sequence turnoff also indicates that SU Cyg is probably not associated with the group. Turner's period-turnoff color relation (unpublished) predicts a turnoff point of $(B-V)_0 = -0.11$ for a Cepheid with the period of SU Cyg, whereas in section 3.2 we found a turnoff colour of $(B-V)_0 = -0.18$. There is some possibility for a later turnoff, however, depending on whether FM3 and FM8 are members of the group.

Turner (private communication) has made the interesting suggestion that SU Cyg might be an overtone pulsator, with the objective to bridge the gap between the implied luminosity from group membership and the PLC luminosity. If $P = 3^{\mathrm{d}}\!.8455466$ is the first overtone period, the corresponding fundamental mode period is $P_0 = 5^{\mathrm{d}}\!.5540247$, and the resulting PLC luminosity is $M_V = -3.65$. While this is in excellent agreement with the predicted "cluster" luminosity, the Fourier parameters of the light curve of SU Cyg (Table 22) would seem to rule out overtone pulsation. We must conclude, therefore, that the available data do not support the membership of SU Cygni in the anonymous group found in this study.

2.3.4 A possible new cluster in the vicinity of SU Cyg

In the course of examination of the POSS photographs of the region surrounding SU Cyg, the author has found what seems to be a new sparse cluster about 17′ to the west of SU Cyg. Figure 32, which shows the cluster (in the centre) and the surrounding area, is an enlargement from a blue POSS photograph. The bright star at the bottom is SU Cyg, and the other bright star above the centre is V1276 Cyg, a low-amplitude δ Scuti star. The reality of the cluster has yet to be confirmed, but an indication that this is an actual cluster is the appearance of the group on very low dispersion objective-prism photographs taken by Turner (private communication) many years ago. With the exception of the brightest star southwest of the cluster centre, all relatively bright objects appear to be early-type stars. That particular star looks like a K star, which does not exclude its membership in the cluster. We have planned further investigation of this area in order to confirm or reject the existence of the cluster.

2.4 Summary and conclusions

We have presented and analyzed photoelectric, photographic and CCD photometry for 163 stars in the field of the Cepheid SU Cyg, with the purpose of searching for a cluster associated with the Cepheid. We have detected the existence of a very sparse, relatively young (~ 4×10^7 yr) group, dominated by faint stars, at a distance of 1040 pc ($V_0 - M_V = 10.08$). There is a possibility that this group is related to the Vul OB4 association which is located a few degrees south of SU Cyg. The use of CCD photometry enabled us to reach faint stars on the main sequence, and compared with the cluster near V1726 Cyg, our photometry goes about $1^m\!\!.5$ fainter.

One of the important results of this study is the new colour excess for SU Cyg. Previous determinations were based on mean values from field stars (Feltz and McNamara

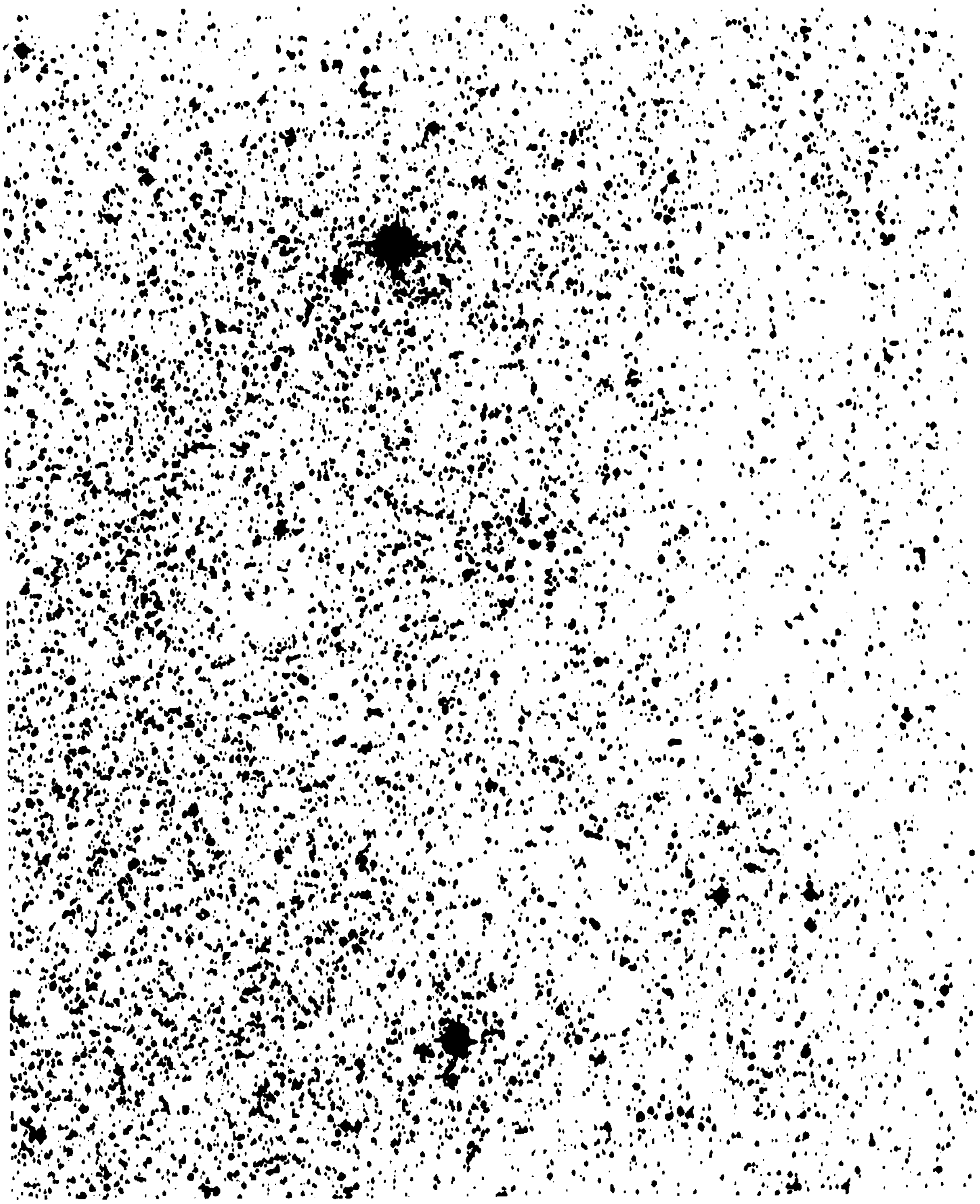

Figure 32. The field of the proposed new cluster, which is clearly visible near the centre. SU Cyg is the bright star at the bottom. The other bright star in the upper part of the field is BD +28° 3447 = V1276 Cyg, a low-amplitude δ Scuti star. The field is approximately 30′× 35′. West is up and north is to the left.

1976) or an assumed interstellar reddening law (Dean, Warren and Cousins 1978). Given the patchiness of the extinction in this area and that colour excesses vary by $0^{m}.35$ within $20'$ from the Cepheid, such reddenings are not very reliable. Our result comes from a star that has an accurate MK spectral type and is only $20''$ from the Cepheid, so the new colour excess is expected to be very close to the true one.

Unfortunately, the currently available data suggest that SU Cyg is not a member of the newly found group. While the difference between the distance modulus predicted from the PLC relation and that expected from group membership is admittedly not very large ($\sim 0^{m}.5$), it is significant given the accuracy of both the group distance modulus and the Cepheid's parameters. Turner (private communication) has suggested overtone pulsation as a way to reconcile the PLC and group luminosities. For an overtone pulsator with the period of the Cepheid, the two luminosities are in excellent agreement; however, there is a very slim chance for SU Cyg pulsating in the first overtone given the current interpretation of the Fourier light curve parameters. We conclude therefore that SU Cyg is not associated with the group, but is a foreground star projected against it.

In the course of the present study the author has discovered a new faint planetary nebula about $3'$ south of SU Cyg, and possibly a new sparse cluster about $17'$ to the west of the Cepheid. While the first object is almost certainly real, the existence of the cluster has yet to be confirmed.

Conclusions

At present, Cepheids that are established members of well-studied open clusters or associations are indispensable for the calibration of the PLC relation. Increasing the number of such Cepheids is the primary reason for carrying out studies such as those presented in this thesis. Regrettably, as far as the currently available data implies, neither V1726 Cyg nor SU Cyg seem to be usable as PLC calibrators. Yet the controversial results for the field of C2128+488 and V1726 Cyg, as well as the unknown nature of the stellar group found in the field of SU Cyg clearly call for further investigation of both fields. In the author's opinion, future studies of the region of SU Cyg should be concentrated on determining the extent of the sparse group of stars at 1040 pc found in this study and examining its relation to the Vul OB4 association. In the case of V1726 Cyg, the establishment of its pulsational mode and, as a more distant goal, the detection of the rate and direction of evolution across the instability strip seem to be the most important objectives.

References

Andreasen, G. K. 1988, A&A, 196, 159

Antonello, E., and Poretti, E. 1986, A&A, 169, 149

Antonello, E., Poretti, E., and Reduzzi, L. 1990*a*, A&A, 236, 138

Antonello, E., Poretti, E., and Reduzzi, L. 1990*b*, in *Confrontation Between Stellar Pulsation and Evolution*, edited by C. Cacciari and G. Clementini (ASP, San Francisco), ASP Conf. Ser., 11, p. 209

Berdnikov, L. N. 1986, Variable Stars, 22,369

Berdnikov, L. N. 1992, Sov. Astron. Lett., 18, 130

Berdnikov, L. N. 1993, IAU Inform. Bull. Variable Stars, No. 3885

Böhm-Vitense, E. 1985, ApJ, 296, 169

Böhm-Vitense, E., and Proffitt, C. 1985, ApJ, 296, 175

Brodie, J. P., and Madore, B. F. 1980, MNRAS, 191, 841

Buser, R. 1978, A&A, 62, 411

Caldwell, J. A. R., and Coulson, I. M. 1987, AJ, 93, 1090

Crawford, D. L. 1978, AJ, 83, 48

Dean, J. F., Warren, P. R., and Cousins, A. W. J. 1978, MNRAS, 183, 569

Ebbighausen, E. G. 1942, AJ, 50, 1

Eggen, O. J. 1980, ApJ, 238, 627

Evans, N. R. 1988, ApJS, 66, 343

Evans, N. R., and Bolton, C. T. 1990, ApJ, 356, 630

Feltz, K. A., Jr., and McNamara, D. H. 1976, PASP, 88, 699

Feltz, K. A., Jr., and McNamara, D. H. 1980, PASP, 92, 609

Fernie, J. D. 1963, AJ, 68, 780

Fernie, J. D. 1979, PASP, 91, 67

FitzGerald, P. M. 1970, A&A, 4, 234

Gieren, W. P., Welch, D. L., Mermilliod, J.–C., Matthews, J. M. and Hertling, G. 1994, AJ, 107, 2093

Johnson, H. L. 1953, ApJ, 117, 353

Johnson, H. L. 1966, Ann. Rev. Astron. Astrophys., 4, 193

Kholopov, P. N., Samus, N. N., Frolov, M. S., Goranskij, V. P., Gorynya, N. A., Kireeva, N. N., Kukarkina, N. P., Kurochkin, N. E., Medvedeva, G. I., Perova, N. B., Shugarov, S. Yu. 1985, *General Catalogue of Variable Stars* (Nauka, Moscow)

Krelowski, J., and Papaj, J. 1993, PASP, 105, 1209

Kron, G. E. 1978, AJ, 83, 1195

Luyten, W. J. 1961, *A Catalogue of 7127 Stars in the Northern Hemisphere with Proper Motions Exceeding 0.2 arcsec Annually (LTT)* (The Lund Press, Minneapolis)

Luyten, W. J. 1979, 1980, *New Luyten Catalogue of Stars with Proper Motions Larger than Two Tenths of an Arcsecond (NLTT)* (University of Minnesota, Minneapolis)

Madore, B. F. 1977, MNRAS, 178, 505

Maeder, A., and Meynet, G. 1988, A&AS, 76, 411

Maeder, A., and Mermilliod, J.–C. 1981, A&A, 93, 136

McNamara, B. J., and Sanders, W. L. 1977, A&AS, 30, 45

Metzger, M. R., Caldwell, J. A. R., McCarthy, J. K., and Schechter, P. L. 1991, ApJS, 76, 803

Metzger, M. R., Caldwell, J. A. R., and Schechter, P. L. 1992, AJ, 103, 529

Platais, I. 1979, Astron. Tsirk. No. 1049, p. 4

Platais, I. 1984, Sov. Astron. Lett., 10, 84

Platais, I. 1986, Nauchnye Inform. Astron. Sov. Akad. Nauk SSSR, 61, 89

Platais, I. 1988, Nauchnye Inform. Astron. Sov. Akad. Nauk SSSR, 65, 119

Platais, I. 1994, Bull. Inform. CDS, No. 44

Platais, I., and Shugarov, S. Yu. 1981, IAU Inform. Bull. Variable Stars, No. 1982

Poretti, E. 1994, A&A, 285, 524

Röser, S., and Bastian, U. 1991, *PPM star catalogue: positions and proper motions of 181731 stars north of −2.5 degrees declination for equinox and epoch J2000.0* (Spektrum Akademischer Verlag, Heidelberg)

Schaefer, B. E. 1981, PASP, 93, 253

Schaltenbrand, R., and Tammann, G. A. 1971, A&AS, 4, 265

Schmidt, E. G. 1975, MNRAS, 170, 39P

Schmidt, E. G. 1984, ApJ, 285, 501

Schwarzenberg-Czerny, A. 1989, MNRAS, 241, 153

Simon, N. R. 1988, in *Pulsation and Mass Loss in Stars*, edited by R. Stalio and L. A. Willson (Kluwer, Dordrecht), p. 27

Simon, N. R., and Lee, A. S. 1981, ApJ, 248, 291

Stellingwerf, R. F. 1978, ApJ, 224, 953

Stetson, P. B. 1987, PASP, 99, 191

Stetson, P. B. 1990, PASP, 102, 932

Szabados, L. 1988, in *Multimode Stellar Pulsations*, edited by G. Kovacs, L. Szabados, and B. Szeidl (Konkoly Observatory, Budapest), p. 1

Turner, D. G. 1976, AJ, 81, 1125

Turner, D. G. 1979, PASP, 91, 642

Turner, D. G. 1980, ApJ, 235, 146

Turner, D. G. 1985, in *Cepheids: Theory and Observations*, edited by B. F. Madore (Cambridge University Press, Cambridge), p. 205

Turner, D. G. 1986, AJ, 92, 111

Turner, D. G. 1989, AJ, 98, 2300

Turner, D. G. 1992, AJ, 104, 1865

Turner, D. G., and Welch, G. A. 1989, PASP, 101, 1038

Turner, D. G., Forbes, D., and Pedreros, M. 1992, AJ, 104, 1132

Turner, D. G., Leonard, P. J., and English, D. A. 1987, AJ, 93, 368

Turner, D. G., Leonard, P. J., and Madore, B. F. 1986, JRASC, 80, 166

Turner, D. G., Mandushev, G. I., and Forbes, D. 1994, AJ, 107, 1796

Turner, D. G., van den Berg, S., Younger, P. F., Danks, T. A., and Forbes, D. 1993, ApJS, 85, 119

Curriculum Vitae

Name:	Georgi Iliev Mandushev
Date and place of birth:	9 July 1962, Varna, Bulgaria
Post-secondary Education and Degrees:	Sofia University, Sofia, Bulgaria 1982-1987 Diploma of Higher Education
	Saint Mary's University, Halifax, Nova Scotia 1992-1994 Master of Science
	University of British Columbia, Vancouver, British Columbia 1994 –
Honours and Awards:	Sofia University Scholarship, 1982-1987
	First Place, National Student Competition in Physics, 1985
	Father Burke-Gaffney Memorial Scholarship, Saint Mary's University, 1992
	Saint Mary's University Graduate Award, 1993
	University of British Columbia Graduate Fellowship, 1994
Related Work Experience:	Visiting Research Fellow, Nagoya University, Japan 1989-1990
	Teaching and Research Assistant, Sofia University, Bulgaria 1990-1992
	Teaching and Research Assistant, Saint Mary's University 1992-1994

Publications:

1. **On the variability of the period of β Lyrae**
   by G. Mandushev, 1988, Astron. Tsirk., No. 1533
2. **Dynamical masses for galactic globular clusters**
   by G. Mandushev, N. Spassova and A. Staneva, 1991, A&A, 252, 94

Publications: (continued)

3. **Galactic clusters with associated Cepheid Variables.**

   IV. C2128+488 (Anon. Platais) and V1726 Cyg

   by D. G. Turner, G. I. Mandushev and D. Forbes, 1994, AJ, 107, 1796

4. **The period and light curve of V1028 Orionis**

   by G. I. Mandushev, A. M. Heiser and D. G. Turner, 1994, IAU Inform. Bull. Variable Stars, No. 3960